Phosphorylation-mediated regulation of cell polarity and auxin transport in plants

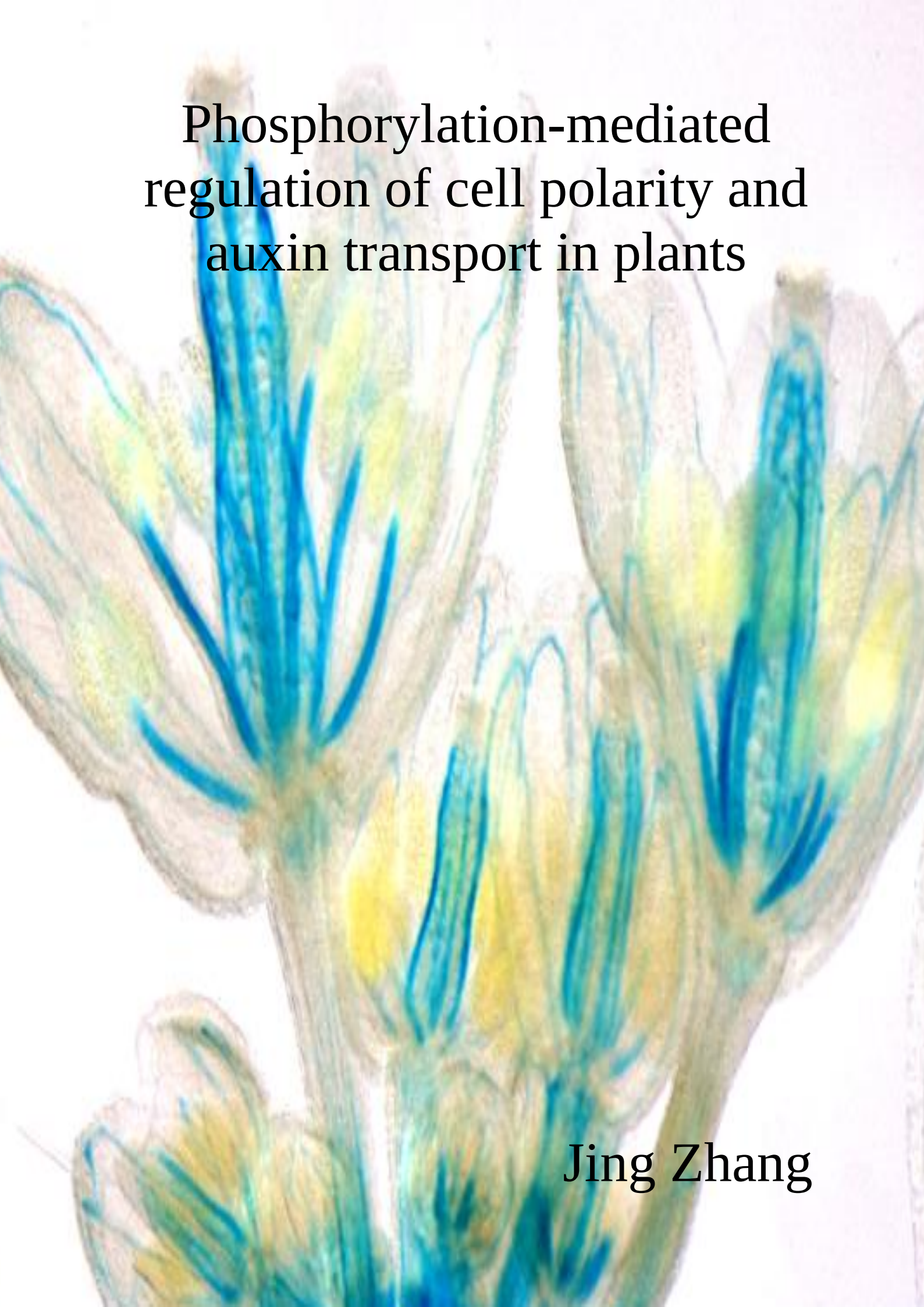

Jing Zhang

Ghent University
Faculty of Science
Department of Molecular Genetics

Phosphorylation-mediated regulation of cell polarity and auxin transport in plants

Jing Zhang

Promotor: Prof. Dr. Jiří Friml

November 2010

Promotion Commission

Promotor:
Prof. Dr. Jiří Friml
E-mail: jifri@psb.vib-ugent.be
VIB/University Gent; Department of Plant Systems Biology

Chair:
Prof. Dr. Ann Depicker
E-mail: anpic@psb.vib-ugent.be
VIB/University Gent; Department of Plant Systems Biology

Prof. Dr. Pierre Hilson
E-mail: pihil@psb.vib-ugent.be
VIB/University Gent; Department of Plant Systems Biology

Dr. Eva Benkova
E-mail: evben@psb.vib-ugent.be
VIB/University Gent; Department of Plant Systems Biology

Dr. Jürgen Kleine-Vehn
E-mail: jukle@psb.vib-ugent.be
VIB/University Gent; Department of Plant Systems Biology

Dr. ZhaoJun Ding
E-mail: zhdin@psb.vib-ugent.be
VIB/University Gent; Department of Plant Systems Biology

Prof. Dr. Remko Offringa
E-mail: r.offringa@biology.leidenuniv.nl
Leiden University

Dr. Stéphanie Robert
E-mail: Stephanie.Robert@genfys.slu.se
SLU/Umea Plant Science Center

Only when you seize today can you not lose tomorrow

只有抓住今天，才能不丢失明天

CONTENTS

SCOPE

The phytohormone auxin is important for various aspects of plant growth and development. Local auxin gradients within tissues correlate spatiotemporally with developmental events such as apical-basal axis and symmetry establishment during embryogenesis, phyllotaxis, organ initiation or tropism. These asymmetric auxin distributions are largely mediated by the activity of auxin efflux carriers PIN proteins. The plasma membrane localized PINs, including PIN1, PIN2, PIN3, PIN4 and PIN7 determine the directional cell-to-cell auxin flow and facilitate the auxin gradient formation in plant. Alterations in the PIN polarity redirect the auxin flow and thus influence the auxin-dependent plant development. However, the mechanisms governing PIN polarity are still elusive. Therefore, broadly speaking, the question of how PIN polar targeting is controlled, and consequently, mediate local auxin gradients and how the polarity regulators interact with PIN-mediated transport is currently of great interest and has been the major subject of the research described in this thesis.

At the beginning of this Ph.D study, the serine/threonine protein kinase PINOID (PID) was the only isolated molecular that unambiguously and directly mediated the decision about the polar delivery of auxin efflux carriers PIN proteins. However, mechanistic insights of how the phosphorylation modulations of PIN proteins affect their polar localization were surprisingly limited. Our first special focuses in this thesis were given on dephosphorylation event, putative phosphorylation targets, and the interaction between the PID and the GNOM that determine PIN polarity. On the other hand, to characterize additional new regulator of PIN function, our chosen approach was to perform a forward genetic screening and look for mutants that suppressed the phenotype of PIN1 gain-of-function alleles. Generally, our studies provide new insights into regulation of PIN polar targeting, auxin transport, and thus auxin-mediated development.

SUMMARY

SUMMARY

Research of the last years showed that activities of the PIN proteins can be regulated by transcription, degradation, phosphorylation and vesicle trafficking. The first indentified component involved in PIN protein trafficking was the GNOM protein. The PIN protein exocytosis process was inhibited in the *gnom* mutant, which was phenocopied by pharmacological treatment with the fungal toxin brefeldin A (BFA). SNX1 was also established as a regulator for the PIN recycling by defining PIN-sorting endosomes. Many studies had indicated that also the phosphorylation processes were important parts of mechanism for PIN-dependent auxin transport. It had been demonstrated that gain-of-function of PID kinase (*35S::PID*) caused the apical targeting of normally basally localized PIN proteins in *Arabidopsis thaliana* roots, which consequently led to auxin depletion in the root meristem and eventually its collapse. In contrast to *35S::PID*, the *pid* loss-of-function alleles led to basal retargeting of apically localized PIN proteins in the shoot apical meristem. The resulting depletion of auxin from this region provoked to strong needle-like defects in organogenesis. These observations indicate that the PID-dependent phosphorylation acts as a binary switch, in which high phosphorylation levels result in apicalization of the PIN proteins, whereas low phosphorylation levels lead to basal PIN targeting. Thus, the PINOID kinase is an important molecular component directly involved in the regulation of the PIN protein targeting and thus the directional auxin flow.

Further research was aimed at identifying a possible phosphatase component that would influence the polar localization of PIN proteins through dephosphorylation events. As a result, the serine/threonine protein phosphatase 2A (PP2A) was identified as an antagonistic molecular partner for the PINOID kinase (**Chapter 2**; Michniewicz et al., 2007). We demonstrated that the *pp2aa* loss-of-function phenotypes strongly resemble PAT-related defects, particularly, the primary root collapse observed in *35S::PID* plants. Through genetic interactions, we observed that loss of the PID function suppressed the *pp2aa* phenotypes, whereas its overexpression enhanced this phenotype. Moreover, similarly to *35S::PID*, the *pp2aa* mutation also induced basal-to-apical shifts in PIN localizations. All these antagonistic activities of PID and PP2A suggest that they act as a kinase/phosphatase pair on common substrates. This hypothesis was further supported by the finding that both proteins partially colocalize with the PIN proteins at the plasma membrane, indicating at least a transient association of these proteins. In addition, *in vivo* and *in vitro* phosphorylation assays revealed that PID directly phosphorylated the central hydrophilic loop of PIN proteins, whereas PP2A counteracted this event by PIN dephosphorylation. In summary, PP2A and PID antagonistically regulate the PIN polar targeting: more phosphorylation leads to apical targeting and more dephosphorylation to basal targeting.

From the abovementioned observations, we know that PID is able to determine the PIN polarity through phosphorylation of the hydrophilic loop of PIN proteins. However, the direct targets of phosphorylation on the PIN proteins were still unknown. One of putative phosphorylation sites was serine 337 and/or threonine 340 (**Chapter 2**; Michniewicz et al., 2007), which are conserved in several members of the PIN gene family. The objective of the research was to analyze the impact of the PIN phosphorylation at this(ese) specific site(s) on the PIN polar targeting, the auxin distribution, and the auxin-mediated development (**Chapter 3;** Zhang et al., 2010). We provided the first direct evidence that the PIN phosphorylation decides about PIN subcellular polar localization. Both loss-of-phosphorylation PIN1(Ala) and phosphomimic PIN1(Asp) protein versions resulted in flower and fruit defects, indicating that PIN1 phosphorylation at this site is required for auxin-related development. Interestingly, PIN1(Ala) induced predominant basal targeting and thus increased the auxin flow to the root tip. Conversely, the phosphomimic PIN1(Asp) mutation led to apical targeting of PIN1 correlating with embryo defects and also increased the auxin flow in the opposite direction. Furthermore, we analyzed the function of PIN1(Ala) and PIN1(Asp) in the endogenous PIN2 expression domain. Apicalized PIN1(Asp) largely rescued the agravitropic root growth of the *pin2* mutant. All these observations suggested that phosphorylation at this particular site is sufficient to redirect the PIN polarity as well as the directionality of the auxin flow. In addition, our genetic interaction data showed that the basally localized PIN1(Ala) partially rescued root collapse in the *PID* gain-of-function allele *35S::PID* and enhanced the frequency of defective cotyledon patterning in *pid* loss-of-function allele *pid wag1 wag2*, whereas the apically localized PIN1(Asp) was not affected in *pid wag1 wag2*. Altogether, the PIN1(Ala) mutation had antagonistic and PIN1(Asp) agonistic effects with the PID action. Nevertheless, our *in vitro* phosphorylation assay suggested this(ese) phosphorylation site(s) are not a direct target of the PID kinase. Collectively, all the data indicated that serine 337 and/or threonine 340 phosphorylation sites could be a target for other potential kinases that act together with PID in the control of the PIN phosphorylation and the apical/basal PIN polar targeting.

As mentioned, several serine- and threonine-containing phosphorylation sites in conserved

motifs had been identified in the PIN proteins as polarity-determining signals. Using engineered dephosphorylated or phospho-mimicking mutant PIN proteins, we found that phosphorylation of these specific residues in the PIN proteins determine the apical-basal polar PIN localization (Zhang et al., 2010; Huang et al., 2010). However, the underlying mechanism of how the phosphorylation-based sequence regulates the polar PIN delivery was still unknown. To date, ARF-GEF GNOM together with PID kinase were the most prominent identified regulators of the polar PIN targeting. The polar localizations of PIN proteins are highly dynamic and to large extent depend on the constant recycling of PIN proteins from and back to the plasma membrane, which require the actine cytoskeleton and the activity of the ARF-GEF GNOM. In **Chapter 4** (Kleine-Vehn et al., 2009), the interaction between the PID and the GNOM polar-targeting mechanisms were examined. We first detected that the PID gain-of-function allele *35S::PID* and GNOM loss-of function allele *gnom*^{R5} had similar effects on PIN polarity, auxin distribution, development of the primary root and lateral root organogenesis, and vascular tissue patterning. Furthermore, the double mutant *35S::PID gnom*^{R5} showed developmental defects in embryos and seedlings that were much more enhanced than those of each of the single mutants and resembled those of the *gnom* complete loss-of-function mutant. All these data suggested that PID and GNOM regulated PIN polar targeting and auxin-related developments in an antagonistic manner. We further observed a reduced BFA sensitivity of PIN1 at the apical plasma membrane in *35S::PID*, *pp2a* and phospho-mimicking mutant *PIN1-GFP* (mutated PID-targeted phosphorylation sites; Huang et al., 2010), suggesting that the PIN phosphorylation promotes its BFA-insensitive, GNOM-independent targeting. Hence, we proposed that both the PID and GNOM proteins are required in dynamic PIN polarity alterations: PIN proteins phosphorylated at the plasma membrane get internalized into endosomes, but fail to get sorted to the GNOM-dependent basal recycling pathway due to a reduced affinity, while they have an enhanced affinity to be recruited to the apical GNOM-independent trafficking pathway, eventually leading to basal-to-apical PIN transcytosis. Meanwhile, PID kinase activity could be counteracted by the PP2A phosphatase activity that eventually restores the PIN recruitment to the GNOM-dependent basal recycling pathway.

The main question discussed in this thesis concerns the mechanism controlling the PIN polarity. Phosphorylation is one of the essential posttranscriptional regulations of PIN proteins. In order to identify and characterize additional molecular components of PIN function and polar targeting, we performed a forward genetic screening and looked for mutants that suppressed the phenotype of PIN1 gain-of-function alleles (**Chapter 5**; Zhang et al., submitted). One recessive mutant locus, suppressor of PIN1 overexpression (*supo1*), restored normal gravitropism of *35S::PIN1* seedlings. Fine mapping revealed that SUPO1 was defective in the gene encoding an inositol polyphosphate 1-phosphatase, which promoted the inositol 1,4,5-trisphosphate ($InsP_3$) content and increased the Ca^{2+} signaling. This mutant showed pronounced defects in cell polarity, auxin distribution and auxin-mediated development. By numerous pharmacological and genetic manipulations, we showed that increasing $InsP_3$ or free Ca^{2+} levels phenocopied the developmental and cellular defects in *supo1* mutants and also rescued the *35S::PIN1* agravitropic root phenotype, whereas inhibition of $InsP_3$-mediated Ca^{2+} signaling had opposite effects on both development and cell polarity. Altogether, we demonstrated that the basis of these defective phenotypes were changes in Ca^{2+} signaling that are a direct consequence of changes in $InsP_3$ homeostasis. Thus, our work firmly establishes a mechanistic link between the major mechanism of patterning and adaptive development in plants, the cell polarity- and transport-mediated auxin gradients with basic regulatory processes of eukaryotic cells such as inositol phosphate-mediated calcium signaling.

Collectively, the work in this Ph.D thesis provides novel insights into the mechanisms underlying the intracellular PIN polar targeting. We showed that the PIN polar plasma membrane localizations can be regulated through the antagonistic action of the protein kinase PID and phosphatase PP2A. We also provide direct evidence that the PIN phosphorylation decides about PIN subcellular polar localization by identifying an evolutionarily conserved phosphorylation site in PIN sequence. We also obtained initial insights into the cellular mechanisms how PID regulates the polar PIN targeting by revealing that PID-dependent phosphorylation of PIN proteins at the plasma membrane mediates the differential recruitment of PIN proteins to a GNOM-independent polar trafficking pathway. Finally, we propose a previously unsuspected mode of regulation of the PIN-mediated auxin transport by one of the major signals of eukaryotic cells, the inositol phosphate-mediated calcium signaling. These findings open novel lines of investigation in areas of cell polarity and signaling crosstalk as well as into the mechanism by which endogenous and environmental signals influence auxin-mediated plant development through regulation of the PID activity and calcium signaling, and provide possible conceptual means to engineer various aspects of auxin-dependent plant development, including plant shape and architecture in different species.

CHAPTER 1

General Introduction

1. 1 PLANT HORMONES

The coordinated development of all multicellular organisms requires a defined and precise communication at the different levels of the biological organization. The chemical messengers mediating the intracellular signaling are traditionally termed hormones. Hormones are produced in specific tissues or cells from which they are transported to their target sites, where they act at low concentrations. Thus, the action of hormones is established by the pattern of their secretion and the signal transduction of the recipient cells.

In plants, auxin was the first hormone to be designated (Kögl and Haagen-Smit, 1931), which had been chemically identified as indole-3-acetic acid (IAA) (Thimann, 1977) and physiologically functioned as mobile signal regulating the formation and growth of plant organs (Darwin and Darwin, 1881). Nowadays, besides auxin, also gibberellin (GA), cytokinin (CK), abscisic acid (ABA) and ethylene belong to the classical plant hormones (Davis, 2004). In addition to these five traditional classes, there is a constantly growing list of other plant signaling molecules considered to be the phytohormones, such as brassinosteroid, jasmonate, salicylic acid, nitrogen monoxide, and strigolactone. In brief, GA is mainly synthesized in young developing tissues and seeds (Stoddart, 1983) from where they are transported to the place of action through the xylem and phloem. It regulates various developmental processes, including stem elongation, germination, dormancy, flowering, sex expression, enzyme induction, and leaf and fruit senescence (Davis, 2004). CK is produced in developing seeds and root tips and from where it is redistributed to the receiving cells via xylem. They are important regulators of cell divisions and plant morphogenesis (Davis, 2004). The biosynthesis of ABA primarily occurs in leaves and roots and distribution occurs through xylem and phloem tissues, but it can also be transported via the parenchyma cells. It plays a central role not only in plant development but also in plant adaptation to both biotic and abiotic stresses (Salisbury and Ross, 1992; Davis, 2004). Ethylene is produced in response to stress or by tissues that undergo senescence or ripening and it most probably redistributed by the diffusion. It is important regulator of fruit ripening, flower and leaf senescence, lateral and adventitious root initiation, etc (Davis, 2004).

Among all these classical hormones, auxin is the only known hormone so far that is transported in a strictly controlled, directional (polar) manner. Below, the aspects of this polar transport and the proteins mediating the process will be described briefly, because they are crucial to the understanding of this work.

1. 2 AUXIN

In higher plants, the highest auxin biosynthetic capacity has been mainly detected in young developing organs (Ljung et al., 2001). It is widely accepted that plants predominantly use two routes to produce auxin: one dependent and one independent of tryptophan (Trp) (Normanly et al., 2004; Woodward et al., 2005). The Trp-independent pathway has been suggested to maintain constitutive levels of auxin, whereas the Trp-dependent one is initiated when higher levels of this hormone are required, such as during organogenesis or upon wounding (Bartel et al. 2001). Interestingly, only small fractions of synthesized auxin in the plant bodies continue to be biologically active, while the bulk undergoes conjugation to amino acids and sugars (Normanly et al., 2004; Woodward et al., 2005). Such conjugated forms of auxin are considered to be hormonally inactive and might serve as protection against oxidative degradation. The very intriguing property of biologically active auxin is its ability to influence many aspects of plant development, such as embryogenesis, all types of organogenesis, root meristem maintenance, vascular tissue differentiation, hypocotyl and root elongation, apical hook formation, apical dominance, fruit ripening, and tropic responses to light and gravity. Initiation of these developmental events is the final result of the directional intracellular auxin transport that leads to local auxin accumulation in the correct tissues and cells (Vieten et al., 2007).

The discovery of genes that are rapidly upregulated by auxin and identifying conserved auxin response element within their promoters allowed engineering highly auxin responsive synthetic promoters, known as DR5. This brought long awaited possibility of monitoring auxin distribution within the plant tissues (Figure 1; Sabatini et al., 1999; Friml et al., 2002b; Ottenschläger et al., 2003; Benková et al., 2003; Friml et al., 2003a). Nowadays, DR5-based reporters supported with other techniques as immunolocalisation with anti-IAA antibodies (Friml et al., 2003a) or direct measurements of auxin content (Casimiro et al., 2001; Marchant et al., 2002; Ljung et al., 2005) constitute reliable tool for indirect visualisation of endogenous auxin level, allowing gaining insight into the spatial and temporal pattern of auxin accumulation.

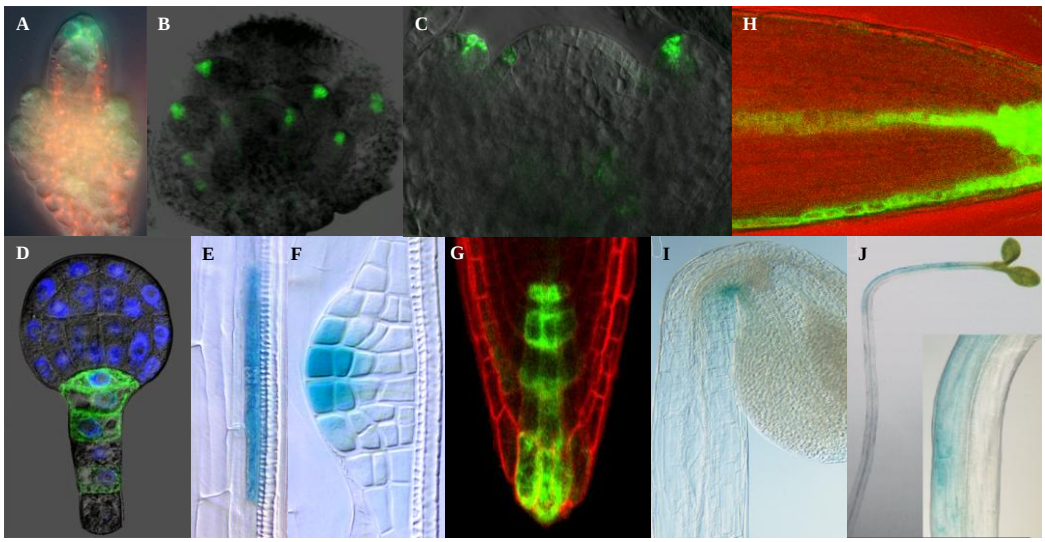

Figure 1. Examples of DR5-monitored local auxin distribution in *Arabidopsis*
(A) *DRrev::GFP* signals visible in the older ovule primordium.
(B) *DR5rev::GFP* signal in developing flowers.
(C) Accumulation of *DR5rev::GFP* signal at the position of incipient primordia in apical meristem.
(D) *DR5rev::GFP* signal in globular embryo.
(E and F) *DR5::GUS* activity gradient gradually established during lateral root primordium development.
(G) *DR5rev::GFP* in columella initial region of the primary root.
(H) *DR5rev::GFP* distributed asymmetrically at the lower side of root after a change in the gravity vector.
(I) Asymmetric expression of *DR5::GUS* in the apical hook of an etiolated seedling.
(J) *DR5::GUS* expression in hypocotyl of light stimulated seedling.

1.3 AUXIN TRANSPORT

Auxin is produced mainly locally in young, apical tissues, but is necessary for almost all the plants parts, suggesting the existence of an auxin transport (Morris et al., 2004). There are two pathways responsible for the redistribution of auxin throughout the plant body: a non-polar transport in phloem and a cell-to-cell polar auxin transport (PAT) in various tissues (Morris et al., 2004). Both transport pathways are connected, as radioactively-labeled auxin transported within the phloem could also be detected in the PAT system (Cambridge and Morris, 1996). Thus, auxin (mostly in conjugated form) together with other assimilates transported in the phloem sap are gradually unloaded to the different sink tissues from where it is further redistributed by a regulated, short-distance PAT.

This polar transport is a feature that is, among plant hormones, unique to auxin. The central characteristics of PAT are: it occurs in a cell-to-cell manner, requires energy, is relatively slow, saturable, and specific for active free auxins, and is sensitive to protein synthesis inhibitors (Friml et al., 2002c). This PAT is required for the formation of the local auxin gradient observed in different developmental processes in plants as mentioned above (Figure 1). Data obtained from manipulation of auxin-responsive promoter DR5 (Ulmasov et al., 1997), immunolocalization of IAA (Friml et al., 2003a), or direct auxin measurements in tissue sections (Casimiro et al., 2001; Marchant et al., 2002; Ljung et al., 2005) collectively suggested that PAT is required for dynamic changes in local homeostasis that occur during plant growth and development.

1.3.1 Chemiosmotic Hypothesis

The significant milestone in the studies on PAT and understanding its unidirectional character was formulation of chemiosmotic theory for polar auxin transport (Rubery and Sheldrake, 1974; Raven, 1975). The model proposed that in the fairly acidic environment of the cell wall (pH 5.5), part of IAA exists in its protonated form (IAAH). IAAH can enter cell by simple diffusion through the PM or be imported by auxin uptake carriers. In the more basic (pH 7.0) cytosolic environment, IAA became deprotonated, and the resulting polar IAA^- anions are largely membrane impermeable and require active efflux carriers to exit the cell (Figure 2). This unidirectional auxin flow can be determined by the proposed asymmetric placement of these auxin carriers at the PM. The chemiosmotic model was further supported by the identification of AUX1/LAX protein family (AUXIN RESISTANT 1/ LIKE

AUX) as candidate auxin influx carriers (Bennett et al., 1996; Yang et al. 2006; Swarup et al., 2008), PIN (PIN-FORMED) family as auxin efflux carriers (Luschnig et al., 1998; Petrášek et al., 2006), and PGP (MULTIDRUG RESISTANCE/P-GLYCOPROTEIN) class of ABC (ATP-binding cassette) protein as auxin transporters (Noh et al., 2001; Geisler et al., 2005; Bandyopadhyay et al., 2007). As the studies in this thesis focus on aspect of PAT mainly regarding auxin efflux carriers, the next paragraphs will focus on what is known about the controlling of the PIN polar targeting.

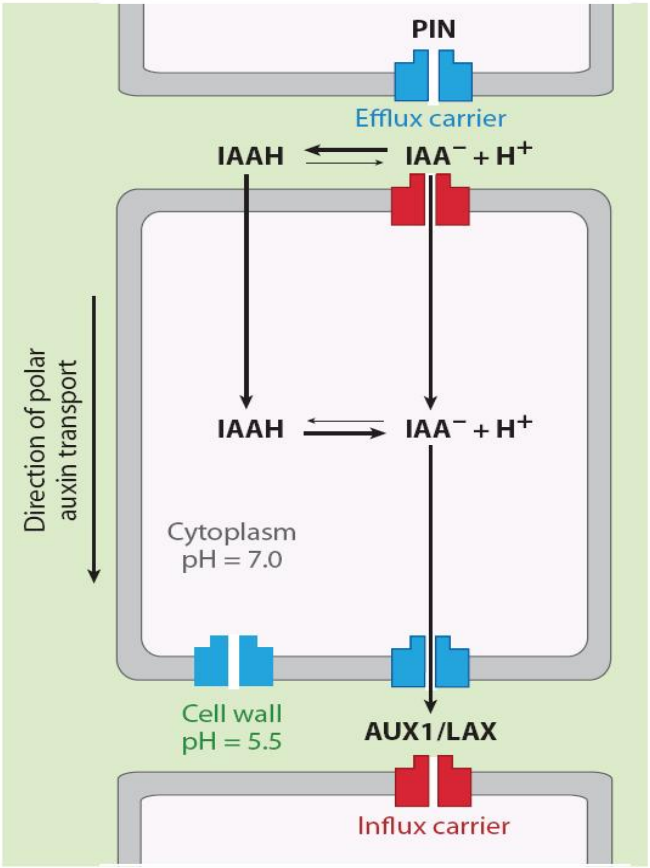

Figure 2. Mechanistic model for PAT based on the chemiosmotic hypothesis.
Figure is adapted from Kleine-Vehn et al., 2008..

1.4 AUXIN TRANSPORTER - EFFLUX CARRIER PIN PROTEINS

The PIN-FORMED (PIN) proteins have been identified and characterized as key regulators of polar auxin transport. The PIN family of *Arabidopsis thaliana* consists of eight members, most of which are polarly localized at the plasma membrane (PM) of the various cell types and act as efflux carriers (Petrášek et al., 2006). The PM localization is correlated and also required for the direction of the auxin flow (Wiśniewska et al., 2006). The first identified putative auxin efflux carrier was PIN1 protein (Gälweiler et al., 1998). The *pin-formed1* (*pin1*) mutant was defective in organ initiation and phyllotaxis, as visualized by needle-like inflorescence. Importantly, this strong defect could be mimicked by growing plants on PAT inhibitors (Okada et al., 1991). Moreover, *pin1* inflorescence showed a reduced basipetal auxin transport (Gälweiler et al., 1998). These data hinted at the involvement of PIN1 in the PAT, particularly, in the auxin efflux. Molecular analysis suggested that PIN1 encoded a plant-specific transmembrane protein sharing topological similarity to bacterial transporter carrier proteins (Gälweiler et al., 1998). The other PIN family proteins were designated after PIN1: PIN2/EIR1/AGR1 is required for root gravitropism (Chen et al., 1998; Luschnig et al., 1998; Müller et al., 1998; Utsuno et al., 1998); PIN3 for hypocotyl or root tropisms (Friml et al., 2002b); PIN4 for root meristem patterning (Friml et al., 2002a); and PIN7 for early embryo development (Friml et al., 2003a).

The asymmetric distribution of these PIN proteins at the PM is determined by the protein type,

cell type and developmental context as well. The polarities of PIN proteins correlate well with the direction of auxin transport and also with the local accumulation in adjacent cells (Vieten et al., 2007). The PIN1 protein is basally localized (towards the root tip) in the vascular tissues of embryos, leaves, and roots (Figure 3A and 3E), whereas they are apically localized (towards the shoot apex) in the epidermis of shoot apices, embryos, and gynoecia (Gälweiler et al, 1998; Benková et al, 2003; Reinhardt et al, 2003; Friml et al, 2003b; Sorefan et al, 2009). PIN2 shows an apical localization in the lateral root cap and root epidermis cells, but is basal in the root cortex cells (Figure 3B and 3E; Müller et al, 1998; Friml et al, 2003a). PIN3, PIN4, and PIN7 are also polarly localized in specific tissues or organs, such as the predominant lateralization of PIN3 at the inner side of shoot endodermis cells (Friml et al, 2002b; Zádníková et al, 2010); the basalization of PIN4 in the central root meristem (Figure 3D and 3E; Friml et al, 2002a); and the apicalization of PIN7 in the basal cells of the zygote and basalization in the basal cells and suspensors at the globular stage (Friml et al, 2003a).

Based on the topology predication and protein structure, PIN5, PIN6 and PIN8 seem to be more distantly related to these PM localized PIN proteins, because of the reduced central hydrophilic loop. Indeed, these proteins have been shown to be localized to the endoplasmic reticulum (ER) and are presumably involved in the regulation of auxin homeostasis by controlling the auxin exchange between the ER and the cytosol (Mravec et al., 2009).

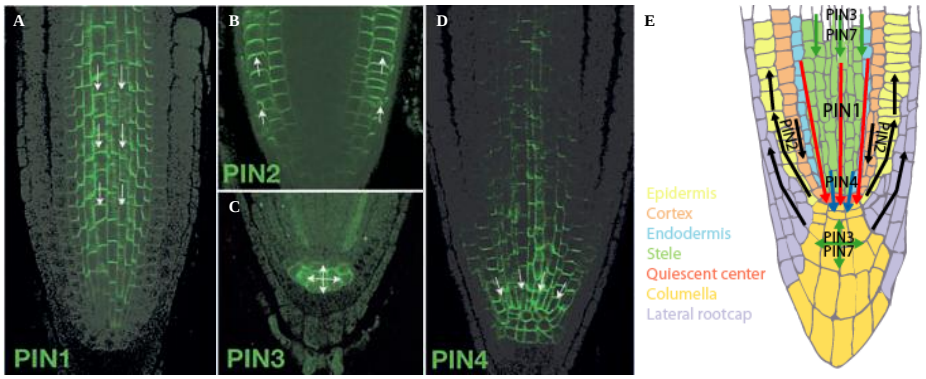

Figure 3. Polar localization of PIN proteins in the *Arabidopsis* root tip.
(A-D) Immunolocalization of PIN proteins: PIN1 is localized at the basal (root apex-facing) side of the root vasculature (A); PIN2 at the basal side of the cortical cells and at the apical (shoot apex-facing) side of the epidermal and root cap cells (B); PIN3 in an apolar manner in the columella cells of the root (C); and PIN4 at the basal side of cells in the central root meristem and with less pronounced polarity in the cells of the quiescent center.
(E) Schematic pattern showing different PIN protein localizations.
Arrows indicate polar PIN localization at the plasma membrane; Figures are adapted from Dhonukshe et al., 2005 and Tanaka et al., 2006.

1.5 CONTROL OF THE PIN POLAR TARGETING

The PIN polar localizations direct the auxin flow and ultimately modify the developmental program of the given tissues or organs in plants. Thus, the mechanisms underlying the establishment and maintenance of the PIN polarity belong to the important themes of developmental and cell biology. The PIN proteins are very dynamic inside the cells (Geldner et al., 2001) and their regulations seem to be extremely complex (Tanaka et al., 2006), namely developmental and environmental signals (Friml et al., 2002b; Benková et al., 2003; Friml et al., 2003a), vesicle trafficking (Geldner et al., 2001, 2003; Dhonukshe et al., 2007, 2008; Kleine-vehn et al., 2008a), and post-translational modulations phosphorylation and ubiquitination (Friml et al., 2004; Abas et al., 2006; Michniewicz et al., 2007) can regulate PIN targeting at the different levels.

1.5.1 Cell Type-Based Determinants

One of the main determinants of PIN polarity is cell type: a single PIN can localize to opposite cell sides depending on the cell type where it is expressed. For instance, PIN2 is localized at the apical side of epidermis cells, whereas it localizes to the basal side of cortex cells (Müller et al., 1998). Similarly, PIN1 is localized at the basal side of vascular cells, but at the apical side of outer cells in the shoot apical meristem (Benková et al., 2003; Reinhardt et al., 2003; Tanaka et al., 2006). Thus, it seems that

the PIN polarity is regulated by some, yet unknown, tissue-specific determinants.

1.5.2 PIN Sequence-Based Determinants

Another main determinant of PIN polarity is encrypted in their amino acid sequences. As different PINs expressed in the same tissue can have different subcellular localizations. For instance, ectopically expressed PIN1 in the epidermis preferentially localizes to the basal cell side, while endogenous PIN2 stays at the apical side of epidermal cells (Wiśniewska et al., 2006). Moreover, insertion of GFP at a specific position in the PIN1 protein sequence causes apical PIN1 localization in epidermal cells. These data demonstrate the existence of specific signals encoded within PIN amino acid sequence to determine PIN polar targeting. The polarity determinant signals are probably related to phosphorylation sites within the PIN proteins (Huang et al., 2010; Zhang et al., 2010), which will be discussed later in this thesis.

1.5.3 Developmental and Environmental Modulations

The modulation of the PIN polar targeting also depends on developmental signals. During early embryogenesis, PIN7 is distributed at the apical side of the suspensor cells and PIN1 is expressed in a non-polar manner in the proembryo. Later on, PIN7 changes its localization to the basal side of the suspensor cells, while PIN1 also polarizes at the basal side of provascular cells (Friml et al., 2003a; Weijers et al., 2005). Such PIN polarity shifts promote the formation of auxin gradients at the lower side of the embryo, establishing the future root pole and thus embryonic axis. Similar cellular relocations happen during postembryonic organogenesis as well, such as during inflorescence development, lateral root formation and phyllotaxis. In these examples, establishment of auxin accumulation in the specific cells trigger subsequent organ formation and positioning (Benková et al., 2003; Reinhardt et al., 2003; Heisler et al., 2005). These processes might involve a feedback between the auxin content of a cell or tissue and the regulation of the directional auxin flow as a means to polarize tissues (Sachs, 1981). This self-regulating mechanism was first described for leaf vascular patterning and conceptually summarized in the canalization hypothesis by Sachs (1981). Only recently, molecular proof of the canalization hypothesis was reflected in dynamic rearrangements of the PIN polarity during leaf vascular pattern formation (Scarpella et al., 2006) and vascular tissue regeneration after wounding (Sauer et al., 2006a). Importantly, auxin was found to influence directly its own transport by modulation of the intracellular PIN trafficking. Recently, it was found that auxin has the capacity to inhibit clathrin-dependent endocytosis (Paciorek et al., 2005; Robert et al., 2010). Thus, through inhibition of the PIN endocytosis auxin could increase the PIN levels at the PM and thus directly stimulates the auxin itself efflux from cells. These feedback regulations of the PIN polarity by auxin itself could occur during multiple regenerative and patterning processes in plants.

Besides changes in the PIN polarity in response to internal signals, switches of the PIN polarity can occur also in response to environmental stimuli. PIN3 is non-polarly distributed in the collumela cells, which contain gravity-sensing statolithes. During gravistimulation, PIN3 follows the sedimenting statolithes and rapidly relocates to the basal side of the same cells, redirecting auxin flow to the new lower side of the root (Friml et al., 2002c). Accumulated auxin further translocated basipetally to the responsive cells in the elongation zone by concerted action of AUX1 (auxin influx carrier) and PIN2 (Müller et al., 1998; Luschnig et al., 1998; Swarup et al., 2001; Swarup et al., 2005). Furthermore, PIN2 gets more stabilized in the cells at the new lower side of the root, internalized, and apparently degraded in cells at the new upper side. During this step, the originally established auxin asymmetry is further enforced by an asymmetric expression of PIN2 along the basipetal route (Abas et al., 2006).

1.5.4 Trafficking Mechanisms

Polarized epithelial cells provide a model system for analyzing the cell polarity in mammalian cells. Intensive research has suggested that PM-destined proteins are first synthesized in the ER and later on sorted into specialized carrier vesicles that deliver the cargo to one particular polar domain (Dhonukshe, 2009). In contrast to mammalian cells, plants seem to utilize a non-polar secretion mode. Recently, the studies of Dhonukshe (2008) identified an endocytosis-dependent, two-step mechanism for the PIN polarity generation at PM. The PIN proteins are first targeted to the PM without apparent asymmetry, and then attain polarity by subsequent endocytic recycling (Dhonukshe et al., 2008). Therefore, the secretion step, endocytic step, and subsequent recycling steps are crucial for the polarity

establishment.

The pathway of polar localization and recycling involves the function of GNOM, encoding a brefeldin A (BFA)-sensitive guanine nucleotide exchange factor (GEF) for ARF GTPases that regulate vesicle formation (Shevell et al., 1994; Geldner et al., 2001). The first hint towards the involvement of vesicular trafficking in PIN polar localization came from the analysis of the *gnom* mutants that displayed an impaired PIN1 polar localization in embryos and eventually led to misshaping of the whole embryo architecture (Mayer et al., 1991; Steinmann et al., 1999). Pharmacological interference of the GNOM function by BFA treatments leads to depletion of PIN1 from the PM and to strong internalization in so-called "BFA compartments" (Geldner et al., 2001). The utilization of *gnom* knockout mutants, a transgenic line expressing a BFA-resistant mutant $GNOM^{M696L}$, demonstrated that GNOM is the entry point for intracellular sorting and recycling of PIN1 to the PM (Geldner et al., 2003). Moreover, GNOM seems to be more crucial for basal polar targeting, because the apical PM localization of PIN proteins and AUX1 is not strongly affected when GNOM function is inhibited (Geldner et al., 2003; Kleine-Vehn et al., 2008a). Hence, the involvement of GNOM in basal versus apical targeting differs substantially. GNOM preferentially regulates the PIN cycling to the basal PM, whereas apically targeted PIN proteins might be controlled by another, BFA-resistant, ARF GEF (Kleine-Vehn et al., 2008a).

In the presence of the phosphatidylinositol-3-kinase (PI3K) inhibitor wortmannin, PIN2 accumulates in a compartment that is different from GNOM-containing BFA compartment. This compartment is defined by the localization of SORTING NEXIN1 (SNX1) (Jaillais et al., 2006). Pharmacological or genetic interferences with the SNX1 compartment do not affect the PIN polarity, but preferentially alter the vacuolar sorting of the PIN proteins (Kleine-Vehn et al., 2008c). Following gravitistimulation, the PIN2 localization in the SNX1 compartment is enhanced, which is consistent with enhanced vacuolar targeting and degradation of PIN2 (Abas et al., 2006; Kleine-Vehn et al., 2008c). SNX1 orthologs are retromer components that assure the retrieval of vacuolar receptors back from the provascular compartment (PVC) to the trans-Golgi network (TGN) in yeast and mammalian system (Seaman, 2005). In plants, a putative plant retromer component VACUOLAR PROTEIN SORTING29 (VPS29) is colocalized with SNX1 at the PVC (Oliviusson et al 2006; Jaillais et al., 2008). VPS29 functions in the regulation of size of SNX1-containing endosomes, indicating that SNX1 and VPS29 form a functional complex. Compared with the *snx1* mutant, polarity defects were observed not only in PIN2, but also in PIN1 in the *vps29* mutant. In the stele cells of the main root, although the PIN1 polar localization is not severely defected, additional accumulation of PIN1 in abnormal intracellular compartments is rather pronounced. In lateral root initial cells, the PIN1 protein is assembled into enlarged SNX1 compartments (Jaillais et al., 2007). These phenotypes observed for *snx1* and *vps29* might be explained by the enhanced vacuolar targeting of PIN proteins (Kleine-Vehn et al., 2008c). Thus, retromer-dependent endosomal trafficking specifically regulates repolarization of the PIN proteins.

1.5.5 Sterol Composition

Localization of PIN proteins seems to depend also on the sterol composition of plasma membranes (Willemsen et al., 2003; Grebe et al., 2003). The Arabidopsis mutant *orc* with mutation in the *STEROL METHYLTRANSFERASE1* (*SMT1*) gene that is involved in membrane sterol biosynthesis shows defects in meristem patterning, cell polarity and auxin distribution in the main root tip (Willemsen et al., 2003). Together with data that the sterol-specific dye filipin labels the intracellular route of PIN2 (Grebe et al., 2003), a connection between the sterol membrane composition and the PIN proper localization is suggested. In mammalian systems, detergent-resistant microdomains (DRMs) (also called lipid rafts) have functions of trafficking different PM cargos. A proteomic analysis of the DRM fraction in plants shows that many plant proteins are associated with DRM (Morel et al., 2006), supporting the involvement of membrane sterol in controlling the PIN targeting.

1.5.6 Reversible Protein Phosphorylation

PIN phosphorylation is an important mean for the PIN polar targeting. Decision about delivery of PIN proteins to the proper cell side is regulated through the antagonistic action of the protein kinase PID and protein phosphatase PP2A (Friml et al., 2004; Michniewicz et al., 2007): phosphorylation leads to a preferentially apical PIN localization, whereas dephosphorylation results in a basal PIN targeting.

The first assumption connecting PID activity with the PAT was based on the observation that the *pid* mutant showed phenotypes similar to those of the *pin1* mutant (Bennett et al., 1995). The *pid*

mutant often develops aberrant numbers of cotyledons at the seedling stage, whereas as an adult plant it produces characteristic needle-like inflorescence and occasionally forms aberrant flowers. This inflorescence phenotype is similar to that of wild-type plants treated with auxin efflux inhibitors (Okada et al., 1991; Bennett et al., 1995; Christensen et al., 2000). Moreover, the auxin transport in the inflorescence of the *pid* mutants is also reduced, although less pronounced than that of the *pin1* (Bennett et al., 1995). Cloning of the *PID* gene revealed that it encoded a plant-specific serine/threonine protein kinase (Christensen et al., 2000). Interestingly, phenotypes of PID gain-of-function allele *35S::PID* were found to be consistent with the disruption of the auxin transport or auxin signaling. Adult plants of *35S::PID* have small, crinkled leaves, reduced apical dominance, and tiny flowers. *35S::PID* seedlings show severe root defects, illustrated by agravitropic growth, primary root collapse, and significantly reduced auxin levels, which can be rescued by exogenous application of auxin efflux inhibitors (Christensen et al., 2000; Benjamins et al., 2001; Friml et al., 2004). All these observed root phenotypes can be explained by the switched polar localizations of PIN1, PIN2, and PIN4. In cells where these proteins normally localize to the basal side, the majority of the proteins is found instead at the opposite apical side (Friml et al., 2004). Importantly, these polarity shifts occur within a few hours after the onset of the increased PID activity, indicating a direct regulation of PID on the PIN polarity. Consistently, in the cotyledons and apices of the *pid* mutant, the PIN localization is switched from the apical to the basal side, explaining the defects in organogenesis of the mutant (Friml et al., 2004).

One of the indications hinting at the involvement of protein dephosphorylation events in the auxin transport came from the analysis of the mutant *rcn1* (*ROOT CURL ON NPA*). *RCN1* was identified in a screen for mutants that maintain root curling in the presence of the auxin efflux inhibitor, *N*-1-naphthylphthalamic acid (NPA) (Garbers et al., 1996). The mutant has phenotypes in apical hook formation, etiolated hypocotyl elongation as well as root elongation and gravity response, which are all PAT-related defects (Garbers et al., 1996). The *RCN1* gene encodes a regulatory A subunit of the trimeric protein phosphatase 2A (PP2A) (Garbers et al., 1996). Further investigation of the *rcn1* mutant showed an increased basipetal auxin transport in the root tip, probably explaining the defects in the roots gravity responses (Rashotte et al., 2001). Importantly, all these defects in the *rcn1* mutant can be phenocopied by treatments with the phosphatase-specific inhibitor, cantharidin (Rashotte et al., 2001). Later on, characterization of two RCN1 paralogs, PP2AA2 and PP2AA3 revealed that they do not act as strong positive regulators of the PP2A activity, while their specific roles are unmasked only when the RCN1 function is abolished (Zhou et al., 2004). Nevertheless, double mutant combinations that include the *rcn1* allele show strong auxin-related developmental defects in root growth and cotyledon formation (Zhou et al., 2004). This role of the PP2A phosphatase in regulation of the PAT is confirmed by further characterization that shows that PP2A acts antagonistically with PID on the decision about the PIN protein delivery (Michniewicz et al., 2007). For a detailed discussion, see Chapter 2.

CHAPTER 2

Antagonistic Regulation of PIN Phosphorylation by PP2A and PINOID Directs Auxin Flux

Marta Michniewicz, Marcelo K. Zago, Lindy Abas, Dolf Weijers, Alois Schweighofer, Irute Meskiene, Marcus G. Heisler, Carolyn Ohno, **Jing Zhang,** Fang Huang, Rebecca Schwab, Detlef Weigel, Elliot M. Meyerowitz, Christian Luschnig, Remko Offringa, and Jiří Friml

Modified from Michniewicz et al., (2007) Cell *130*, 1044-1056

Author's Contributions: JZ performed experiments presented in Figure 5G-I.

ABSTRACT

In plants, cell polarity and tissue patterning are connected by intracellular flow of the phyto-hormone auxin, whose directional signaling depends on polar subcellular localization of PIN auxin transport proteins. The mechanism of polar targeting of PINs or other cargos in plants is largely unidentified, with the PINOID kinase being the only known molecular component. Here, we identify PP2A phosphatase as an important regulator of PIN apical-basal targeting and auxin distribution. Genetic analysis, localization, and phosphorylation studies demonstrate that PP2A and PINOID both partially colocalize with PINs and act antagonistically on the phosphorylation state of their central hydrophilic loop, hence mediating PIN apical-basal polar targeting. Thus, in plants, polar sorting by the reversible phosphorylation of cargos allows for their conditional delivery to specific intracellular destinations. In the case of PIN proteins, this mechanism enables switches in the direction of intracellular auxin fluxes, which mediate differential growth, tissue patterning, and organogenesis.

INTRODUCTION

Polarity is one of the elementary properties of eukaryotic cells and is inseparable from other fundamental processes such as division, differentiation, and cellular signaling. The intimate relation between cell polarity and patterning is particularly prominent in plants, since even fully differentiated cells often retain the potential to redefine their polarity, enabling crucial adaptation processes such as directional growth, tissue regeneration or de novo organ formation (Sauer et al., 2006a). The molecular mechanisms of polarized cargo traffic are conserved from yeast to humans and have been extensively characterized in animal epithelial cells, which exhibit a clearly discernible asymmetry between the apical and the basolateral plasma membrane domains (Mostov et al., 2003).

Substantially less is known about the mechanism(s) of cell polarity establishment in plants. Much of our knowledge has been acquired by studying the asymmetric targeting of plant-specific plasma membrane-resident PIN proteins, which show distinct polar subcellular localizations. PIN proteins have emerged as key regulators of a plethora of developmental processes including axis formation in embryogenesis (Friml et al., 2003a), postembryonic organogenesis (Okada et al., 1991; Benková, et al., 2003; Reinhardt et al., 2003), root meristem organization (Friml et al., 2002a; Blilou et al., 2005) and tropisms (Luschnig et al., 1998; Friml et al., 2002b). PIN proteins facilitate the polar efflux of the plant growth regulator auxin from cells (Petrášek et al., 2006) and their polar localization determines the direction of local intracellular auxin transport (Wiśniewska et al., 2006).

Distinct polar localizations of PIN proteins in different cell types depend on so far unidentified cell type-specific and PIN sequence-based signals (Wiśniewska et al., 2006). Furthermore, PIN localization can be modulated by environmental (e.g., gravity) or developmental cues (Friml et al., 2002b, 2003; Benková, et al., 2003; Reinhard et al., 2003; Scarpella et al., 2006). The rapid retargeting of PINs to different polar domains is possibly related to the constitutive endocytosis and recycling of PIN proteins (Dhonukshe et al., 2007). Such flexible regulation of PIN polarity provides a way to integrate multiple signals at the level of single cells, translating them into intracellular auxin fluxes, relevant for diverse developmental processes (reviewed in Friml, 2003).

Despite the importance of PIN polarity control for plant development, the underlying mechanisms are still not well understood. Genetic and pharmacological studies have indicated involvement of (de)phosphorylation processes in regulation of PIN-dependent auxin transport (Garbers et al., 1996; Benjamins et al., 2001; Friml et al., 2004; Shin et al., 2005). The protein serine/threonine (Ser/Thr) kinase PINOID (Christensen et al., 2000; Benjamins et al., 2001) is the only as yet identified molecular component directly involved in the regulation of polar delivery of PIN proteins. Loss of PINOID (PID) function causes an apical-to-basal shift in PIN polarity, correlating with defects in embryo and shoot organogenesis. On the other hand, PID gain-of-function results in an opposite basal-to-apical PIN polarity shift, which leads to auxin depletion from the root meristem, ultimately leading to its collapse (Friml et al., 2004). These results indicate that PID-dependent phosphorylation leads to preferentially apical PIN localization, whereas low phosphorylation levels result in basal PIN targeting. In such a scenario, reversible phosphorylation of components of the apical versus the basal targeting machinery could regulate their activities, which are decisive for polar targeting of membrane proteins. Alternatively, direct phosphorylation of cargo proteins, such as PINs, could determine their intracellular targeting.

Here, we identify a phosphatase activity required for apical-basal PIN targeting and auxin transport-dependent development. We show that protein phosphatase 2A (PP2A) and PID act

antagonistically on phosphorylation of PIN proteins. Our findings demonstrate that decisions about apical or basal targeting in plants require reversible phosphorylation of cargo proteins.

RESULTS

PP2AAs Are Required for Auxin-Related Seedling Development

To identify a possible phosphatase component of the mechanism responsible for PIN polar targeting, we analyzed the three closely related regulatory A subunits of the protein phosphatase 2A (PP2A) complex in *Arabidopsis* - *PP2AA1*, *PP2AA2* and *PP2AA3*. We focused preferentially on the PP2A class since a loss-of-function mutation in one of the A regulatory subunits (PP2AA1), called ROOT CURLING ON NPA1 (RCN1) causes various developmental defects, some of which are in processes governed by auxin transport (Garbers et al., 1996; Rashotte et al., 2001). We analyzed the expression pattern of *PP2AA* genes using *PP2AA1::GUS*, *PP2AA2::GUS*, *PP2AA3::GUS* and *PP2AA1::PP2AA1:GFP* fusions. Analysis of seedlings 4 and 8 days after germination revealed high and overlapping transcriptional activity for all three genes (Figures S1A-S1D). In the root, *PP2AA1* was expressed in the whole root tip, *PP2AA2* prominently in the elongation zone and columella root cap, and *PP2AA3* more restricted to the columella root cap (Figure 1A). These overlapping expression patterns of *PP2AAs* have been confirmed by analysis of global transcription data (http://www.weigelworld.org/resources/microarray/AtGenExpress) and are in accordance with previous reports (Zhou et al., 2004).

To test the requirement of PP2AA activities for plant development, we isolated and analyzed phenotypes of *pp2aa1*, *pp2aa2* and *pp2aa3* double and triple mutant combinations. In line with previous observations (Zhou et al., 2004), the *pp2aa2* and *pp2aa3* single mutants, and *pp2aa2 pp2aa3* double mutants showed largely normal development (data not shown), but double-mutant combinations that included the *pp2aa1* suffered from increasingly severe developmental aberrations (Figure 1B). Both *pp2aa1 pp2aa2/+* and *pp2aa1 pp2aa3/+* mutants displayed defects in root growth and root gravity response (n = 90) (Figures S2A and S2B). Also homozygous seedlings for *pp2aa1 pp2aa2* and *pp2aa1 pp2aa3* showed identical but more severe defects (Figures S2A and 1C). Primary root meristems typically collapsed at 6-8 day (76% for *pp2aa1 pp2aa2*, n=40; 80% for *pp2aa1 pp2aa3*, n = 50) as evident from the disturbance of proper patterning and lack of columella-specific lugol staining (Figure 1L). During subsequent development, initiation of numerous lateral roots substituted for a defective primary root (Figure 1D). About 30% (n = 90) of *pp2aa1*-containing double-mutant seedlings showed defects in cotyledon development. These included collar-shaped or fused cotyledons (10%) as well as aberrant positioning and irregular numbers of cotyledons (19%) (Zhou et al., 2004; Figure 1C). Because *pp2aa1 pp2aa2 pp2aa3* triple mutant seedlings were not recovered among progeny of pp2aa1 pp2aa2 pp2aa3/+ plants (n = 87), we constructed transgenic lines with estrogen (4-hydroxytamoxifen)-inducible overexpression of two different artificial microRNAs (amiRNAs) (Schwab et al., 2006) that simultaneously target all three *PP2AA* genes. In both amiRNA lines, we observed identical defects that were similar to but more severe than the phenotypes observed in *pp2aa1* double mutants. These included root and cotyledon defects (Figure 1E), which resembled phenotypes seen in mutants compromised in auxin signaling (*monopteros*, Hardtke and Berleth, 1998) or auxin transport (*pins*, Friml et al., 2003). Functional primary and lateral root meristems were not established (n = 120), causing arrest of further growth at the seedling stage (Figure 1E).

These results extend previous findings (Zhou et al., 2004) that PP2A activity (as assessed by downregulation of its regulatory A subunits) is important for seedling development. Importantly, our additional analysis highlighted that some features of loss of PP2AA function phenotypes including root agravitropism, cotyledon defects and root meristem collapse resemble auxin transport-related defects (reviewed in Friml, 2003) and in particular gain-of-function PID Ser/Thr kinase phenotypes (*35S::PID*, Benjamins et al., 2001; Friml et al., 2004).

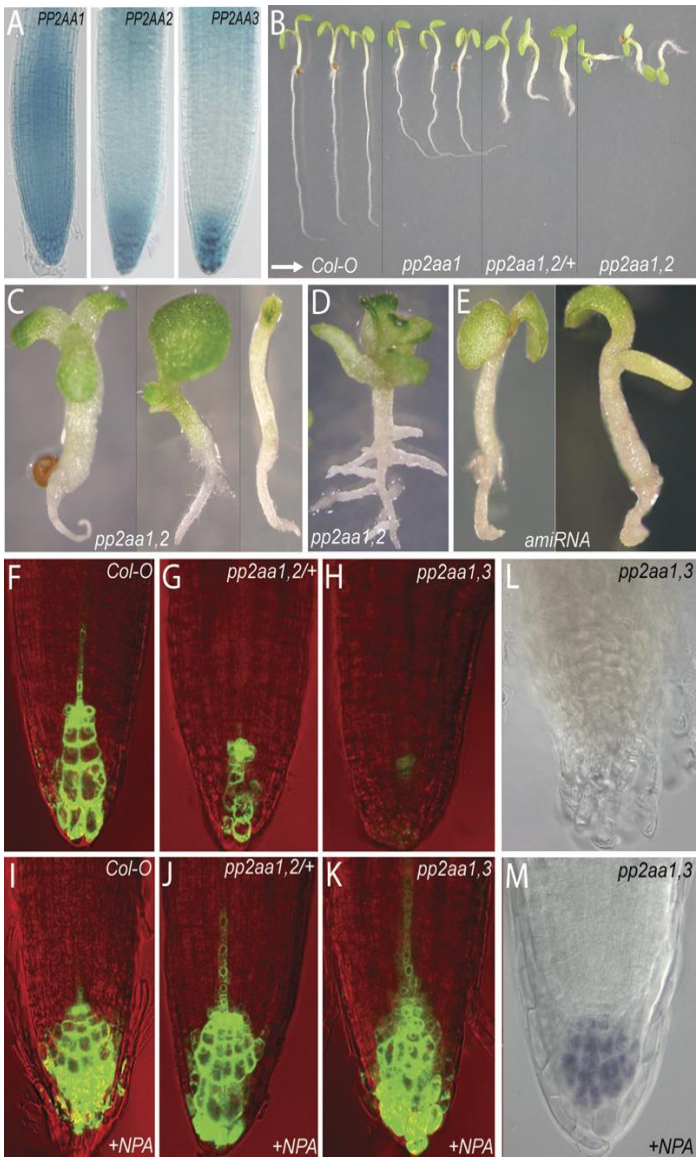

Figure 1. Expression and Developmental Roles of PP2AAs during Seedling Development
(A) GUS staining shows overlapping expression patterns of *PP2AA1::GUS*, *PP2AA2::GUS* and *PP2AA3::GUS* in primary roots.
(B) Increasingly stronger defects of *pp2aa1*, *pp2aa1 pp2aa2/+*, *pp2aa1 pp2aa2* seedlings include impaired gravity response and defects in primary root growth. Arrow indicates new gravity vector.
(C and D) Phenotypes of 4-day-old *pp2aa1 pp2aa2* seedlings: strong primary root defects, aberrant cotyledon number, fused cotyledons, and no cotyledons (C). No primary root growth but excessive lateral root development in 14- day-old seedlings (D).
(E) Strong developmental defects in two independent amiRNA, which target all three PP2AAs.
(F-H) Reduced *DR5rev::GFP* expression in *pp2aa1 pp2aa2/+* (G) and *pp2aa1 pp2aa3* (H) root tips as compared to wild-type (F).
(I-K) Restoration of *DR5rev::GFP* expression in the *pp2aa1 pp2aa2/+* (J) and *pp2aa1 pp2aa3* (K) following auxin transport inhibition by NPA. (L and M) Collapse of root meristem in *pp2aa1 pp2aa3* (L) and its restoration following NPA treatment (M) reflected by absence (L) and presence (M) of columella cells as visualized by lugol staining.

PP2AAs Are Required for Auxin-Related Embryo Development

The pronounced seedling patterning defects in *pp2aa* loss-of-function mutants suggested that PP2A activity is already required during embryo development. Analysis of *PP2AA1,2,3::GUS* embryos revealed transcriptional activity of all three genes from the 8-cell-stage onward. *PP2AA1::GUS* and *PP2AA1::PP2AA1:GFP* reporters showed strong expression throughout the whole embryo (Figures 2A and 2B). Expression of the *PP2AA2::GUS* was similar but slightly weaker and *PP2AA3::GUS* was

only weakly detectable (data not shown).

Next, we analyzed the development of mutant embryos from *pp2aa1 pp2aa2/+* and *pp2aa1 pp2aa3/+* plants. These embryos showed identical strong developmental aberrations as early as at the preglobular stages (Figures 2D-2I). Affected embryos (70%, n = 80) displayed a range of defects, including root pole (68%) and cotyledon (36%) misspecifications (Figures 2G and 2H). The most severe cases were characterized by embryos lacking a clearly defined apical-basal axis (3%) (Figure 2I). All these embryonic phenotypes resemble those of embryos with defects in auxin transport (Friml et al., 2003), or those observed in PID gain-of-function embryos (*RPS5A* > > *PID*; Friml et al., 2004).

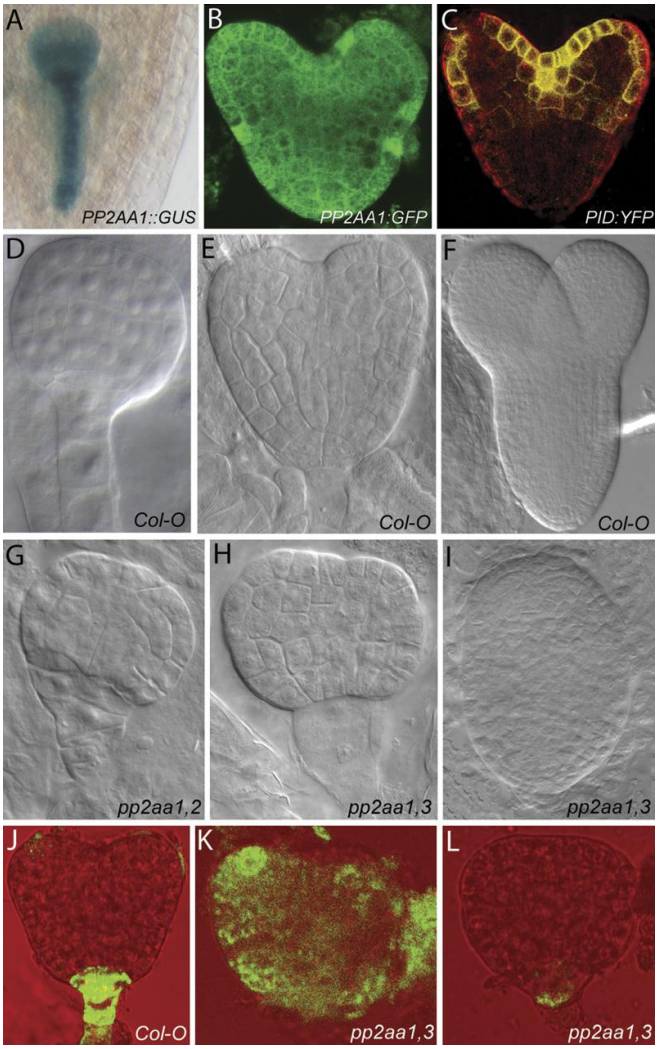

Figure 2. Expression and Developmental Roles of PP2AAs during Embryo Deveopment
(A) *PP2AA1::GUS* expression in globular stage embryo.
(B and C) Localization of PP2AA1 (*PP2AA1:: PP2AA1: GFP*) (B) and PID (*PID:: PID: YFP*) (C) proteins in heart stage embryos.
(D-I) Embryonic defects of *pp2aa1 pp2aa2* (G) or *pp2aa1 pp2aa3* (H and I) with failure of root pole and cotyledon specification. Wild-type control (D-F).
(J-L) *DR5rev::GFP* auxin activity gradients in wild-type (J) and *pp2aa1 pp2aa3* (K and L) embryos; mislocalized (K) or strongly reduced (L) DR5 signals.

PP2AAs Are Required for Asymmetric Auxin Distribution in the Embryo and Seedling Root

Several of the phenotype features in *pp2aa* loss-of -function embryos and seedlings suggested defects in auxin transport-related processes as an underlying cause. To test this hypothesis, we analyzed local auxin distributions in *pp2aa* mutant backgrounds using a reporter system based on the synthetic auxin-responsive promoter *DR5* (Ulmasov et al., 1997), which can be employed for the in planta visualization of auxin activity gradients (Sabatini et al., 1999; Friml et al., 2003; Benková et al., 2003;

reviewed in Friml, 2003). In globular and post-globular wild-type embryos, strong *DR5* activity can be seen at the root pole (Figure 2J) and at later stages at tips of developing cotyledons (Friml et al., 2003). In embryos excised from *DR5rev::GFP pp2aa2/+* and *DR5rev::GFP pp2aa1 pp2aa3/+* plants, we still observed the correct pattern of *DR5* activity in about one-half of the analyzed embryos (56%, n = 80), but with reduced signal intensity (Figure 2L). In some embryos (18%), the *DR5* activity maximum was misplaced (Figure 2K) whereas in others (26%) it was not detectable at all (data not shown).

Next we examined the *DR5* activity pattern in roots (Figures 1F-1H). We analyzed young (2.5 day) *pp2aa* seedlings well before the collapse of the root meristem. In *pp2aa1 pp2aa2/+* (Figure 1G) and *pp2aa1 pp2aa3/+* (data not shown) root tips, the *DR5* signal was strongly decreased. This reduction was even more pronounced in *pp2aa1 pp2aa2* (data not shown) and *pp2aa1 pp2aa3* (Figure 1H) double homozygous mutants. 53% (n = 40) of these roots showed strongly reduced *DR5* intensity and in 20% the *DR5* signal was not detectable at all.

The observed changes in *DR5* activity could be either due to alterations in auxin response or auxin distribution. To address this question, we treated *pp2aa1 pp2aa2* and *pp2aa1 pp2aa3* roots with the synthetic auxin 2,4-dichlorophenoxyacetic acid (2,4-D) or the auxin transport inhibitor 1-N-naphthylphthalamic acid (NPA). 2,4-D caused a comparable induction of DR5 in both wild-type and mutant roots, suggesting that auxin response is unaffected (Figures S2G-S2J). Notably, NPA did rescue the decrease in the DR5 expression and the root meristem collapse of the *pp2aa1* double mutants (Figures 1F-1M), as previously observed for *35S::PID* seedlings (Figures 3A, 3F, and 3G; Benjamins et al., 2001), indicating that the mutants are affected in auxin transport. To substantiate these observations, we assessed a possible defect in auxin transport of *pp2aa* mutants by monitoring auxin redistribution during gravity response. It is well established that the root gravitropic response is mediated by transport-dependent redistribution of auxin to the lower side of the responding root tip (e.g., Luschnig et al., 1998). In contrast to wild-type roots, which all responded (100%, n = 25), only about 23% of *pp2aa1 pp2aa2/+* and *pp2aa1 pp2aa3/+* roots (total n = 48) showed weak relocation of the *DR5* signal following gravistimulation (Figures S2C-S2F; not shown).

In Summary, these data suggest that PP2A activity is required for transport-dependent auxin distribution in embryos and seedling roots.

PP2AA Acts Antagonistically to PINOID on Seedling Development

The same phenotypes as those caused by loss of PP2AA function, including embryo patterning defects, agravitropic root growth and decreased *DR5* activity in roots followed by meristem collapse have also been observed in PID kinase gain-of-function seedlings (Benjamins et al., 2001; Friml et al., 2004).

To test for genetic interactions between PID and PP2A, we introduced PID gain- and loss-of-function alleles (*35S::PID* and *pid*, respectively) into the *pp2aa1 pp2aa3* background. *pp2aa1 pp2aa3 35S::PID* seedlings showed more severe phenotypes than either parental line (Figures 3B and 3C). Typically, the primary root meristem of *35S::PID* seedlings collapses followed by essentially normal lateral root development (Benjamins et al., 2001). In contrast, *pp2aa1 pp2aa3 35S::PID* plants (n = 36) failed to establish lateral root meristems and arrested growth as seedlings (Figures 3B and 3C). These defects were similar to those observed in amiRNA lines (see Figure 1E), in which all three *PP2AA* genes are downregulated. Conversely, the *pid* mutation partially suppressed *pp2aa1 pp2aa3* double-mutant phenotypes. In *pp2aa1 pp2aa3 pid* mutant seedlings (n = 20), defects in root growth and root meristem maintenance, that are seen in *pp2aa1 pp2aa3* double mutants, were rescued (Figures 3E and 3H). Nonetheless, additive phenotypes were observed in *pp2aa1 pp2aa3 pid* inflorescence axes (Figure 3D), suggesting additional, divergent roles of PID and PP2AA at later stages of above-ground development.

Taken together, our genetic analysis strongly suggests that PP2AA Ser/Thr phosphatases and PID Ser/Thr kinase represent antagonistically acting regulators of embryo and root development.

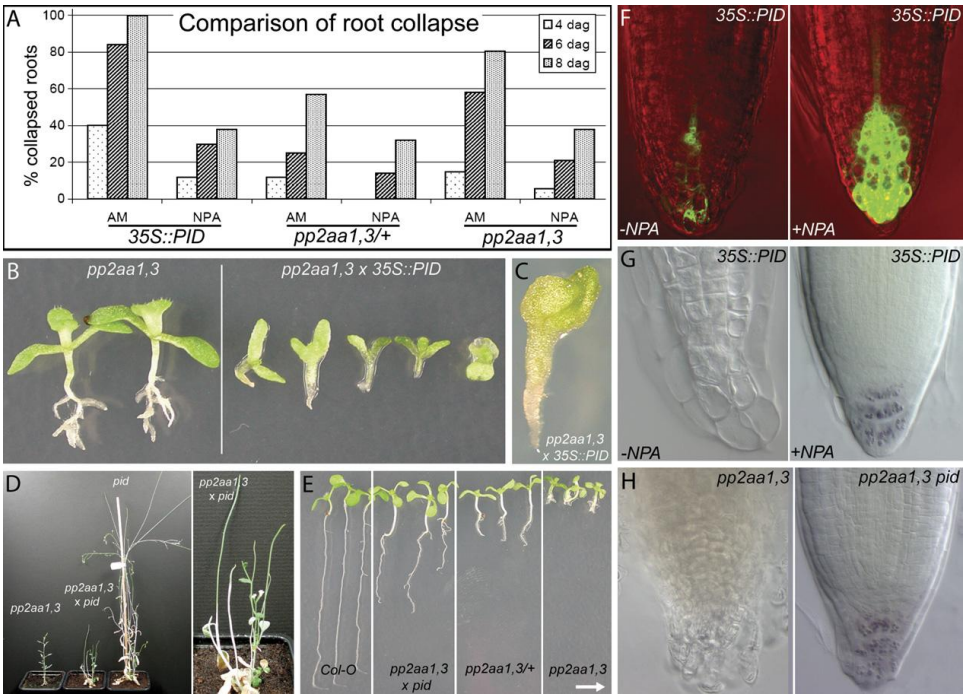

Figure 3. PP2AAs Act Antagonistically to PID on Root Development
(A) Comparison of frequency of primary roots collapse in 4-, 6-, and 8-day-old *35S::PID*, *pp2aa1 pp2aa3*/+ and *pp2aa1 pp2aa3* seedlings grown in the presence or absence of NPA; in all mutant combinations, inhibition of auxin transport by NPA rescues the root collapse.
(B and C) Strongly enhanced phenotypes of *pp2aa1 pp2aa3 35S::PID* seedlings as compared to *pp2aa1 pp2aa3* double mutants of the same age. (D) Additive shoot phenotypes of an adult *pp2aa1 pp2aa3 pid* plant in comparison to *pp2aa1 pp2aa3* and *pid*.
(E) Partial rescue of *pp2aa1 pp2aa3* double-mutant phenotype in *pp2aa1 pp2aa3 pid* seedlings; rescue of root growth and root meristem activity. Arrow indicates new gravity vector.
(F and G) As in case of *pp2aa* mutants (see Figure 1), reduced *DR5* activity (F) and resulting root collapse (G) in *35S::PID* root tips is rescued following auxin transport inhibition by NPA.
(H) Collapsing root meristem of *pp2aa1 pp2aa3* is rescued in *pp2aa1 pp2aa3 pid* triple mutant.

Loss of PP2AA Function Leads to Basal-to-Apical PIN Polarity Shift in Embryos and Roots

It has been suggested that PID kinase exerts its effect on polar auxin transport by controlling apical-basal targeting of the PIN auxin efflux carriers (Friml et al., 2004). This prompted us to examine subcellular localization of PIN proteins in different *pp2aa* loss-of-function mutants.

In *pp2aa1 pp2aa2* and *pp2aa1 pp2aa3* double-mutant embryos (total n = 45), the localization of PIN1 was impaired. Generally, basal (lower, root pole-facing) polarity of PIN1 localization was much less pronounced; in some cells a basal-to-apical polarity shift was detectable (Figure 4A). Also, the polarity of the PIN4 protein was affected during embryo development (n = 57) occasionally resulting in a complete apicalization of signal (data not shown).

During postembryonic development, polar localization of PIN proteins in roots of 2.5 day seedlings was also affected in all *pp2aa1* double-mutant combinations. PIN2, which in the wild-type localizes to the basal side of young cortical cells, changed its polarity to apical (upper, shoot apex-facing) in approximately 60% (n = 110) of *pp2aa1* double-mutant roots, whereas the apical localization in the epidermis cells remained unaffected (Figure 4B). Similarly, PIN4, which is basally localized in proximal initials and daughter cells of the wild-type root meristem, shifted to the apical side in approximately 20% (n = 90) of *pp2aa1* double-mutant roots (Figure 4C). Basal localization of PIN1 as observed in wild-type stele cells was also affected in *pp2aa1* double-mutant roots. Although no complete apicalization of PIN1 localization was detectable, the subcellular polarity of PIN1 was less pronounced in these double mutants (data not shown).

When activity of all three PP2AAs was decreased in tamoxifen-inducible amiRNA lines, a pronounced basal-to-apical shift of PIN1, PIN2 and PIN4 polarity could be observed following tamoxifen treatment (Figure 4D and data not shown). In control experiments, the same transgenic

seedlings grown without tamoxifen (Figure 4D) as well as tamoxifen-treated transgenics harboring the empty T-DNA vector (data not shown) did not show changes in PIN polarity (Figure 4D).

These data collectively show that loss of PP2AA function leads to a basal-to-apical shift in PIN polarity, a phenomenon identical to PIN polarity changes in PID gain-of-function plants. Furthermore, the observed reversal of basal PIN localization fully explains all observed auxin transport-related aspects of *pp2aa* mutant phenotypes.

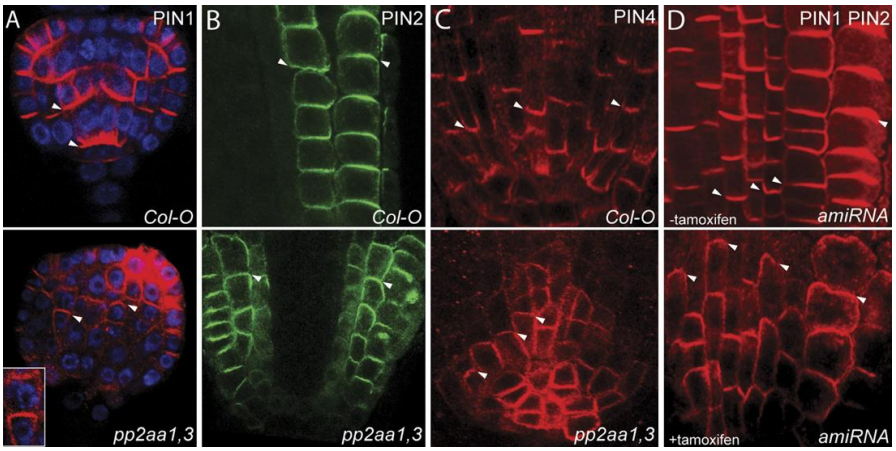

Figure 4. Basal-to-Apical Shift of PIN Proteins in *pp2aa* Loss-of-Function Mutants
(A) Immunolocalization of PIN1 in embryos: disturbed polarity of PIN1 with visible apicalization in *pp2aa1 pp2aa3* as compared to the basal localization of PIN1 in wild-type.
(B and C) Immunolocalization of PIN2 and PIN4 in roots of 2- to 3-day-old seedlings: apicalization of PIN2 (in cortex) (B) and PIN4 (in the whole expression domain) (C) in *pp2aa1 pp2aa3* mutants as compared to basal localization of PIN2 (cortex) (B) and PIN4 (C) in wild-type roots.
(D) Immunolocalization of PIN1 and PIN2 in conditional amiRNA transgenic seedlings: basal-to-apical shift of PIN1 and PIN2 in roots germinated on inductor tamoxifen as compared to basal localization of PIN2 (cortex) and PIN1 (stele) in untreated roots.
Arrowheads indicate polarity of PIN localization.

PP2AA and PINOID Partially Colocalize with PINs at the Plasma Membrane

To obtain further insight into the potentially common action of PID and PP2A on PIN polar trafficking, we determined the subcellular localization of both proteins in *PP2AA1::PP2AA1:GFP* and *PID::PID:YFP* lines. For both constructs, functionality was demonstrated by complementation of the corresponding loss-of-function mutant (see Experimental Procedures).

At the subcellular level, *PP2AA1:GFP* protein showed a broad intracellular distribution including endoplasmic reticulum-, cytosol-, and cell boundaries-associated signals (Figures 5A and 5D). Closer examination by immunolocalization revealed colocalization of a fraction of *PP2AA1:GFP* with PIN1 and PIN2 at the plasma membrane (Figures 5A-5F). Quantitative analysis demonstrated that about 7% of the detected PP2AA1 signal colocalizes with PIN1, whereas 80% of PIN1 overlaps with PP2AA1. These results indicate that a sub-fraction of PP2AA1 colocalizes with PIN proteins at the plasma membrane.

Analysis of *PID::PID:YFP* transgenic lines showed that *PID:YFP* is expressed in embryos (Figure 2C) and seedlings root tips (Figure S1E) where it is associated with the plasma membrane, corroborating previous observations on *PID:GFP* expressed in root hair cells (Lee and Cho, 2006). Immunolocalization studies in roots revealed that *PID:YFP* is localized intracellularly and at the apical and basal cell sides thus partially co-localizing with PIN2 at apical plasma membrane of epidermis cells (Figures 5G-5I). Quantitative analysis of co-localization revealed that 23% of *PID:YFP* colocalizes with PIN2, whereas 89% of PIN2 colocalizes with PID:YFP.

The association of PP2AA and PID with membranes was further substantiated by subcellular fractionation of protoplast extracts (see below) followed by Western blotting revealing a proportion of both proteins associated with the membrane fraction (data not shown).

As PP2AA and PID do not represent intrinsic membrane proteins, their localization at the

membrane structures necessitates at least transient association with membrane protein(s) or other membrane components.

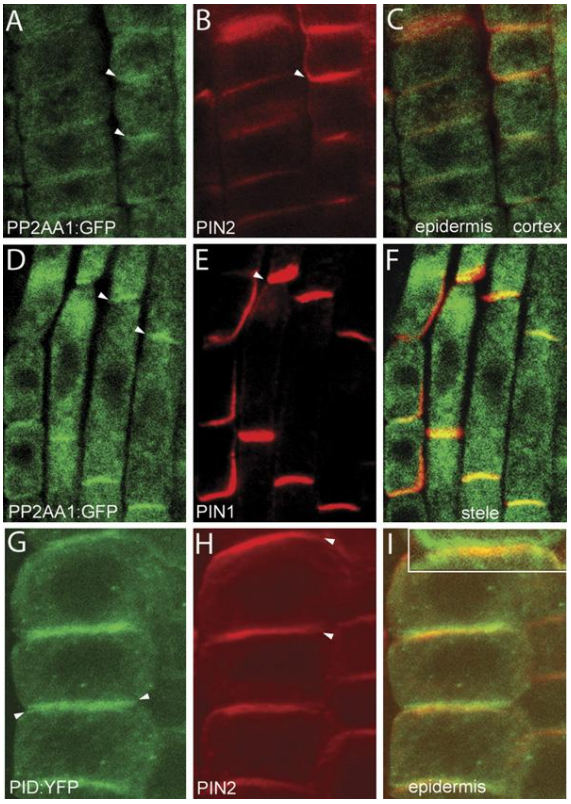

Figure 5. Subcellular Localization of PP2AA1, PID, and PIN Proteins
(A-F) Immunolocalization of PP2AA1 (*PP2AA1::PP2AA1:GFP*) (A and D), PIN1 (E), and PIN2 (B) proteins: PP2AA1 signal is associated with cytosol, ER and plasma membrane (A and D), where it partially colocalizes with PIN1(F) and PIN2 (C).
(G-I) Immunolocalization of PID (*PID::PID:YFP*) (G) and PIN2 (H): localization of PID at the transversal plasma membranes; colocalization with PIN2 (I). Inset shows detail of colocalization at the apical cell side.

PIN1 Is Phosphorylated in a PINOID-Dependent Manner *In Vivo*

The opposite effects of both PP2AA and PID on PIN polar targeting and partial colocalization of these proteins suggest a scenario in which PINs are phosphorylation substrates of a pathway that depends on PID kinase and PP2AA phosphatase activities. To test the involvement of PID and PP2A in phosphorylation of PIN1 in vivo, we performed phosphorylation assays using extracts from *Arabidopsis* protoplasts (Meskiene et al., 2003). Protoplasts were transfected with the *35S::PIN1:GFP* construct in combination with *35S::PID:FLAG* and/or *35S::PP2AA1:HA*. *PIN1:GFP* was observed by microscopy predominantly at the protoplast plasma membrane (Figure 6A). Both *PID:FLAG* and *PP2AA1:HA* were detected on protein blots with the expected molecula weight (Figure 6B). *PID:FLAG* was found as a double band and, as the upper band disappeared upon phosphatase treatment (data not shown), this presumably reflects PID autophosphorylation, which was reported before (Zegzouti et al., 2006). Protein blots from extracts of protoplasts transfected with *PIN1:GFP* alone produced a single band of expected size for *PIN1:GFP*. When *PIN1:GFP* was cotransfected with *PID:FLAG* with or without *PP2AA1:HA*, we observed additional high molecular weight *PIN1:GFP* signals, in which two distinct, other bands could be distinguished (Figure 6C). This result was confirmed by immunoprecipitation from cell extracts - *PIN1:GFP* was pulled down as a compact band when expressed alone, but was accompanied by increased molecular weight PIN1-specific products when coexpressed with PID (Figure S3B). These results demonstrate PID-dependent modification of *PIN1:GFP* protein. Overexpression of *PP2AA1:HA* did not mitigate the effect of *PID:FLAG* on *PIN1:GFP*. This might be due to the dominance of PID- over PP2A activity, or due to the failure to increase the activity of the whole PP2A complex by overexpression of just the A

regulatory subunit.

To test whether the observed shift in molecular weight includes PIN1 phosphorylation, we incubated protein extracts with l-phosphatase and/or phosphatase inhibitors. The higher molecular weight bands of *PIN1:GFP* were sensitive to incubation with l-phosphatase. This effect was blocked by cotreatment with phosphatase inhibitors (Figure 6D), demonstrating that these additional *PIN1:GFP* signals with reduced mobility are the result of phosphorylation.

The comparable effect of *PID:FLAG* on endogenous PIN1 in protoplasts cotransfected with *PIN1:GFP* was difficult to observe, due to transfection efficiencies of about 10% (data not shown). In addition, *PIN1:GFP* levels in the cotransfected cells was estimated to be about 10-fold higher than levels of endogenous PIN1 leading to preferential PID-dependent modification of *PIN1:GFP*. However, when we omitted *PIN1:GFP* and transfected protoplasts with only *PID:FLAG* with or without *PP2AA1:HA*, similar higher molecular weight bands for endogenous PIN1 were observed that disappeared upon l-phosphatase treatment (Figure S3A). In Summary, these data show that the PIN1 protein is phosphorylated in a PID-dependent manner in vivo.

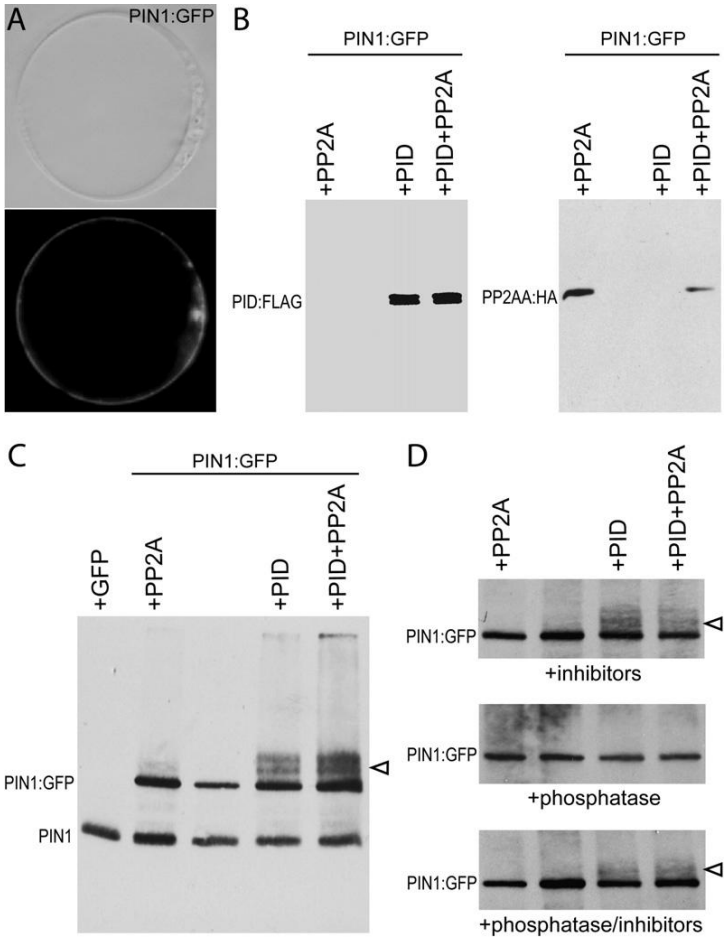

Figure 6. PID-Dependent Phosphorylation of PIN1 in *Arabidopsis* Protoplasts
(A) Transiently expressed *PIN1:GFP* localizes predominantly to the plasma membrane of protoplasts.
(B-D) Western blot demonstrating *PID:FLAG*, *PP2AA1:HA* and *PIN1:GFP* expression following (co)transfections of protoplasts (B). When cotransfected with *35S::PID:FLAG* (with or without *35S::PP2AA1:HA*), higher molecular weight bands of *PIN1:GFP* (arrowheads) appear (C). The appearance of additional *PIN1:GFP* bands is sensitive to l-phosphatase treatment but stable in the additional presence of phosphatase inhibitors (D).

PINOID and PP2A Antagonistically Act on Phosphorylation of PIN Proteins in Their Central Hydrophilic Loop

To test whether PINs are present in a phosphorylated state in planta, we immunoprecipitated *PIN1:GFP* protein from seedling roots and performed Mass Spectrometry (nLC-MS/MS) on tryptic

peptides. Seven different PIN1 peptides were identified, all falling within the large central hydrophilic loop (Supplementary Table). One of these peptides was found both in a nonphosphorylated and phosphorylated state (Figure 7A; Supplementary Table). From the MS/MS spectrum, it cannot be determined whether the phosphorylation occurs at Serine 337 or at Threonine 340, both of which are conserved in several members of the PIN gene family. These results together with previous reports (Nühse et al., 2004; Benschop et al., 2007) demonstrate that PIN1 and possibly also other PIN proteins are phosphorylated in their central hydrophilic loop in *Arabidopsis*. Next we tested whether the central hydrophilic loop of PIN proteins can be directly phosphorylated by PID. The HIS-tagged hydrophilic loop (HL) of PIN1 and GST-tagged PID were heterologously expressed in E. coli, and coincubated in an in vitro phosphorylation reaction. Following electrophoretic separation of the proteins, clear PID-dependent phosphorylation of *HIS:PIN1HL* was detected (Figure 7B). In addition, PID autophosphorylation and phosphorylation of the standard Ser/Thr kinase substrate Myelin Basic Protein (MBP), but not of an unrelated myosin-like protein (MLP) was detected. In another experiment, both *GST:PID* and *HIS:PID* were able to phos- phorylate *HIS:PIN2HL* as well (Figure 7C). These results demonstrate that the PID kinase is able to phosphorylate the hydrophilic loop of PIN proteins in vitro.

Furthermore, we tested the ability of protein extracts derived from wild-type, *35S::PID* and *pp2aa* mutants to phosphorylate *HIS:PIN2HL*. The phosphorylation of *HIS: PIN2HL* was enhanced upon incubation with *35S::PID* protein extract when compared to extracts from wild-type (Figure 7D). Similarly, protein extracts derived from plant material lacking *PP2AA1* and either *PP2AA2* or *PP2AA3* had increased ability to phosphorylate *PIN2HL* (Figure 7D). These data confirm that PID activity positively regulates phosphorylation of PIN hydrophilic loops, whereas PP2A activity has a negative effect.

When taken together, the results obtained in in vitro and the in vivo phosphorylation assays corroborate the genetic and cell biological studies and provide strong support for a scenario in which PID kinase and PP2A phosphatase activities antagonistically regulate phosphorylation of PIN proteins in their middle, hydrophilic loop.

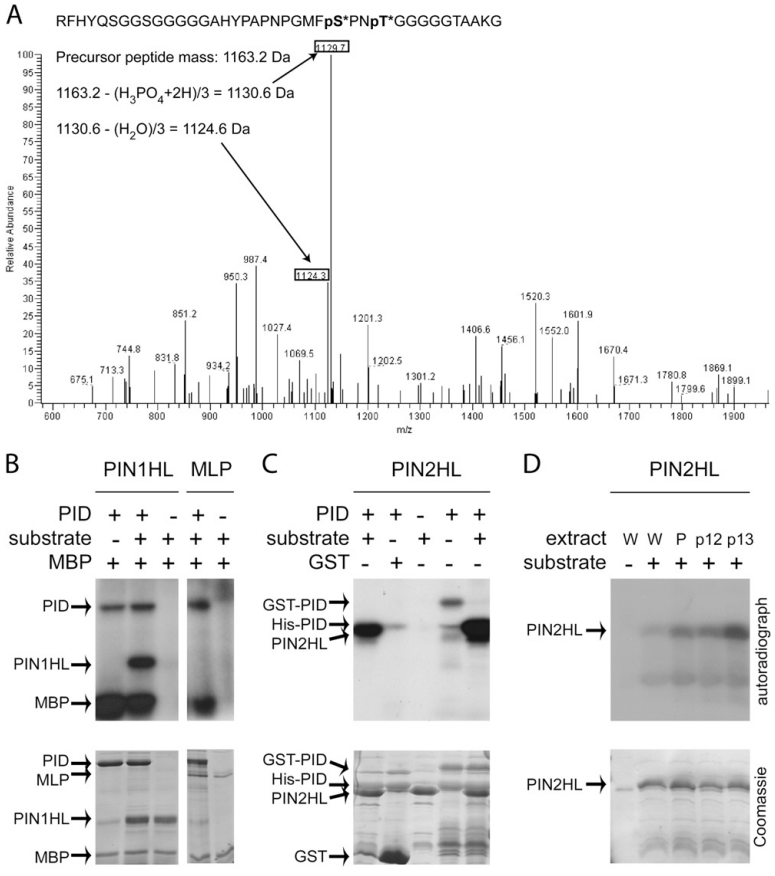

Figure 7. PID and PP2A Activities Mediate Phosphorylation of PIN Proteins in Their Hydrophilic Loop

(A) MS/MS spectrum of phosphorylated peptide derived from PIN1 hydrophilic loop. The sequence of the precursor peptide. Asterisks indicate Serin and Threonin, one of which is phosphorylated. The major peak in the spectrum corresponds to the precursor peptide (Mass: 1163.2 Da) with neutral loss of a single phosphate group (1130.6 Da). A second major peak is consistent with the precursor peptide losing both a phosphate group and a water molecule (1124.6 Da).
(B and C) *GST:PID* or *HIS:PID* autophosphorylates and efficiently phosphorylates the large hydrophilic loop of PIN1 (*HIS:PIN1HL*) and Myelin Basic Protein (MBP) (B) or the loop of PIN2 (*HIS:PIN2HL*) (C) in vitro. GST (C) and the myosin-like protein (*HIS:MLP*) (B) are not phosphorylated by PID. (D) Increased phosphorylation of the *HIS:PIN2HL* by protein extracts of *35S::PID* (P), *pp2aa1 pp2aa2* (p12) and *pp2aa1 pp2aa3* (p13) as compared to wild-type (w) extracts. Lane 1 contains wild-type extract without *HIS:PIN2HL*.

DISCUSSION

PP2A Phosphatase and PINOID Kinase Act Antagonistically on Auxin Transport-Dependent Development and PIN Apical-Basal Targeting

Functional characterization of the Ser/Thr protein kinase PINOID revealed a role for protein phosphorylation in PIN polar targeting, auxin transport and auxin-related development (Christensen et al., 2000; Benjamins et al., 2001; Friml et al., 2004). Moreover, loss-of-function of the A regulatory subunits of PP2A was shown to cause severe developmental defects (Garbers et al., 1996; Rashotte et al., 2001; Zhou et al., 2004), many of which correlate with defects in auxin distributions. Our detailed observations on *pp2aa* mutants showed that the loss-of- function phenotypes affecting root and embryo development are strikingly similar to PID gain-of-function phenotypes (Benjamins et al., 2001; Friml et al., 2004), and that *pid* and *pp2aa* show antagonistic genetic interactions. The antagonistic activities of PID and PP2A were also apparent at the cellular level, since both, PP2A and PID activities influence the apical versus basal polar targeting of PIN proteins. In wild-type plants, basal polarity of PIN localization in the inner embryo and root tissues mediates auxin flow toward the root pole, thereby triggering and, later, maintaining the activity of the root meristem (Friml et al., 2002a, 2003; Blilou et al., 2005). In the PID gain-of-function or PP2A loss-of-function alleles, PIN localization is to a large extent apicalized, causing auxin depletion in the root pole, and resulting in meristem collapse. These results imply that PP2A phosphatase and PID kinase act on the same auxin transport-related developmental processes, by antagonistically regulating PIN polar targeting.

PP2A phosphatase is a heterotrimeric protein consisting of a C catalytic subunit together with A and B regulatory subunits. 5 Arabidopsis loci encode C subunits, 17 loci were found to encode B subunits, whereas 3 loci code for A subunits. Different combinations of these subunits form holoenzymes with distinct properties, which in animals are known to regulate a wide range of developmental processes (reviewed in Janssens and Goris, 2001). Considering this, it is quite surprising that a general decrease of PP2A activity in *Arabidopsis* roots and embryos primarily affects auxin transport-related patterning. This may reflect both the specificity of PP2A action in auxin transport-related processes as well as high susceptibility of root and embryos to perturbations in the auxin distribution. On the other hand, in inflorescence and flower development, PP2A have been reported to mediate additional auxin-unrelated processes (Zhou et al., 2004) and show additive rather than antagonistic effects to PID. This suggests a broader specificity of PP2A action as compared to PID at these developmental stages.

PINOID and PP2A Act Antagonistically on Phosphorylation of PIN Proteins

Antagonistic action of PID and PP2A implies that they might act as a kinase/phosphatase pair on common substrates. As expected for soluble proteins, PID and in particular PP2AA show a broad intracellular distribution. Nevertheless, a fraction of both proteins was detected together with PIN proteins associated with the plasma membrane. Similar localization of a kinase was found in mammalian epithelial cells, where the atypical protein kinase C, which mediates apicalization of early blastomeres, localizes to the apical plasma membrane (Chalmers et al., 2005). The demonstration of close subcellular association of PID, PP2AA and PINs favors a scenario in which PID/PP2AA pairs directly control phosphorylation of PIN proteins. This model is further reinforced by observations that the hydrophilic parts of PIN proteins are phosphorylated *in vitro* and *in vivo* in PID-dependent manner. In addition, protein extracts from both PID gain-of-function and PP2A loss-of-function plants show increased ability to phosphorylate PIN proteins. There are two scenarios consistent with these data: (1) Both PP2A and PID act directly on (de)phosphorylation of PINs or (2) PP2A acts on

dephosphorylation of PID, thus downregulating its kinase activity on PINs. In either case, the data clearly show that the PID kinase and PP2A trimeric phosphatases act antagonistically on reversible phosphorylation of PIN proteins, which in turn determines the apical-basal targeting of these auxin efflux carriers.

Reversible Phosphorylation of Cargos as a Means for Conditional Apical-Basal Targeting in Plants

We propose a model for conditional apical or basal delivery of polarly localized cargos in plants. Cargos such as PIN proteins can be targeted either to the apical or to the basal side of cells, depending on their phosphorylation status. Conditions in which PID kinase activities are relatively high would result in predominantly phosphorylated PIN proteins, causing their targeting to the apical side of cells. In the converse situation, when PID activities are lower than those of PP2A phosphatase, PIN proteins will be dephosphorylated and targeted preferentially to the basal side of the cell.

Regulation of polar delivery of membrane components in mammalian and plant cells may share important features. In mammalian epithelial cells, phosphorylation of cargos has been shown to influence their delivery. For example, delivery of the immunoglobulin receptor to the apical cell surface largely depends on its phosphorylation status (Casanova et al., 1990). Our demonstration of the kinase/phosphatase regulation of PIN1 polarity shows that similar processes occur in plants. The suggested mechanism might also help to answer outstanding questions about the regulation of auxin flow, such as how differences between distinct PIN proteins and cell types together contribute to the decision of apical or basal PIN delivery. Variations in phosphorylation of different PIN proteins could, for example, arise as a consequence of divergent phosphorylation sites, some of which would be phosphorylated more efficiently, whereas others might represent rather poor substrates for PID. In parallel, relative expression levels of PID and/or PP2A in different cell types could play a decisive role. Furthermore, activities of PID and PP2A may be downstream of different signaling pathways, which by this mechanism could redirect auxin flow through modulation of PIN polar targeting. In this scenario, a combination of constitutive endocytosis of PINs (Dhonukshe et al., 2007) and their reversible phosphorylation would allow for flexible retargeting of PINs to different subcellular destinations in response to various signals. Overall, control of PIN protein phosphorylation appears to represent a hitherto unappreciated level of regulation of directional auxin fluxes, which are causal in plant pattern formation, organogenesis and tropisms.

EXPERIMENTAL PROCEDURES

Material

The following mutants and transgenic plants have been described previously: *DR5$_{rev}$::GFP* (Benková et al., 2003), *pp2aa1* (*rcn1)* (Garbers et al., 1996), *35S::PID* and *pid* (EN197) (Benjamins et al, 2001). Double mutants were generated by crosses and F2 progeny from five independent crosses for each combination of mutants were screened for phenotypes and confirmed by PCR genotyping. In an attempt to obtain *pp2aa1 pp2aa2 pp2aa3* triple mutants among 120 genotyped F2 seedlings (all revealing strong phenotypes) no triple homozygous plants were found.

PP2AA promotor::*uidA* (GUS) fusions were generated using approximately 2 kb of At1g25490 (*PP2AA1*), At3g25800 (*PP2AA2*) and At1g13320 (*PP2AA3*) 5'UTRs. The promotor fragments were amplified from genomic DNA by using the following primers combinations: 5'-TCACTTACCAAGCTTCGGATGATCCA-3' and 5'-CGCGGATCCCTTATGTGAAAGTTCGAATCA-3' for *PP2AA1*; 5'-CGCGAGCTCCCTGAGATTGATACATTGA-3' and 5'-CGCGGATCCCTTCAACAACACCAACAAC-3' for *PP2AA2* and 5'-ACGCGTCGACCATCGTATTCAATTCCAAGCTC-3' and 5'-CGGGATCCCCTCACCAAAACTCAAATCACT-3' for *PP2AA3*. Fragments were cloned into pSDM 7006, pVKH-35S-GUS-pA and pCAMBIA-1391Z binary vectors, respectively (Weijers et al., 2003; Hamann et al., 2002; McElroy et al., 1995). The *PP2AA1:GFP* C-terminal translational fusion was created inserting *PP2AA1* genomic fragment between 2035 bp upstream and 3194 bp downstream from ATG into pGreenII Kan-tNOS (Hellens et al., 2000) and its functionality was confirmed in *pp2aa1* and *pp2aa1 pp2aa3* mutants. The *PID:YFP* translational fusion was created by cloning a BamHI fragment containing the complete *PID* promoter plus coding region from *PID:GUS* (Benjamins et al., 2001) upstream and in frame with a 9X poly-alanine linker and the GFP variant VENUS (Nagai

et al., 2002). Functionality of the PID:YFP translational fusion was confirmed by transformation into *pid-6 /PID* heterozygotes using the binary vector pMLBART (Eshed et al., 2001). Two independent amiRNAs were engineered according to Schwab, et al., 2006 and placed under the *UAS* promotor. 21 bp oligonucleotides used for PCR were: 5'- TATTGCCCATTCAGGACCGAA-3' for amiRNA-1 and 5'-TTGCATGCAAAGGGCACCGAG-3' for amiRNA-2 construct. The predicted miRNA targets were: At1g25490 (*PP2AA1*), At3g25800 (*PP2AA2*) and At1g13320 (*PP2AA3*). Artificial microRNA fragments were engineered into miR319 and cloned into to pGIIB-UAS-tNOS (Schwab et al., 2006) and the construct was transformed into tamoxifen-inducible pINTAM activator line (Friml et al. 2004). *GST:PID* (Benjamins et al., 2003), pET-*PIN1HL* (amino acids 288-452; Paciorek et al., 2005) and pGEX-*PIN2HL* (Abas et al., 2006) have been described previously. *HIS*:*PID* was created by ligating the *PID* cDNA (Benjamins et al., 2001) into pET16H (pET16B derivative, J. Memelink, unpublished results). *35S::PID:FLAG* was constructed by replacing the BsiWI XhoI 3'fragment in pSDM70671 (pEF-*PID*; Friml et al., 2004) with a fragment encoding a C-terminal fusion between PID and the FLAG tag and subsequently cloned behind the *35S* promoter. *HIS:MLP* (At5g08120) was obtained by PCR amplification of the cDNA using the primers 5'-ACGCTTGTCGACTATATGTATGAGCAGCAGCAACAT-3' and 5'-CGGGATCCAAACAACCCAAGGAGAGAAATATC-3'. The resulting PCR fragment was cloned into pET16B (Novagen). MBP (myelin basic protein) was purchased from Sigma. *Arabidopsis thaliana* (ecotype *Col-0*) plants were transformed into wild-type or pINTAM (amiRNA) activator line. T2 or T3 seedlings for each transgene were identified by antibiotic selection and segregation analysis. T-DNA insertion lines were obtained from NASC: SALK_042724 (*pp2aa2-1)* and SALK_017541 (*pp2aa2-3*); SALK_014113 (*pp2aa3-1*) and SALK_099550 (*pp2aa3-2*). Genotypes of all insertion lines were confirmed by PCR and further analyzed by RT-PCR.

Growth Conditions and Phenotypic Analysis

Seeds were grown as described (Benková et al., 2003). Short-time incubation of 3-5 day seedlings with 5 mM 2,4-dichlorophenoxyacetic acid (2,4-D; Sigma) was performed in 24-well cell-culture plates in liquid AM medium with 1% sucrose for 4 hr. Long-time treatment was done by growing seedling on MS medium supplemented with 0.3 mM NPA (Sigma). Seeds carrying inducible amiRNA system were germinated on MS medium supplemented with 1 or 5 mM tamoxifen (Sigma). Root gravitropic assays (Paciorek et al., 2005) and embryo analyses (Friml et al., 2003) were performed as described. Seedlings were analyzed at 3, 4, 6, 8, and 14 day. Nine independent amiRNA lines were analyzed (four for amiRNA-1 and five for amiRNA-2). For *pp2aas pid* and *pp2aas 35S::PID* triple mutants five independent segregating lines of ($n > 500$ individuals) were examined. Microscopy was done with a Zeiss Axiophot equipped with Axiocam HR CCD camera.

In Situ Expression and Localization Analysis

Histochemical stainings for GUS activity and whole-mount immunolocalization were performed as described (Friml et al., 2003; Sauer et al., 2006b). Each experiment was done on three to ten independent lines with minimum of two repetitions. Antibodies were diluted as follows: anti-PIN1 (1:1000; Paciorek et al., 2005), anti-PIN2 (1:1000; Abas et al., 2006), anti-PIN4 (1:400; Friml et al., 2002a), anti-GFP (1:500; Molecular Probes); FITC- and CY3-conjugated anti-rabbit secondary antibodies (Dianova) were both diluted 1:500. For in vivo GFP inspections, plant material was mounted in 5% glycerol. Analysis was done using a Leica TCS SP2 confocal laser scanning microscope. Images were processed in Adobe Photoshop and assembled in Adobe Illustrator. The colocalizations were quantitatively analyzed using MetaMorph (Molecular Devices).

Immunoprecipitation and Mass Spectrometry

PIN1:GFP seedlings were grown vertically for 5 days and crude protein extract was prepared from excised roots (Karlova et al., 2006). Following preclearing protein extract with Tris-conjugated Microlink agarose matrix (Pierce), *PIN1:GFP* was precipitated by overnight incubation with anti-YFP antibody-coupled Microlink agarose matrix (R. Karlova, W. van Dongen, and S. de Vries, personal communication; details available upon request). The immunocomplexes were washed and Trypsin-digested as in Karlova et al. (2006). After Trypsin digestion, peptides were separated by nano-Liquid Chromatography and subjected to tandem Mass Spectrometry using an LCQ Classic (Thermo Electron, San Jose, CA). Spectra were compared with a custom- made database encompassing the Arabidopsis

proteome using Bio- works 3.2 (Thermo Electron) software. The experiments were performed with three biological replicas giving comparable results.

In Vivo Phosphorylation Assays

Arabidopsis protoplasts were isolated from suspension culture, transformed according to Meskiene et al. (2003) and harvested after 10-22 hr. Cell pellets were lysed by freeze-thaw cycles followed by a Dounce-type homogenizer. The extraction buffer used was based on Abas et al. (2006) except that PVPP was excluded, and 20% sorbitol was used instead of glycerol. Phosphorylation assays were performed using protoplasts extracted as above, but omitting the phosphatase inhibitors. Total cell extracts or membrane fractions were solubilised with 0.1% Brij35 and reheated at 65ºC for 10 min to inactivate endogenous enzymes. After l-phosphatase buffer (Sigma P9614) was added, four treatments were performed in a final volume of 30 or 50 ml: (a) sample plus 3 mM MnCl2; (b) sample plus 3 mM MnCl2 and 100 U l-phosphatase (Sigma P9614); (c) sample plus phosphatase inhibitors (20 mM EDTA, 13 mM EGTA, 40 mM betaglycerolphosphate, 0.5 mM sodium orthovanadate, 1 mM sodium molybdate, 5 nM okadaic acid, 50 mM sodium fluoride); (d) sample plus 100 U l-phosphatase and phosphatase inhibitors as in (c). All samples were incubated at 30ºC for 5-20 min. Reactions were stopped by adding phosphatase inhibitors to (a) and (b) and freezing all samples. Protoplasts transformed with GFP and subjected to phosphatase treatment as above showed no change in GFP specific bands as detected by Western blotting, indicating that GFP itself was not phosphorylated when overexpressed in protoplasts (data not shown). Samples were separated as described (Abas et al., 2006) and probed with the following antibodies: affinity purified rabbit polyclonal anti-PIN1 (Paciorek et al., 2005), mouse monoclonal anti-FLAG (Sigma, clone M2, used at 2.5 mg/ml), mouse monoclonal anti-GFP (Roche, clones 7.1 and 13.1, used at 0.4 mg/ml), rat monoclonal anti-HA (Roche, clone 3F10, used at 0.2 mg/ml). Secondary antibodies (HRP-conjugated goat anti-rabbit, anti-mouse or anti-rat IgG, all from Jackson) were used at 0.02-0.08 mg/ml. Detection was performed using enhanced chemiluminescence (Pierce Super Signal).

In Vitro Phosphorylation Assays

Approximately 1 mg of purified protein expressed in E. coli (PID and substrates) wereadded to kinase reaction mix (20 ml total volume), containing 1x kinase buffer (25 mM Tris-HCl [pH 7.5]; 1 mM DTT;5 mM MgCl2) and 1x ATP solution (100 mM MgCl2/ATP; 1 mCi 32P-g-ATP). For the assays with seedling extracts, 3-4 day seedlings were harvested in aliquots of 50 seedlings and stored at -80ºC. Approximately 4 mg of the PIN2HL was incubated with 50 mg total protein extracted from seedlings, 1x kinase buffer and 1x ATP solution (see above) in a total volume of 150 ml. Reactions were incubated at 30ºC for 30 min. and stopped by the addition of respectively 5 or 40 ml of 5x protein loading buffer (310 mM Tris-HCl [pH 6.8]; 10% SDS; 50% Glycerol; 750 mM b-Mercaptoethanol; 0,125% Bromophenol Blue) and 5 min. boiling. Reactions were subsequently separated over 12,5% acrylamide gels, which were washed 3 times for 30 min. with kinase gel wash buffer (5% TCA [trichoroacetic acid]; 1% Na2H2P2O7), Coomassie stained, destained, dried, and exposed to X-ray films for 24 to 48 hr at -80ºC using intensifier screens.

ACKNOWLEDGMENTS

We thank S. Boeren, R. Karlova, J. Kleine-Vehn, F. Maraschin and H. Robert for technical help and advice; S. Peck for helpful discussions; J. Strauss and L. Mach for sharing reagents. We gratefully acknowledge financial support from the VolkswagenStiftung and EMBO Young Investigator Program (J.F.), the Deutsche Forschungsgemeinschaft -SFB 446 (M.M.), Brazilian Funding Agency for Post-Graduation Educa- tion-CAPES (M.K.Z.), the Austrian Research Fund - P16311; P18440 (L.A., C.L.),- P16409; P19005 (A.S., I.M.), the Netherlands Proteomic Center (NPC; Grant to S. de Vries; D.W.), the China Scholarship Council (F.H.), the National Science Foundation FIBR 0330786 and Department of Energy FG02-88ER13873 (M.G.H., C.O. and E.M.M.).

SUPPLEMENTAL FIGURES

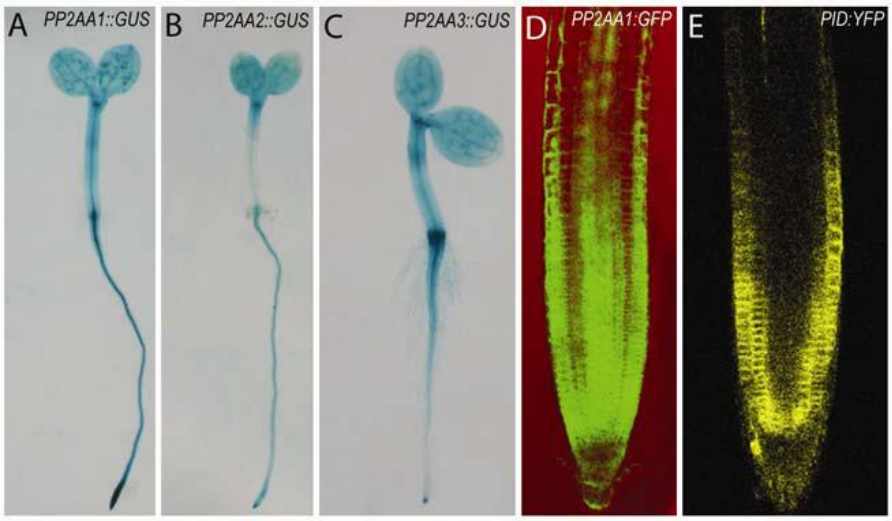

Figure S1. Expression of *PP2AA*s during seedling development
(A-C) GUS staining shows overlapping expression patterns of *PP2AA1::GUS* (A), *PP2AA2::GUS* (B) and *PP2AA3::GUS* (C) in transgenic seedlings. GUS activity was found predominantly in primary root, lateral roots (with exception of *PP2AA3*), root-shoot junction, cotyledons and shoot apical meristem.
(D-E) Localization of PP2AA1 (*PP2AA1::PP2AA1:GFP*, D) and PID (*PID::PID:YFP*, E) proteins in primary roots.

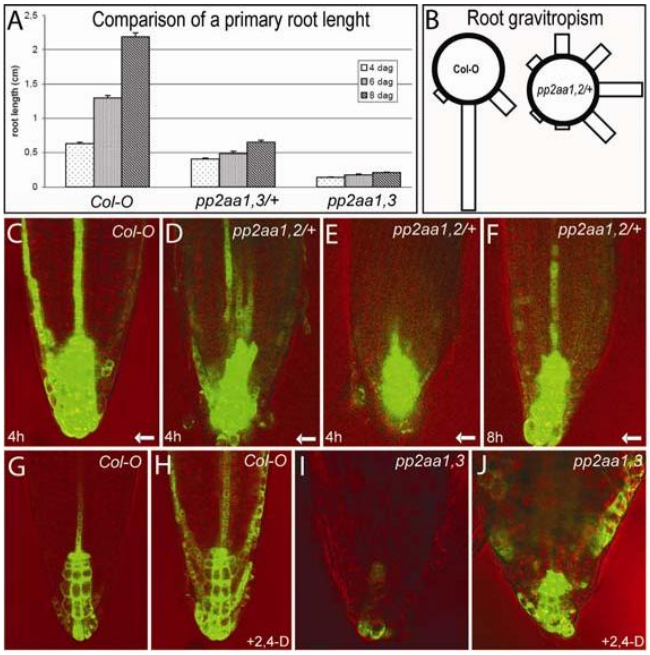

Figure S2. Development and DR5 activity in *pp2aa* primary roots
(A, B) Root phenotypes of *pp2aa1 pp2aa2/+*, *pp2aa1 pp2aa3/+* and *pp2aa1 pp2aa3* as compared to wild-type include defects in primary root growth (A) and impaired gravity response (B).
(C-F) Distribution of *DR5rev::GFP* expression in gravistimulated roots exhibit no or only weak relocation of DR5 signal 4 or 8 hours after gravistimulation as compared to wild-type. Whereas all wild-type roots exhibited asymmetric DR5 activity accumulation along the lower side of roots within 3-4 hours (n = 25) (C), only about 23% (n = 48) of *pp2aa1 pp2aa2/+* mutant roots showed a slight (D) or no (E) relocation of the GFP signal even after 8 hours (F). Arrows indicate direction of gravity vector.
(G-J) Increased DR5 expression in roots incubated in 2,4-D for 4 hours (H,J) as compared to untreated controls (G,I) in both wild-type (G,H) and *pp2aa1 pp2aa3* (I,J) roots.

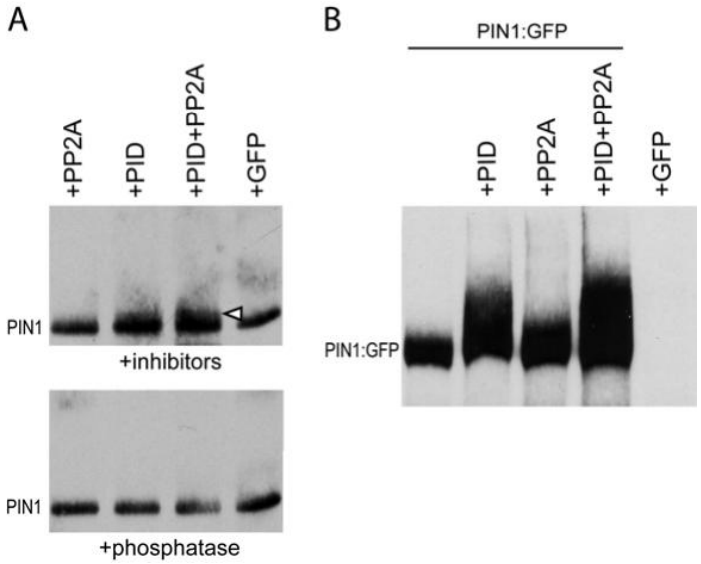

Figure S3. PID-dependent phosphorylation of PIN1 in Arabidopsis protoplasts.
(A) When co-transfected with *35S::PID:FLAG* (with or without *35S::PP2AA1:HA*), higher molecular weight bands of endogenous PIN1 (arrowheads) appear. The appearance of additional PIN1 bands is sensitive to λ-phosphatase treatment. This effect of PID on endogenous PIN1 is to large extent masked when co-transfected with *35S::PIN1:GFP* (see Figure 6C). This is due to the low transfection efficiency; only about 10% of endogenous PIN1 that is seen on the blot was derived from successfully transfected cells and thus accessible to any overexpressed PID. The remaining 90% of endogenous PIN1 would be not modified in a PID-dependent manner as it originates from non-transfected cells. In contrast, almost 100% of co-transfected *PIN1:GFP* originates from *PID:FLAG*-positive protoplasts. Moreover, similar signal intensities that we observed, when comparing endogenous PIN1 vs. *PIN1:GFP*, demonstrated much higher abundance of *PIN1:GFP* in transfected cells. This explains the preferential phosphorylation of *PIN1:GFP* over endogenous PIN1in these cells.
(B) Phosphorylation assays in Arabidopsis protoplasts: immunoprecipitation of *PIN1:GFP* by anti-PIN1 antibodies confirms PID-dependent modification of PIN1.

SUPPLEMENTAL TABLE

Table S1. Sequences of recovered peptides from the *PIN1:GFP* immunoprecipitation as derived from MS/MS data. Note peptide 5, which was recovered in both phosphorylated and non-phosphorylated form.

No	Peptide	Pos.	z	Score (XC)[a]	Ions (MS/MS)
1	KVLATDGGNNISNKT	435	2	2.91	20/24
2	RPSNYEEDGGPAKPTAAGTAAGAGRF	288	2	4.16	21/46
3	KGPTPRPSNYEEDGGPAKPTAAGTAAGAGRF	283	3	3.78	34/112
4	KISVPQGNSNDNQYVERE	406	2	2.76	17/30
5a	RFHYQSGGSGGGGGAHYPAPNPGMF**pS**PNTGGGGGTAAKG	312	3	3.99[b]	53/216
	RFHYQSGGSGGGGGAHYPAPNPGMFSPN**pT**GGGGGTAAKG			3.82	55/216
5b	RFHYQSGGSGGGGGAHYPAPNPGMFSPNTGGGGGTAAKG	312	3	3.90	37/144
6	RPSNLTNAEIYSLQSSRN	229	2	4.99	22/30
7	RNSNFGPGEAVFGSKG	269	2	3.59	18/26

[a] Cross-correlation (XC) significance thresholds after Peng et al. (2003) are 1.5 and 3.3 for doubly- and triply-charged peptides, respectively.
[b] The MS/MS spectrum of this peptide fits almost equally well with phosphorylation at Serine 337 (3.99) as on

Threonine 340 (3.82).

PIN1 protein sequence with recovered peptides highlighted:

```
  1 MITAADFYHV MTAMVPLYVA MILAYGSVKW WKIFTPDQCS GINRFVALFA
 51 VPLLSFHFIA ANNPYAMNLR FLAADSLQKV IVLSLLFLWC KLSRNGSLDW
101 TITLFSLSTL PNTLVMGIPL LKGMYGNFSG DLMVQIVVLQ CIIWYTLMLF
151 LFEYRGAKLL ISEQFPDTAG SIVSIHVDSD IMSLDGRQPL ETEAEIKEDG
201 KLHVTVRRSN ASRSDIYSRR SQGLSATPRP SNLTNAEIYS LQSSRNPTPR
251 GSSFNHTDFY SMMASGGGRN SNFGPGEAVF GSKGPTPRPS NYEEDGGPAK
301 PTAAGTAAGA GRFHYQSGGS GGGGGAHYPA PNPGMFSPNT GGGGGTAAKG
351 NAPVVGGKRQ DGNGRDLHMF VWSSSASPVS DVFGGGGGNH HADYSTATND
401 HQKDVKISVP QGNSNDNQYV EREEFSFGNK DDDSKVLATD GGNNISNKTT
451 QAKVMPPTSV MTRLILIMVW RKLIRNPNSY SSLFGITWSL ISFKWNIEMP
501 ALIAKSISIL SDAGLGMAMF SLGLFMALNP RIIACGNRRA AFAAAMRFVV
551 GPAVMLVASY AVGLRGVLLH VAIIQAALPQ GIVPFVFAKE YNVHPDILST
601 AVIFGMLIAL PITLLYYILL GL
```

329 aa cytoplasmic loop
137 aa (42%) coverage of the cytoplasmic loop in MS
Transmembrane domains; Peptides recovered in MS

CHAPTER 3

PIN Phosphorylation is Sufficient to Mediate PIN Polarity and Direct Auxin Transport

Jing Zhang, Tomasz Nodzyński, Aleš Pěnčík, Jakub Rolčík, and Jiří Friml

Modified from Zhang et al., (2010) Proc. Natl. Acad. Sci. USA 107, 918-922.

Author's Contributions: JF initiated the projects; JZ and JF designed experiments; JZ carried out most of the experiments; NT performed experiments presented in Figure 4D and Figure S3; PA and RJ contributed Figure 3C; JZ assembled the figures; and JZ and JF discussed the resultes and wrote the manuscript.

ABSTRACT

The plant hormone auxin plays a crucial role in regulating plant development and plant architecture. The directional auxin distribution within tissues depends on PIN transporters that are polarly localized on the plasma membrane. The PIN polarity and the resulting auxin flow directionality are mediated by the antagonistic actions of PINOID kinase and protein phosphatase 2A. However, the contribution of the PIN phosphorylation to the polar PIN sorting is still unclear. Here, we identified an evolutionarily conserved phosphorylation site within the central hydrophilic loop of PIN proteins that is important for the apical and basal polar PIN localizations. Inactivation of the phosphorylation site in PIN1(Ala) resulted in a predominantly basal targeting and increased the auxin flow to the root tip. In contrast, the outcome of the phosphomimic PIN1(Asp) manipulation was a constitutive, PINOID-independent apical targeting of PIN1 and an increased auxin flow in the opposite direction. Furthermore, the PIN1(Asp) functionally replaced PIN2 in its endogenous expression domain, revealing that the phosphorylation-dependent polarity regulation contributes to functional diversification within the PIN family. Our data suggest that PINOID-independent PIN phosphorylation at one single site is adequate to change the PIN polarity and, consequently, to redirect auxin fluxes between cells and provide the conceptual possibility and means to manipulate auxin-dependent plant development and architecture.

INTRODUCTION

The plant hormone auxin acts, on account of its differential distribution (gradients) within tissues, as a major determinant of plant architecture (Kepinski et al., 2005; Mockaitis et al., 2008; Vanneste et al., 2009). Auxin is distributed throughout the plant by a network of carrier proteins (Bennett et al., 1996; Blakeslee et al., 2007; Geisler et al., 2005; Petrášek et al., 2006; Yang et al., 2006), and the directionality of the auxin flow is determined by asymmetrically localized plasma membrane PIN transporters (Wiśniewska et al., 2006). The differentially expressed and polarly localized PIN proteins constitute the backbone of a transport network for directional auxin distribution in different parts of the plant (Petrášek et al., 2009). The local biosynthesis (Stepanova et al., 2008; Tal et al., 2008; Zhao et al., 2008) together with the PIN-dependent transport (Vieten et al., 2007) largely account for the formation of local auxin maxima and minima that regulate various developmental processes, including embryonic axis establishment, tropic growth, root meristem patterning, lateral organ and fruit formation, and vascular tissue differentiation and regeneration (Tanaka et al., 2006; Sorefan et al., 2009). The polar PIN localization determines direction of the auxin flow; thus, any signal that acts upstream to control the cellular PIN localization and activity can be translated into changes in the auxin distribution that modulate multiple aspects of the plant development. Phosphorylation has been shown to be important for auxin transport and distribution (Christensen et al., 2000; Benjamins et al., 2001; Sukumar et al., 2009; Zourelidou et al., 2009). So far, the only known regulators that specifically regulate the PIN polar targeting are the serine/threonine protein kinase PINOID (PID) (Christensen et al., 2000; Benjamins et al., 2001; Sukumar et al., 2009) and the protein phosphatase 2A (PP2A) (Zhou et al., 2004; Michniewicz et al., 2007) that mediate antagonistically the phosphorylation of PIN proteins (Michniewicz et al., 2007). Loss-of-function *pid* mutant leads to a preferentially basal (lower cell side) PIN localization (Friml et al., 2004), whereas *pid* gain-of-function and *pp2a* loss-of-function mutants favor an apical (upper cell side) PIN localization (Friml et al., 2004; Michniewicz et al., 2007). These results suggest that phosphorylated and dephosphorylated PIN proteins might be recruited into the apical and basal polar targeting pathways, respectively. Thus, PIN phosphorylation would determine the directional aspects of auxin transport. To test this model, we analyzed the impact of the PIN phosphorylation at a specific site on the PIN polar targeting, auxin distribution, and auxin-mediated development.

RESULTS

PIN1 Phosphorylation at Ser337/Thr340 is Required for Auxin-Related Development

A putative phosphorylation site of PIN1 had been isolated by mass spectrometry at Ser337 and/or Thr340 in the central hydrophilic loop of the PIN1 coding sequence (Michniewicz et al., 2007). These Ser and Thr of the phosphorylation site are conserved in all plasma membrane-localized PIN proteins in *Arabidopsis thaliana* (Figure 1A) and other species (Figure S1) when compared to the endoplasmic

reticulum-localized subfamily of PIN proteins (Mravec et al., 2009). To test the involvement of the phosphorylation site in the polar PIN targeting *in vivo*, site-directed mutagenesis of the conserved residues within the PIN1 sequence was carried out (Figure 1A). Ser and Thr were both converted into Ala, which is a nonphosphorylatable residue, and to Asp, which mimics phosphorylation. The *PIN1* genes, fused to the green fluorescent protein (GFP) (*PIN1::PIN1-GFP*) and the hemagglutinin (HA) (*PIN2::PIN1-HA*), were mutagenized and the constructs were transformed into the wild type and the *pin1* and *pin2* mutants, respectively. *PIN1-GFP(Ala)* and *PIN1-GFP(Asp)* partially rescued a shoot phenotype of the *pin1* mutant, but the rescued lines displayed various developmental defects in adult plants. The independent transgenic lines *PIN1-GFP(Ala)* (5/7) as well as *PIN1-GFP(Asp*) (7/9) caused defective phyllotaxis and floral morphology, discernible by fused flowers with two pistils, outgrowth of two siliques from the same position and nondeveloped pistils (Figure 1B). The same range of the phenotypes (Figure 1B) with comparable frequencies (*PIN1-GFP(Ala)* [6/8] and *PIN1-GFP(Asp*) [6/7]) was observed when *PIN1-GFP(Ala)* and *PIN1-GFP(Asp)* were transformed into the wild type, demonstrating the dominant effect of the mutations. In contrast, whereas *PIN1-GFP(Asp)* rescued to a large extent the shoot development, it completely failed to complement embryonic and cotyledon phenotypes of *pin1*; the transformants still showed a defective embryo development, reflected by monocots, tricots or fused cotyledons at the seedling stage (Figure 1C). To investigate why the *PIN1-GFP(Asp)* could not rescue the embryonic phenotype, we examined the subcellular localization of PIN1-GFP(Asp) during embryogenesis. Consistently, defects in the polar PIN1 localization were observed in triangular-stage embryos (n=62), predominantly manifested by the loss of the basal polar localization facing the root pole in the inner embryo cells and its replacement by an apolar or preferentially apical localization (Figure 1D). These results reveal that the PIN1 phosphorylation at the site involving Ser337/Thr340 is important for the PIN1 function, particularly during flower and embryo development. Moreover, the flower defects in the wild type plants highlight the dominant effect of these mutations.

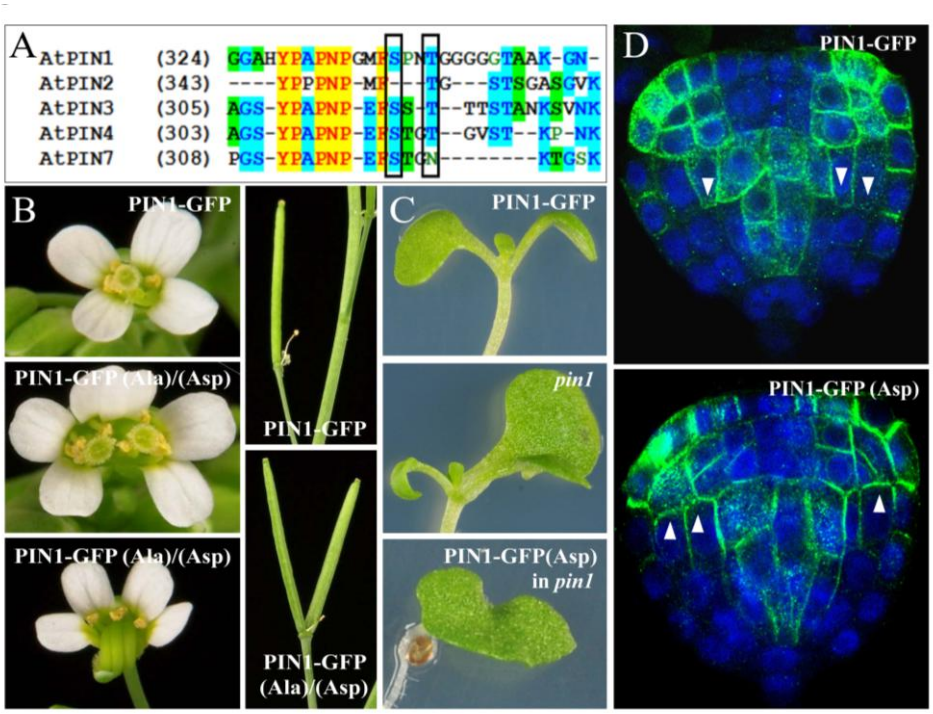

Figure 1. Developmental consequences of the mutations in Ser337/Thr340 of *PIN1-GFP*
(A) Amino acid sequence alignment of PIN1 and other PIN family members in the putative phosphorylation site-spanning region. Framed Ser and Thr were mutagenized to Ala or Asp.
(B) Morphological defects of flowers and silliques in adult plants of *PIN1-GFP(Ala)* and *PIN1-GFP(Asp)* in pin1 or wild type.
(C) Defects on cotyledon formation: *PIN1-GFP(Asp)* fails to complement the pin1 mutant at the cotyledon stage.
(D) Immunolocalization of GFP-tagged PIN1 in triangular-stage embryos of pin1: *PIN1-GFP(Asp)* localizes more apically in the inner cells as compared to the basally localized *PIN1-GFP* facing the root pole. Arrowheads mark polarity of the PIN localization.

Phosphomimic PIN1-HA(Asp) Can Functionally Replace PIN2

We tested the effects of PIN1-HA(Ala) and PIN1-HA(Asp) in the PIN2 expression domain (*PIN2::PIN1-HA* constructs) in the *pin2* mutant background. PIN2 is a key regulator of root gravitropism; it localizes to the apical side of epidermis cells and, after gravistimulation, it mediates the auxin flow along the lower side of the root from the tip toward the elongation zone where the auxin response is activated and inhibits elongation (Luschnig et al., 1998; Swarup et al., 2005; Abas et al., 2006). The expression of *PIN1-HA* in *pin2* mutants was not sufficient to restore either the gravitropic response or the asymmetric auxin accumulation as monitored by the GFP-fused artificial auxin-responsive reporter *DR5rev::GFP* (Wiśniewska et al., 2006). *PIN1-HA(Ala)* slightly enhanced the agravitropic phenotype of the *pin2* mutant (n=45) and did not rescue the activation of the *DR5*-visualized auxin response at the lower side of roots (n=25) (Figure 2A and B). In contrast, *PIN1-HA(Asp)* rescued to a large extent the agravitropic phenotype of the *pin2* mutant (n=39) and also restored the *DR5*-visualized auxin response along the lower side of the root (n=30) during gravitropic responses (Figure 2A and B). These results reveal that mutation of the phosphorylation site in PIN1 is sufficient to acquire a PIN2-like function in root epidermal cells and to efficiently mediate the auxin flow for the root gravitropic response.

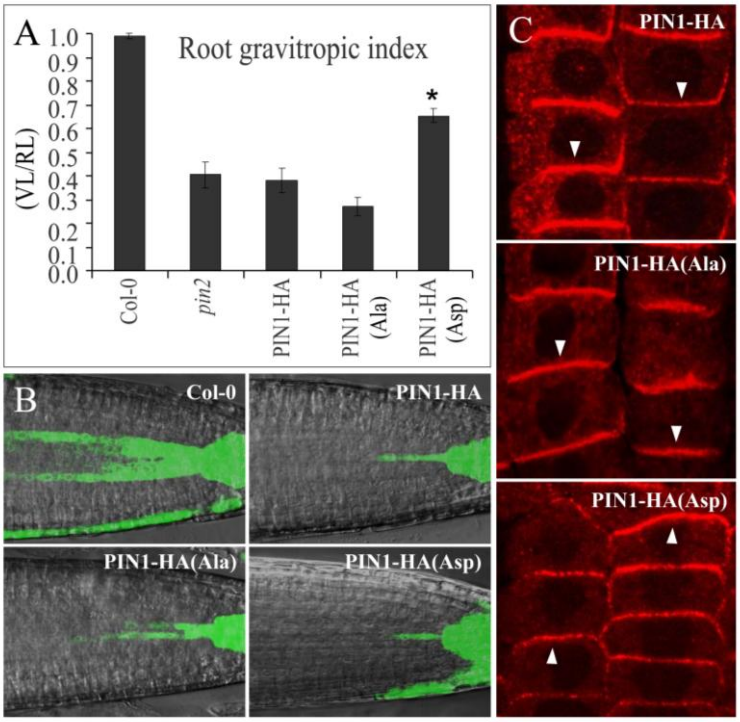

Figure 2. Effects of Ser337/Thr340 mutations in *PIN1-HA* on root gravitropism and polarity
(A) Quantitative evaluation of root gravitropism: the *pin2* agravitropic phenotype is slightly enhanced by *PIN1-HA(Ala)*, but partially rescued by *PIN1-HA(Asp)*. Data are means ± s.e.m., *, P<0.05 (t test).
(B) Auxin relocation during root gravitropic response: *PIN1-HA(Asp)*, but not *PIN1-HA* nor *PIN1-HA(Ala)*, when introduced into the *pin2* mutants, mediated the auxin translocation to the lower side of the root after gravistimulation as visualized by *DR5rev::GFP*.
(C) Immunolocalization of PIN1-HA in the *pin2* root epidermal cells: the basal localizations of *PIN1-HA* and *PIN1-HA(Ala)* contrast with the predominantly apical localization of *PIN1-HA(Asp)*. Arrowheads mark polarity of the PIN localization.

PIN Phosphorylation at Ser337/Thr340 Mediates PIN Polarity and Auxin Distribution

All observations in the *PIN1::PIN1-GFP* and *PIN2::PIN1-HA* transgenic lines suggest that the Ala and Asp mutation-induced phenotypes result from the modulated polar targeting of mutated PIN1 variants. Therefore, we investigated the subcellular polar targeting of PIN1-HA(Ala) and PIN1-HA (Asp)

proteins in epidermal cells. Ectopically expressed PIN1-HA in the epidermis localizes predominantly to the basal side of cells, whereas the endogenous PIN2 localizes to the apical side (Wiśniewska et al., 2006). PIN1-HA(Ala) localized at the basal side of epidermal cells, but, importantly, PIN1-HA(Asp) predominantly to the opposite apical side, similar to the endogenous PIN2 (Figure 2C). Accordingly, only PIN1-HA(Asp) was able to functionally replace PIN2 in the *pin2* mutant.

Similarly to PIN1-HA, the mutations in Ser337/Thr340 influenced also the PIN1-GFP targeting. In roots of the wild type, PIN1 localizes to the basal side of stele cells (Friml et al., 2002a). In comparison to PIN1-GFP, the polar localization of PIN1-GFP(Asp) was dramatically disturbed (n=83 roots). Generally, the basal polarity of PIN1 was much less pronounced and resulted in a largely nonpolar (68%) or preferentially apical distribution (7%) (Figure 3A). In contrast, PIN1-GFP(Ala) had a largely strict basal localization (n=56; Figure 3A). Importantly, these polarity changes correlated well with the incidence of the auxin response in the root tip as visualized indirectly by the auxin response reporter *DR5::GUS*. *PIN1-GFP(Ala)* lines revealed an increased *DR5* activity in the root tip, contrasting with the dramatically decreased *DR5* signal in the roots of *PIN1-GFP(Asp)* (Figure 3B). The changes in *DR5* activity were confirmed by direct auxin measurements in the 1-mm seedling root tips. Consistently with the *DR5* observations, *PIN1-GFP(Ala*) and *PIN1-GFP(Asp)* showed a higher and lower auxin content than that of *PIN1-GFP*, respectively (Figure 3C). These results demonstrate that preferentially the basally localized PIN1(Ala) promotes, whereas more apically localized PIN1(Asp) diminishes the auxin accumulation at the root tips. These quantitative changes in *DR5* activity and auxin content show that the PIN phosphorylation-mediated PIN polarity changes have a direct impact on the auxin distribution.

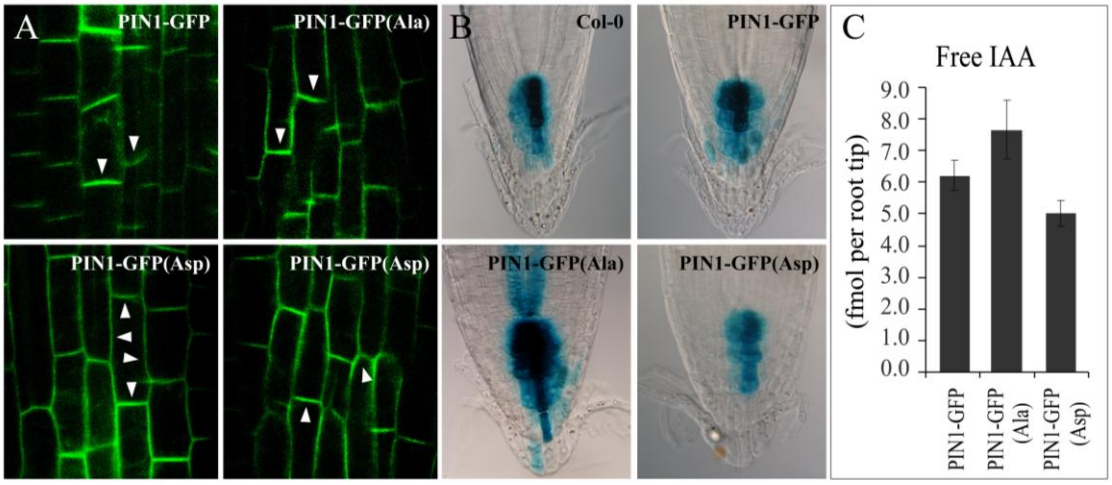

Figure 3. Effects of Ser337/Thr340 mutations in *PIN1-GFP* on polarity and auxin distribution
(A) Live images of GFP-tagged PIN1 in the stele of wild type roots: normal, predominant basal localization of *PIN1-GFP(Ala)* as compared to either nonpolar localization or basal-to-apical shift of PIN-GFP(Asp). Arrowheads mark polarity of the PIN localization.
(B) Auxin distribution in the root tip as inferred from the *DR5::GUS* expression: the *DR5* signal is increased in *PIN1-GFP(Ala)* roots, but reduced in *PIN1-GFP(Asp)* when compared to the wild type. (C) Measurement of the endogenous auxin content in the 1 mm root tips: *PIN1-GFP(Ala)* has higher whereas *PIN1-GFP(Asp)* lower auxin levels as compared with the PIN1-GFP control.

PIN1 Phosphorylation at Ser337/Thr340 is Related to the PID Action in Polar Targeting

The observed changes of PIN1 polarity, auxin distribution and resulting phenotypes revealed that phosphorylation of Ser337/Thr340 site is sufficient to redirect the PIN polarity as well as directionality of the auxin flow, similarly as shown for manipulations of the PID kinase activity (Christensen et al., 2000; Friml et al., 2004). Therefore, we addressed the question of whether this particular phosphorylation site is related to the PID kinase action in the PIN polarity determination. PID gain-of-function (*35S::PID*) leads to a basal-to-apical PIN polarity shift, which causes auxin depletion from the root meristem, ultimately leading to its collapse (Friml et al., 2004). Several independent transgenic lines of *PIN1-HA(Ala)* and *PIN1-HA(Asp)* showed the consistent changes in the root collapse frequency. We

observed that *PIN1-HA(Ala)* significantly delayed the *35S::PID*-mediated root collapse (n=96) when compared to that of the wild type *PIN1-HA* (n=85) (Figure 4A). In contrast, the collapse of the root meristem in *PIN1-HA(Asp)* (n=97) and *PIN1-HA* seedlings did not differ significantly (Figure 4A), which might be due to the already near maximum effect of *35S::PID* on PIN apicalization and root collapse.

Next, we tested PID loss-of-function line. We introduced *PIN1-GFP(Ala)* and *PIN1-GFP(Asp)* transgenes into the *pid*$^{+/-}$ *wag1 wag2* allele. WAG1 and WAG2 are the closest homologs of PID in the family of the AGC serine/threonine protein kinases of *Arabidopsis* and the triple mutant *pid wag1 wag2* displays a completely disrupted cotyledon formation (Cheng et al., 2008; Robert et al., 2008). We analyzed the F2-segregating progeny and quantified the seedlings with defective cotyledon patterning. The frequency of the seedlings that failed to make any cotyledon was increased by *PIN1-GFP(Ala)* and reduced by *PIN1-GFP(Asp)* transgenes. We observed 16% (n=816) and 4% (n=454) aberrant seedlings without cotyledons in *PIN1-GFP(Ala)* and *PIN1-GFP(Asp)*, respectively, when compared to 8% (n=788) in the F2 progeny of control crosses with the wild type *PIN1-GFP* (Figure 4B). Furthermore, the *pid wag1 wag2* mutations did not affect the PIN1-HA(Ala) and PIN1-HA(Asp) localizations at the basal and apical sides of the epidermal cells, respectively (Figure 4C). Altogether, these data show that PIN1(Ala) have antagonistic and PIN1(Asp) mutations agonistic effects with the PID action, consistently with the PID regulating the PIN polarity targeting this and/or other phosphorylation sites. Importantly, the apical localization of PIN1(Asp) does not require the function of PID and related kinases, suggesting that other potential phosphorylation sites targeted by PID or other kinases cannot override the effect of the phosphomimic mutation at the Ser337/Thr340 site. These results reveal that Ser337/Thr340 phosphorylation site is involved in the similar mechanism of PIN polarity regulation as PID action; nonetheless these results cannot discriminate whether Ser337/Thr340 is a target of PID.

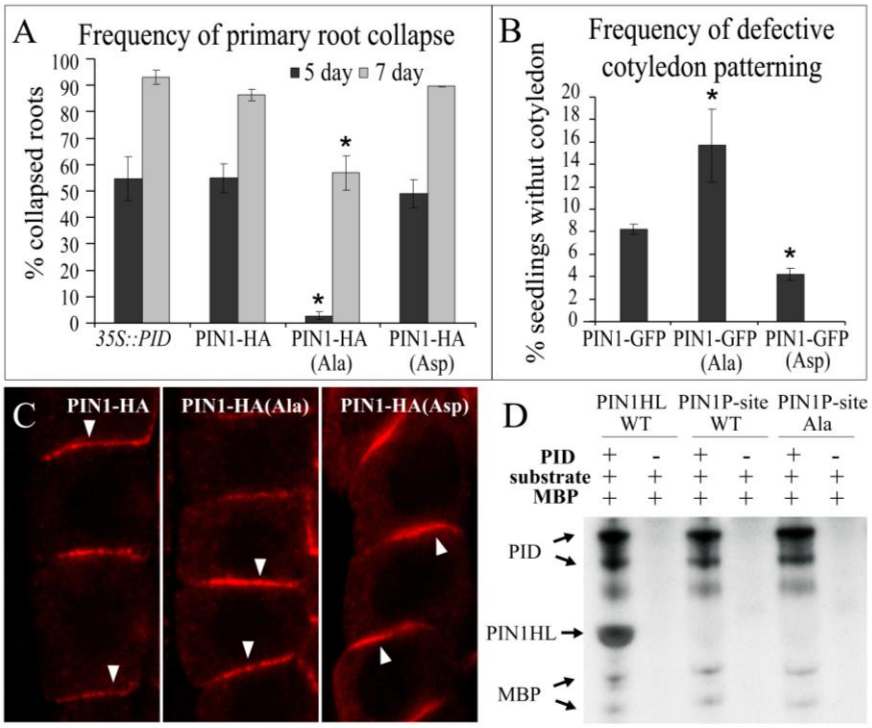

Figure 4. Effects of Ser337/Thr340 mutations similar to PID action

(A) Quantification of frequencies of primary root collapse in 5-day-old and 7-day-old seedlings in *35S::PID*: the collapse of root meristems mediated by *35S::PID* is significantly delayed by *PIN1-HA(Ala)*. Data are means ± s.e.m., *, $P<0.05$ (Fisher Exact test).

(B) Quantification of frequencies of defective cotyledon patterning in *pid wag1 wag2* triple mutant: the failure to make cotyledons in the progeny of *pid*$^{+/-}$*wag1 wag2* is increased by the *PIN1-GFP(Ala)* but decreased by *PIN1-GFP(Asp)*. Data are means ± s.e.m., *, $P<0.05$ (Fisher Exact test).

(C) Immunolocalization of PIN1-HA in the root epidermal cells of the *pid wag1 wag2* mutant: PIN1-HA and PIN1-HA(Ala) show a normal basal localization, whereas PIN1-HA(Asp) displays a basal-to-apical polarity shift, also in the absence of the PID function. Arrowheads mark polarity of the PIN localization.

(D) Autoradiograph of an *in vitro* phosphorylation assay: GST-PID autophosphorylates and efficiently phosphorylates

the large wild type hydrophilic loop of PIN1 (HIS-PIN1HL) and myelin basic protein (MBP); both wild type and the Ala mutant version of the short peptide (GST-PIN1P-site) are probably not phosphorylated by PID. + and - indicate incubated with or without the PID kinase, substrate, and MBP, respectively. Arrows mark positions of the different proteins.

PID Might not Directly Target Ser337/Thr340

Next, we tested whether the Ser337/Thr340 site of the PIN proteins can be directly phosphorylated by PID. The HIS-tagged wild type hydrophilic loop of PIN1 (HIS-PIN1HL, amino acids 288-452; Figure S2), GST-tagged PID (GST-PID), and a 30-amino-acid stretch encompassing the Ser337/Thr340 site (GST-PIN1P-site, amino acids 321-350; Figure S2) as well as its Ala-substituted version were heterologously expressed in *Escherichia coli* and coincubated in an *in vitro* phosphorylation reaction. After electrophoretic separation of the proteins, PID autophosphorylation was detected as well as phosphorylation of HIS-PIN1HL and the standard Ser/Thr kinase substrate myelin basic protein (MBP) (Figure 4D and S3). In contrast, we failed to observe any PID-dependent phosphorylation of both the wild type and mutated version of the GST-PIN1P-site (Figure 4D and S3). These results show that the PID kinase phosphorylates the large hydrophilic loop of PIN1 *in vitro*, but is probably not able to phosphorylate the Ser337/Thr340 site in the same assay.

Taken together, the results obtained in *in vivo* genetic and cell biological studies and *in vitro* phosphorlyation assays are consistent with a scenario in which the Ser337/Thr340 phosphorylation site could be a target for the other potential kinases that act together with PID in regulating the PIN phosphorylation and the apical/basal PIN polar targeting.

DISCUSSION

Our work demonstrates that phosphorylation of the PIN proteins regulates their polar targeting and the directionality of the auxin flow, which mediates various developmental processes. We identified a phosphorylation site that is required and sufficient to promote the PIN polar targeting, similarly to the activity of the PID kinase. Our *in vitro* phosphorylation results do not support that this site is a target of PID, although we cannot exclude that the short PIN1P-site peptide might not form the appropriate tertiary structure or not provide enough binding energy as offered by the large protein substrate essential for PID phosphorlyation. Alternatively, it is possible that residues important for recognition of the substrate are more distant from the targeted phosphorylation site (Kallunki et al., 1996). On the other hand, protein kinases have been also shown to recognize and phosphorylate minimal peptide segments encompassing a very few residues (Sondhi et al., 1998; Hawkins et al., 2000). Altogether, we believe that this site might be a phosphorylation target of other kinases, presumably MAP kinases, because the site shares sequence similarities to a consensus MAP kinase target characterized by a Pro following the Ser or Thr in the phosphorylation site (Pearson et al., 2001; Liu et al., 2004). Furthermore, Ser337 of PIN1 has been found to be phosphorylated in *Arabidopsis* cells treated with flg22, which induces the activation of multiple MAPKs (Benschop et al., 2007). Our data are also consistent with a view of multiple phosphorylation sites, of which some are targets of PID (Huang et al., 2010), that all mediate decisions about the PIN polar targeting.

Manipulation of Ser337 and Thr340 is sufficient to change the PIN polarity and to redirect the auxin flow. This observation provides a conceptual explanation for how various signaling pathways that control the expression (e.g. Sorefan et al., 2009) or activity of upstream kinases can, via the PIN phosphorylation, regulate the auxin distribution and, thus, influence different developmental processes. Identification of the upstream components in the phosphorylation cascade will be the challenge for the coming years and will fill the mechanistic gap on the integration of various external and internal signals into re-arrangements in the auxin distribution. Moreover, similar manipulations of this evolutionarily conserved site in other PIN proteins, in other species (Figure S1), and in a cell-type-specific fashion will enable a targeted engineering of auxin fluxes to achieve the desired changes in plant architecture and development.

EXPERIMENTAL PROCEDURES

Materials

The following mutants, transgenic plants, and constructs have been described previously: *pin1* (*pin1-1*) (Okada et al., 1991), *pin2* (*eir1-1*) (Luschnig et al., 1998), *pid*$^{+/-}$ *wag1 wag2* (kind gift of Remko Offringa, Leiden University, The Netherlands), *PIN1::PIN1-GFP* (Benková et al., 2003), *PIN2::PIN1-HA* (Wiśniewska et al., 2006), *DR5rev::GFP* (Friml et al., 2003a), *DR5::GUS* (Ulmasov et al., 1997), *35S::PID* (Benjamins et al., 2001), *pHIS-PIN1HL* (amino acids 288-452; Paciorek et al., 2005), and *pGST-PID* (Benjamins et al., 2003). Myelin basic protein (MBP) was purchased from Sigma.

The constructs *pPIN1::PIN1-GFP(Ala)*, *pPIN1::PIN1-GFP(Asp)*, *pPIN2::PIN1-HA(Ala)*, and *pPIN2::PIN1-HA(Asp)* were generated from the original *pPIN1::PIN1-GFP* (Benková et al., 2003) and *pPIN2::PIN1:HA* (Wiśniewska et al., 2006) by converting the two residues Ser337(TCG) and Thr340(ACT) on the PIN1 fragment to Ala(GCG) and Ala(GCT) or Asp(GAC) and Asp(GAT), respectively, through the PCR-based site-directed mutagenesis kit (Stratagene Quickchange XL). The mutated strands were synthesized with the following primer combinations: 5'-CCCAGGGATGTTTGCGCCCAACGCTGGCGGTGGTGGAG-3' and 5'-CTCCACCACCGCCAGCGTTGGGCGCAAACATCCCTGGG-3'for the Ala mutation and 5'-CCCAGGGATGTTTGACCCCAACGATGGCGGTGGTGGAGGC-3' and 5'-GCCTCCACCACCGCCATCGTTGGGGTCAAACATCCCTGGG-3'for the Asp mutation. The resulting constructs were transformed into the wild type and the *pin1*, *pin2*, and *35S::PID* lines. *DR5rev::GFP*, *DR5::GUS* markers, and *pid*$^{+/-}$ *wag1 wag2* mutations were introduced into the phosphorylation transgenic mutant lines by crosses. For the *in vitro* phosphorylation assay, the sequences of wild type *PIN1P-site* and mutant *PIN1P-site(Ala)* encompassing 30 amino acids surrounding the Ser337 were generated by PCR amplification with the primer pairs containing *attB* recombination sites (underlined): 5'-GGGGACAAGTTTGTACAAAAAAGCAGGCTGCGGTGGCGGTGGAGGAGCGCAT-3' and 5'-GGGGACCACTTTGTACAAGAAAGCTGGGTGTCATCCTTTCGCCGCCGCGCCTCCACC-3' from the *pPIN1::PIN1-GFP* and *pPIN1::PIN1-GFP(Ala)* constructs, respectively.
E. coli. BL21 Star™ (DE3) cells were used for heterologous expression of wild type HIS-PIN1HL and Rosetta™ cells for the other recombinant proteins.

Growth Conditions and Phenotypic Analyses

Arabidopsis thaliana (L.) Heynh. plants were grown on soil or half-strength Murashige and Skoog medium with sucrose as described (Friml et al., 2002a) under a 16-h light/8-h dark cycle at 21°C or 18°C. All phenotypic comparisons were done at least in duplicate, with three to nine independent lines of minimum 25 seedlings each time. For evaluation of root gravitropism in 6-day-old seedlings, we used the quantification tool Image J (rsbweb.nih.gov/ij/download.html) and calculated the vertical growth index (VGI=vertical length [VL]/root length [RL]) (Grabov et al., 2005). For the timing of the *35S::PID*-mediated collapse of the primary root meristem, we assayed 5-day-old and 7-day-old seedlings with a Leica binocular. The root collapse becomes visually apparent a few days after germination, and can be recognized by the thin and pointed appearance of the root tip (Benjamins et al., 2001). Results are presented as means with standard error bars and all claimed comparisons are based on statistical evaluations with *t*-test or Fisher Exact test.

***In Situ* Expression and Localization Analyses**

Histochemical stainings for GUS activity and whole-mount immunolocalizations in 5-day-old seedlings were carried out as described (Benková et al., 2003; Friml et al., 2003c; Sauer et al., 2006). Each experiment was done on three to nine independent lines with three repetitions (homozygous lines, n>15; segregating lines, n>300 individuals). Antibodies were diluted as follows: 1:1000 for rabbit anti-PIN1 (Paciorek et al., 2005); 1:500 for mouse anti-HA (Babco); 1:500 for mouse anti-GFP (Roche); and 1:600 for CY3- (Sigma) and Alex- (Invitrogen) conjugated anti-rabbit and anti-mouse secondary antibodies, respectively. For the HA-tagged PIN proteins, colocalization of anti-PIN1 and anti-HA were always carried out to confirm the identity of the proteins. For *in vivo* GFP inspection, 6-day-old seedlings were mounted in 5% glycerol without fixation for live-cell imaging. Regarding the auxin translocation assay, confocal imaging was done in 6-day-old seedlings, immediately after 3 h of a 90° gravistimulation in the dark. All the fluorescence signals were evaluated on a Zeiss LSM 510 or Leica TCS SP2 confocal laser scanning microscope. Always the same microscope settings were used for

each independent experiment and pixel intensities were taken into account when comparing the images between control and mutants. Images were finally processed with Adobe Photoshop 7.0 and Adobe Illustrator 8.0.

Auxin Measurements

1 mm-long root tips were transferred immediately after harvest to tubes containing 1 ml of methanol kept at 0°C. To each tube, $^{2}H_5$-IAA was added at the concentration of 10 fmol per root tip. The samples were put into a freezer (-20°C) and centrifuged at 36,000*g* after 24 h. Supernatants were transferred into glass tubes, evaporated to dryness, and methylated with ethereal diazomethanol. Further processing by immunopurification was performed as described (Pěnčík et al., 2009) and final analysis was done with a UHPLC coupled to a Waters Xevo™ TQ MS detector.

In Vitro Phosphorylation Assays

Approximately 3 µg of purified protein expressed in *E. coli* (PID and substrates) were added to the kinase reaction mix, containing 1× kinase buffer (25 mM Tris-HCl [pH 7.5], 1 mM DTT, 5 mM $MgCl_2$, 2 mM $CaCl_2$) and 1× ATP solution (100 µM $MgCl_2$, 100 µM ATP-Na_2, 2 µCi ^{32}P-γ-ATP). Reactions were incubated at 30°C for 45 min and stopped by addition of 5 µl of 5× protein loading buffer (310 mM Tris-HCl [pH 6.8], 10% SDS, 50% glycerol, 750 mM β-mercaptoethanol, 0.125% bromophenol blue) and boiling for 5 min. Reactions were subsequently separated over 12% acrylamide gels, which were washed 3 times for 30 min with kinase gel wash buffer (5% trichoroacetic acid, 1% $Na_2H_2P_2O_7$), coomassie stained, destained, and dried. Autoradiography was done for 48 h with Hyperfilm MP films and a Hyper-cassette (GE-Healthcare Life Sciences).

ACKNOWLEDGMENTS

We acknowledge our ex-colleague Pankaj Dhonukshe for triggering the final stage of this project. We thank Remko Offringa for providing unpublished material and for helpful discussions and inspiration, Hélène Robert-Boisivon for supervising the *in vitro* phosphorylation assay, Agnieszka Bielach for helping with the statistic analysis, Jürgen Kleine-Vehn for critical reading of the manuscript; and Martine De Cock for help in preparing it. This work was supported by the Odysseus program of the Research Foundation-Flanders (J.F., J.Z. and T.N.), the Ministry of Education, Youth and Sports of the Czech Republic (MSM 6198959216) (J.R. and A.P.).

SUPPLEMENTAL FIGURES

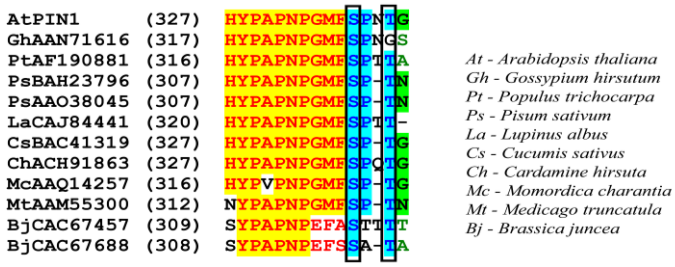

Figure S1. Evolutionarily conserved phosphorylation residues in PIN proteins
The amino acid sequence of AtPIN1 is aligned with the PIN family members from other plant species; the PIN1 protein from A. thaliana is indicated as AtPIN1 and the others by their accession numbers. The conserved Ser and Thr are framed.

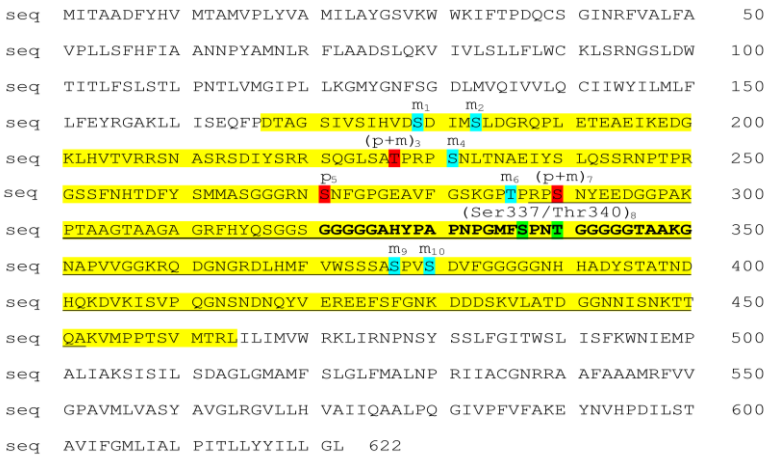

Figure S2. Putative phosphorylation sites in the central hydrophilic loop of the PIN1 protein
(A) PIN1 protein sequence. The hydrophilic loop is highlighted in yellow and all potential phosphorylation sites are marked. p indicates phosphorylation sites predicted by PhosPhAt 3.0; m indicates sites that were identified empirically (1-3). Ser337/Thr340, PIN1HL (amino acids 288-452; underlined), and the PIN1P-site (amino acids 321-350; bold) are indicated as well.
(B) Predicted topology of the PIN1 protein, including transmembrane domins and a large central hydrophilic loop (predicted by HMMTOP 2.0 and visualized by TMRPres2D). All marks are identical to those in (A).

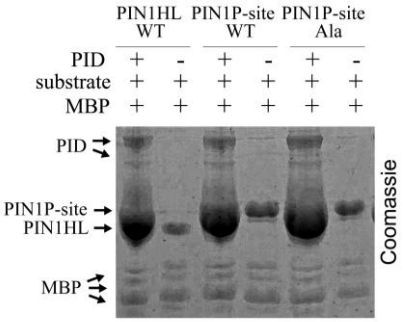

Figure S3. Coomassie-stained gel of an in vitro phosphorylation assay
+ and – indicate incubated with or without the PID kinase, substrate, and myelin basic protein (MBP), respectively. Arrows mark positions of the different proteins.

CHAPTER 4

PINOID Controls PIN-FORMED Polarity by Phosphorylation-Mediated Recruitment into the ARF-GEF GNOM-Independent Trafficking Pathway

Jürgen Kleine-Vehn, Fang Huang, Satoshi Naramoto, **Jing Zhang,** Marta Michniewicz, Remko Offringa, and Jiří Friml

Modified from Kleine-Vehn et al., (2009) Plant Cell *21*, 3839-3849

Author's Contributions: JZ performed experiments presented in Figure 1.

ABSTRACT

The phytohormone auxin plays a major role in embryonic and postembryonic plant development. The temporal and spatial auxin distribution largely depends on the subcellular polar localization of the auxin efflux carrier of the PIN-FORMED (PIN) protein family. The serine/threonine protein kinase PINOID (PID) catalyzes PIN phosphorylation and crucially contributes to the control of the apical-to-basal PIN polarity. The ARF-GEF GNOM preferentially mediates PIN recycling at the basal cell side. Interference with GNOM activity leads to dynamic PIN transcytosis between different cell sides. Our genetic, pharmacological, and cell biological approaches illustrate that PID and GNOM control PIN polarity and plant development in an antagonistic manner and that the PID-dependent PIN phosphorylation results in GNOM-independent polar PIN targeting. The data suggest that PID and the protein phosphatase 2A not only regulate the static PIN polarity, but also act antagonistically on the rate of GNOM-dependent polar PIN transcytosis We propose a model that encompasses the PID-dependent PIN phosphorylation at the plasma membrane and the subsequent sorting of PIN proteins to a GNOM-independent pathway for polarity alterations during developmental processes, such as lateral root formation and leaf vasculature.

INTRODUCTION

Postembryonic plant growth results in shapes that are not predictable by their previous embryonic architecture. Plants have evolved the outstanding ability to redefine the polarity of an already specified tissue, eventually leading to de novo postembryonic organ formation. The flexible nature of plant development most probably compensates for the plant's sessile life style. A decisive role in establishing and redefining the polarity of plant tissues is played by the phytohormone auxin (Sauer et al., 2006; Scarpella et al, 2006). Spatial and temporal auxin accumulation (auxin gradients) determine positional cues for the presumptive sites of embryonic and postembryonic primordia development (Benková et al., 2003; Friml et al., 2003; Heisler et al., 2005). Hence, insights into the control of the auxin distribution and, subsequently, signaling are key to understand this type of plant growth regulation.

The PIN-FORMED (PIN) auxin efflux carriers catalyze the cell-to-cell transport of auxin and largely mediate the spatial and temporal auxin distribution (Petrášek et al., 2006; reviewed in Tanaka et al., 2006). The coordinated polar localization of PIN proteins at different cell sides determines the direction of the auxin flux within a tissue (Wiśniewska et al., 2006). Thus, directional PIN activity has the capacity to translate cellular polarizing signals into polarity of the whole tissue. Moreover, the dynamic nature of the polar PIN localization regulates the plant development by rearranging the auxin fluxes that initiate embryonic and postembryonic developmental programs (Friml et al., 2003; reviewed in Kleine-Vehn and Friml, 2008).

A valuable tool for unravelling polar PIN-targeting mechanisms is the fungal toxin brefeldin A (BFA), which is known to interfere with various vesicle trafficking processes in cells. The molecular targets of BFA are GDP-to-GTP exchange factors (GEFs) for small G proteins of the ADP-ribosylation factor (ARF) class that activates the ARF proteins and, thus, direct the formation of vesicle coats (reviewed by Donaldson and Jackson, 2000).

In *Arabidopsis thaliana* roots, because PIN1 exocytosis is sensitive to BFA it accumulates rapidly and reversibly into so-called BFA compartments, hinting at a constitutive PIN1 cycling mechanism (Geldner et al., 2001). By means of a green-to-red photoconvertible fluorescent reporter (EosFP) that captures the internalization of PIN2 proteins and their subsequent recycling to the plasma membrane, PIN proteins have been confirmed to cycle constitutively between the plasma membrane and some endosomal compartments (Dhonukshe et al., 2007). This constitutive cycling mechanism might have several functions, such as PIN polarization after originally nonpolar secretion (Dhonukshe et al., 2008) or dynamic intracellular resorting of PIN proteins for transcytosis-like polarity alterations during plant development (Kleine-Vehn et al., 2008a).

In *Arabidopsis*, the BFA-sensitive endosomal ARF-GEF GNOM is required for the polar localization and recycling of PIN1 (Steinmann et al., 1999; Geldner et al., 2001). The inhibitory effect of BFA on PIN1 cycling in the root stele cells is due to its effect specifically on GNOM (Geldner et al., 2003). Hence, the vesicle transport regulator GNOM seemingly defines the recycling rate of the PIN1 protein to the basal (root apex-facing) cell side. Moreover, the GNOM activity is also involved in dynamic transcytosis of PIN proteins from one cell side to the other, eventually regulating the PIN-dependent tissue repolarization (Kleine-Vehn et al., 2008a).

Remarkably, while PIN1 localizes preferentially to the basal, PIN2 is targeted to the apical (shoot apex-facing) cell side in the same cell, suggesting polarity determinants in the protein sequence itself (Wiśniewska et al., 2006). The polarity signals are probably related to the phosphorylation sites within the PIN proteins (Huang et al., 2010; Zhang et al., 2010), because the Ser/Thr protein kinase PINOID (PID) and also the protein phosphatase 2A (PP2A) act on the PIN phosphorylation, thus determining the apical or basal PIN targeting, respectively (Friml et al., 2004; Michniewicz et al., 2007). The *pid* mutants display apical-to-basal PIN polarity shifts that cause defects during embryo and shoot organogenesis (Christensen et al., 2000; Benjamins et al., 2001; Friml et al., 2004), whereas the *PID* gain-of-function specifically mistargets the PIN proteins to the apical cell side in the primary root, with auxin depletion from the root meristem and its collapse as a consequence (Benjamins et al., 2001; Friml et al., 2004). Similarly, basal-to-apical PIN polarity shifts in the primary root meristem can be observed in the loss-of-function mutants of the A regulatory subunits of PP2A (Michniewicz et al., 2007).

Recently, several Ser- and Thr-containing phosphorylation sites in conserved motifs have been identified in the PIN proteins. By using engineered "dephosphorylated" or phosphorylation-mimicking mutant PIN proteins, phosphorylation of these specific residues in the PIN proteins have been found to determine the apical-to-basal polar PIN localization (Huang et al., 2010; Zhang et al., 2010). However, the underlying mechanism of how the phosphorylation-based sequence modulation of PIN proteins affects their polar localization is unknown. In particular, the question of how the PID-dependent pathway relates to the GNOM-dependent recycling of PIN proteins remains to be addressed.

Here, we specifically investigated the interaction between the PID and the GNOM pathways. Based on our findings, we propose a model in which the PIN proteins are phosphorylated by PID that decreases their affinity to the GNOM-dependent basal recycling pathway. The increased PIN affinity to the distinct and presumably ARF-GEF-dependent apical targeting pathway eventually initiates PIN transcytosis from the basal to the apical cell side. This mechanism might be functionally important for various dynamic PIN polarity alterations during plant development, such as lateral root primordia formation or vascular development.

RESULTS

The Localization of PID and PIN Suggests a Preferential Interaction at the Plasma Membrane

To address the question how PID regulates the polar PIN targeting in planta, we initially investigated the PID localization and targeting. PIN2 and PID display substantial colocalization at the plasma membrane (Michniewicz et al., 2007) (Figure 1A). As a strong internal PID-yellow fluorescent protein (YFP) signal was observed, we analyzed the endosomal PIN and PID distributions, but the colocalization of endogenous PIN2 and functional PID-YFP was not detectable in the endosomes (Michniewicz et al., 2007) (Figure 1A). To elaborate on this observation, we induced PIN2 internalization in root epidermal cells. Whereas PIN2 strongly accumulated in intracellular compartments after latrunculin B (LatB)-dependent actin depolymerization (Figure 1B) or BFA treatment (Figure 1C), PID localization was less sensitive and accumulating endosomes were more dispersed (Figures 1B and 1C), resulting into only faint endoplasmic colocalization with PIN2.

As no pronounced endosomal colocalization or cotrafficking of PID and PIN proteins could be induced, a largely PIN-independent endosomal trafficking or membrane recruitment of PID was assumed. Besides the weak endoplasmic colocalization, both PIN and PID proteins reside and colocalize mainly in/at the plasma membrane; therefore, we hypothesized that the plasma membrane was the most likely site of the PID-PIN interaction for the regulation of the PIN polarity. This finding suggests that the PID-dependent PIN phosphorylation at the plasma membrane might affect the PIN residence or recycling and, eventually, impose intracellular resorting of PIN proteins.

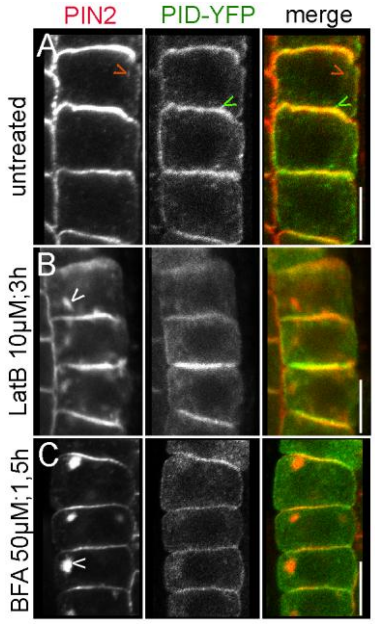

Figure 1. Subcellular localization of PIN2 and PID in root epidermal cells
(A) Pronounced colocalization of PIN2 (in red/left panel) and PID-YFP (in green/medium panel) at the plasma membrane, whereas no pronounced colocalization in the endosomes could be detected.
(B) and (C) Strong intracellular PIN2 localization induced by Latrunculin B (B) and BFA (C) treatments, but weaker and more dispersed endosomal PID-YFP accumulations.
Bars = 10 µm.

PID and GNOM have Opposite Effects on PIN Polarity and Auxin Accumulation in the Primary Root

In animals and plants, the polar targeting to the plasma membrane ultimately requires polar sorting processes at endosomes (Farr et al., 2009; reviewed in Kleine-Vehn and Friml, 2008). The predominant colocalization of PID and PIN at the plasma membrane suggests that the polar PIN distribution is regulated upstream of the actual endosomal sorting event. Hence, we investigated how PID-dependent PIN phosphorylation relates to the constitutive PIN recycling that is presumably related to intracellular polar sorting.

The endosomal ARF-GEF GNOM is known to mediate the PIN recycling preferentially to the basal cell side, and pharmacologically or genetically reduced GNOM activity leads to a dynamic basal-to-apical PIN transcytosis (Kleine-Vehn et al., 2008a). Intriguingly, the similar apical PIN polarity shift is triggered also by the *pp2aa* loss-of-function (Michniewicz et al., 2007) and *PID* gain-of-function (*35S$_{Pro}$:PID*) (Friml et al., 2004) (Figures 2A and 2B). In agreement with these similar cellular phenotypes, *PID* gain-of-function and reduced GNOM function also result in root meristem collapse (Benjamins et al., 2001; Geldner et al., 2004) (Figure 2C), Notably, the severity of the PIN apicalization in *35S$_{Pro}$:PID* and *gnom^{R5}* correlated well with the frequency of root meristem abortion (Figures 2A to 2C). Moreover, auxin seemed to be depleted from the root tip after the increased rate of PIN phosphorylation in *35S$_{Pro}$:PID* and *pp2aa* mutants (Michniewicz et al., 2007). Similarly, pharmacological inhibition of GNOM decreased the ectopic auxin response as monitored by *DR5$_{Pro}$:GFP* activity (Figures 2D and 2E; Figures S1E and 1F), consistent with the auxin depletion from the root tip by the upward-directed auxin flux. In line with the requirement of PIN-mediated auxin accumulation in the root tip for root meristem activity (Friml et al., 2002a), the expression pattern of the quiescent center and columella markers was altered after BFA treatment (see Supplemental Figures 1A to 1D). These and previous observations reveal that *PID* gain-of-function and *gnom* loss-of-function alleles have similar effects on PIN polarity, auxin distribution, and development of the primary root.

PID and GNOM have Opposite Effects on the Formation of Lateral Roots and Vascular Tissues

Dynamic PIN polarity alterations during lateral root development have been shown to depend on GNOM; accordingly, partial loss of *gnom* mutant alleles display severely reduced numbers of lateral roots (Benková et al., 2003; Geldner et al., 2004; Kleine-Vehn et al., 2008a) as well as *35S$_{Pro}$:PID* lines (Benjamins et al., 2001), but the primary root collapse precedes the lateral root induction in the *35S$_{Pro}$:PID* background (Benjamins et al., 2001; Friml et al., 2004), making the interpretation of this observation difficult. Therefore, we studied the PID function in lateral root development prior to the root collapse by inducing lateral root organogenesis with auxin. We observed an aberrant development of lateral root primordia and strongly reduced primordium spacing after auxin treatment in *PID* gain-of-function lines (Figures 2F, 2G, and 2H), undistinguishable from those in weak *gnom* alleles.

Dynamic PIN polarity rearrangements also accompany and regulate leaf vascular development (Scarpella et al., 2006). According to the anticipated function of GNOM for dynamic PIN polarity alterations (Kleine-Vehn et al., 2008a), weak *gnom* mutant alleles display severe defects in leaf vasculature development (Koizumi et al., 2000; Geldner et al., 2004) (Figures 2O and 2P). Therefore, we analyzed the PID involvement in leaf vasculature development. Both *PID* gain-of-function and *pid* loss-of-function seedlings showed defects in leaf vasculature development (Figures 2I to 2N), suggesting that PID might also regulate dynamic PIN polarity alterations during vascular development. Intriguingly, *35S$_{Pro}$:PID* seedlings had lost the main vein polarity in cotyledons and ectopic vasculature development at the leaf margin, largely phenocopying the partial loss of the *gnom^{R5}* function (Figures 2M to 2P, arrowheads). These and previous observations show that *PID* gain-of-function and *gnom* loss-of-function alleles similarly affect lateral root organogenesis and vascular tissue development.

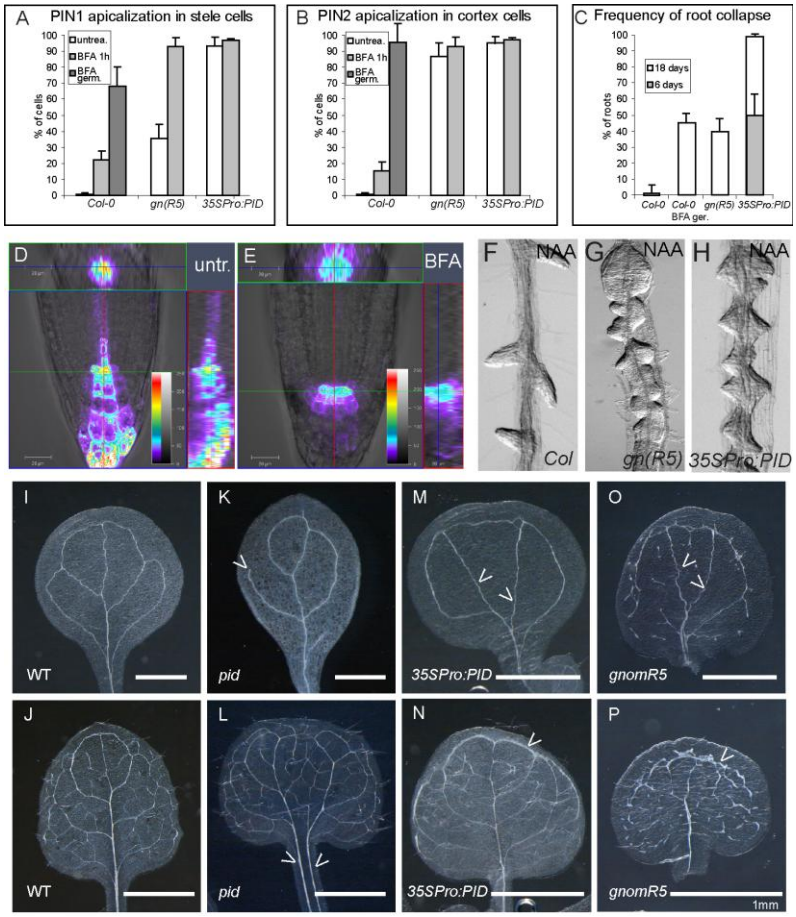

Figure 2. Opposite actions of GNOM and PID on PIN polarity and plant development
(A) and (B) Apicalization of PIN1 (A) in stele and PIN2 (B) cortex cells in the wild type, partial GNOM loss of function (*gnom^{R5}*), and PID gain of function (*35S$_{Pro}$:PID*). White bars represent the untreated condition and gray bars illustrate BFA treatment for 1 h (light gray) or germination on BFA (dark gray).
(C) Correlation of the severity of the PIN apicalization with root collapse in *35S$_{Pro}$:PID*, BFA-treated plants and the

weak *gnom*^{R5} allele after 18 days.
(D) and (E) Z-stack analysis and subsequent fluorescent intensity profiling (red/yellow depicts high and blue/purple low fluorescent intensities) of the auxin-responsive promoter element *DR5rev*$_{Pro}$*:GFP* in untreated (D) and BFA-treated (E) seedlings. The central image shows a single medium confocal section, while the top and right insets represent the radial and longitudinal distributions of the signal, respectively, giving three-dimensional information of the signal intesity. Under untreated conditions, DR5 signaling is the highest in the quiescent centre and outermost tier of columella cells (D). In contrast, BFA-dependent inhibition of GNOM function leads to depletion of the response maximum in the root tip and radial expansion of the signal (E).
(F) to (H) Auxin treatment induces enhanced, but spaced, lateral root development in wild-type seedlings (F). In contrast, both *gnom*^{R5} (G) and *35S*$_{Pro}$*:PID* (H) mutants display defective primordium spacing and development after naphthaleneacetic acid (NAA) treatment, respectively.
(I) to (P) Vascular development of cotyledons (I, K, M, O) and leaves (J, L, N, P) in wild-type (I and J), *pid* (K and L), *35S*$_{Pro}$*:PID* (M and N), and *gnom*^{R5} (O and P) backgrounds. Arrows point out vein discontinuity (K), vein polarity defects (L, M, O), and enhanced cortical vascularization (N and P).

PID and GNOM Show an Antagonistic Genetic Interaction

The similar effects of *PID* gain-of-function and *gnom* loss-of-function on polar PIN deposition, auxin distribution; and plant development suggest an antagonistic action of PID and GNOM. We introduced *PID* gain-of-function into the partial loss of the *gnom*^{R5} mutant background. The *gnom*^{R5} mutant embryos were defective in apical and basal embryo patterning (Figures 3A and 3B). However, only one-third of the mutant seedlings had fused cotyledons and never displayed rootless development (Geldner et al., 2004) (Figure 3F). The *35S*$_{Pro}$*:PID /gnom*^{R5} double mutants showed notably stronger embryonic apical-basal patterning phenotypes being defective in root and shoot formation (Figure 3C, D). In the most affected embryos, apical-basal polarity had disappeared completely (Figure 3D), strongly resembling the complete *gnom* loss-of-function (Shevell et al., 1994; Steinmann et al., 1999). Consistently with the defects observed during embryo development, the *35S*$_{Pro}$*:PID gnom*^{R5} double mutants showed pronounced patterning defects during seedling development, resulting in an early developmental arrest (Figure 3G). Remarkably, all observed aspects of the *35S*$_{Pro}$*:PID gnom*^{R5} phenotypes were markedly stronger than those of each of the single mutants and resembled those of the complete *gnom* loss-of-function (Steinmann et al., 1999; Shevell et al., 1994). This synergistic genetic interaction between *PID* gain-of-function and partial *gnom* loss-of-function together with the similar phenotypes of the single alleles in a range of developmental and cellular processes suggest an antagonistic action of PID and GNOM in the same process.

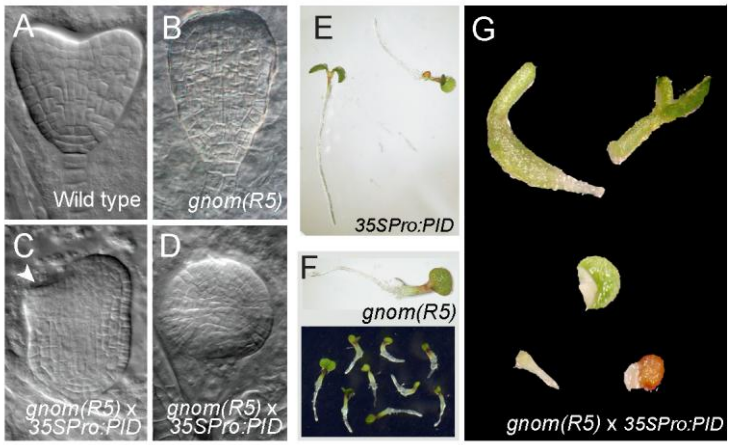

Figure 3. Genetic interaction of PID and GNOM
(A) to (D) Patterning defecst in embryos compared to wild-type embryos (A). Apical and basal patterning defects in *gnom*^{R5} mutant embryos (B). More severe apical-to-basal embryonic patterning defects in *35S*$_{Pro}$*:PID gnom*^{R5} double mutants, leading to the complete loss of apical basal patterning (C) and (D).
(E) and (F) Viable seedling development in *35S*$_{Pro}$*:PID* (E) and *gnom*^{R5} (F)
(G) Strongly affected seedling morphology and growth arrest in *gnom*^{R5} x *35S*$_{Pro}$*:PID* crosses, resembling full *gnom* knock-out mutants.

GNOM Localization is Independent of PID Activity

Next we addressed the mechanism underlying the antagonistic action of PID and GNOM. One possibility is that PID might regulate subcellular GNOM localization and thus influence its activity. We initiallye analyzed the localization of GNOM that resides in an endosomal compartment, functionally defined as recycling endosome (Geldner et al., 2003). GNOM-MYC occurred closely to and regularly colocalized with anti-ARF1-labeled endomembranes (Figure 4A; Figures S2A to 2D). This partial colocalization of ARF1 and GNOM might indicate a potential function for the polar PIN targeting at ARF1-positive endosomes. In agreement with this assumption, a GTP-locked, constitutively active *arf1*^{QL} mutant is defective in the polar PIN targeting (Xu and Scheres, 2005; Kleine-Vehn et al., 2008b).

By means of the endocytic tracer FM4-64 that labels GNOM-positive endosomes only within 10-15 min (Geldner et al., 2003), GNOM had been found not to reside at early endosomes (Chow et al., 2008). In support of this, the early endosomal ARF GEF BEN1/MIN7 does not colocalize with GNOM (Tanaka et al., 2009).

Whereas both ARF1 and GNOM-MYC showed a pronounced sensitivity to BFA (Figure 4C), they were not sensitive to treatment with the phosphatidylinositol-3-kinase inhibitor wortmannin that targets late endocytic trafficking to the vacuole by affecting the prevacuolar compartment (PVC) maturation (Matsuoka et al., 1995; daSilva et al., 2005; Kleine-Vehn et al., 2008b) (Figure 4B). These findings imply that GNOM and its potential substrates of the ARF1 subclass do not function at the PVC and substantiate previous assumptions that GNOM acts at a late endosome required for PIN recycling (Geldner et al., 2003; Chow et al., 2008), but is not directly involved in PVC-dependent PIN trafficking to the lytic vacuole for degradation (Kleine-Vehn et al., 2008c).

Notably, the *PID* overexpression did not visibly alter the expression (Figures 4D and 4E) nor the subcellular distribution of GNOM (Figure 4F). We utilized the stabilizing effect of BFA on ARF/ARF-GEF intermediates to study the GNOM functionality in the *PID* gain-of-function. GNOM proteins accumulated normally after BFA treatments in *35S*$_{Pro}$*:PID*, indicating that the overall interaction of GNOM and ARF proteins was largely unaffected (Figure 4F, inset). These findings suggest that PID does not directly regulate the subcellular GNOM localization or its BFA-sensitive ARF-binding activity.

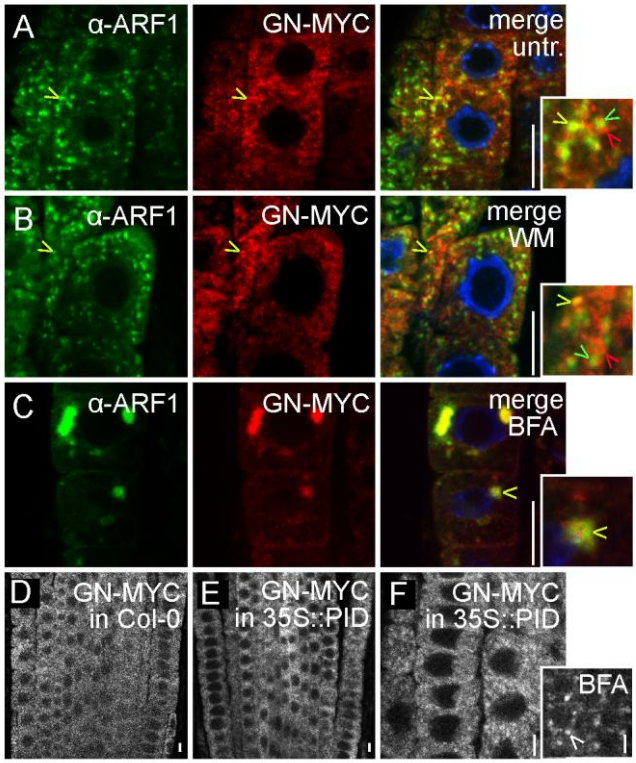

Figure 4. PID-independent GNOM localization
(A) to (C) Partial anti-ARF1 (green) and GNOM (GN-MYC) (red) colocalization in untreated seedlings (A) and treated with wortmannin (WM; 30 µM, 2 h) (B), and BFA (50 µM, 1 h) (C).
(D) and (E) Similar expression pattern of GNOM in wild type (D) and in *35S$_{Pro}$:PID* (E).
(F) Normal subcellular distribution and response to BFA (inset) of GNOM-MYC in *35S$_{Pro}$:PID*-expressing seedlings.
Bars = 10 µm.

PID and PP2A Antagonistically Affect PIN Sorting into a GNOM-independent Pathway

To further investigate by which mechanism PID and GNOM functions were connected, we assessed the GNOM-dependent recycling of the PIN1 protein in *PID* gain-of-function mutants, by using BFA that inhibits GNOM with rapid intracellular PIN1 accumulation as a consequence (Geldner et al., 2003) (Figure 5B). While GNOM remained sensitive to BFA (Figure 4F), the effect of BFA on the PIN1 localization was severely compromised in *35S$_{Pro}$:PID* lines, as manifested by the strongly reduced BFA-induced PIN1 internalization and PIN1 retention at the plasma membrane (Figure 5D; Figure S3A).

The partial loss of the phosphatase activity in *pp2aa1 pp2aa3* double mutants similarly reduced the BFA-induced PIN1 accumulation in BFA compartments (Figure 5F; Figure S3A). This finding suggests that gain of PID kinase and loss of PP2A phosphatase activity both result in PIN recruitment to a BFA-insensitive and, hence, GNOM-independent apical targeting pathway.

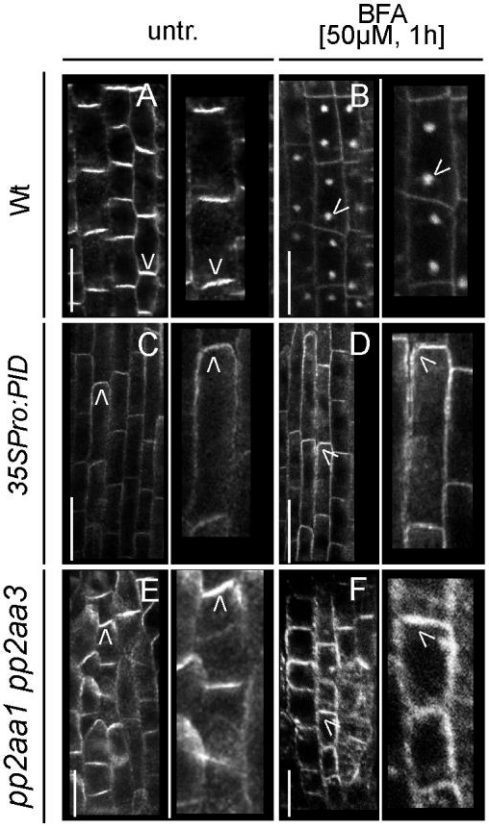

Figure 5. BFA-insensitive PIN trafficking by antagonistic PID and PP2A action
(A) Basal PIN1 localization in stele cells of wild-type seedlings.
(B) Rapid PIN internalization after BFA treatment, because of its inhibitory effect on the ARF-GEF GNOM (Geldner et al., 2003).
(C) Apical PIN1 localization in stele cells as a consequece of *PID* gain-of-function.
(D) Largely BFA-insensitive PIN1 localization in *35S$_{Pro}$:PID*, displaying a reduced accumulation in BFA compartments and persistent labeling of the plasma membrane.
(E) Preferentially apical PIN1 localization due to partial loss of PP2A function in *pp2aa1 pp2aa3* double mutants.
(F) Reduced sensitivity to BFA of PIN1 trafficking in *pp2aa1 pp2aa3* double mutants.
Bars = 10 µm.

PID and PP2A Antagonistically Determine the Affinity of PIN Proteins to Distinct Apical and Basal Targeting Machineries

BFA preferentially interferes with the basal PIN recycling and, hence, leads in time to the artificial recruitment to the apical targeting pathway and basal-to-apical translocation of basal cargos, reminiscent of transcytosis in animal epithelial cells (Kleine-Vehn et al., 2008a). The reduced sensitivity of the PIN protein trafficking to BFA treatments in *35S$_{Pro}$:PID* and *pp2aa* hints at a favored recruitment of phosphorylated PIN proteins to a BFA-insensitive, GNOM-independent recycling pathway. In an alternative scenario, BFA could also preferentially inhibit PIN internalization at the apical cell side, reducing PIN accumulation in BFA compartments. To distinguish between these two scenarios, the PIN basal-to-apical shift was analyzed and the GNOM function was partially inhibited by BFA. A mild 1-h BFA treatment induced only weak or no basal-to-apical PIN2 transcytosis in the lower cortex cells of wild-type seedlings (Figures 6A and 6B; Figure S3B). In contrast, PP2A phosphatase-deficient *pp2aa1* mutants showed an enhanced BFA-induced basal-to-apical PIN transcytosis in cortex cells (Figures 6C and 6D; Figure S3B). In contrast, in *pid* loss-of-function mutants, the apical PIN incidence after prolonged (3 h) GNOM inhibition was lower than that of the wild type (Figures 6E and 6F; Figure S3B). However, PID was not absolutely required for the BFA-induced apical shift of PIN proteins because a complete apical PIN polarity shift was induced after 12 h of BFA treatment in *pid* mutants as well (Figure 6G), indicating a functional redundancy within the PID pathway or a partial PID kinase-independent BFA-induced PIN transcytosis. These data suggest that a higher PIN2 phosphorylation state in a *pp2aa1* mutant background (Michniewicz et al., 2007) promotes the PIN affinity to the apical targeting machinery, whereas a reduced PIN phosphorylation in a *pid* mutant background results in decreased PIN affinity for the apical targeting pathway (Figure 6H). Hence, we conclude that the PID and PP2A activities determine the affinity of the PIN proteins for the basal GNOM-dependent or the apical GNOM-independent polar targeting pathways.

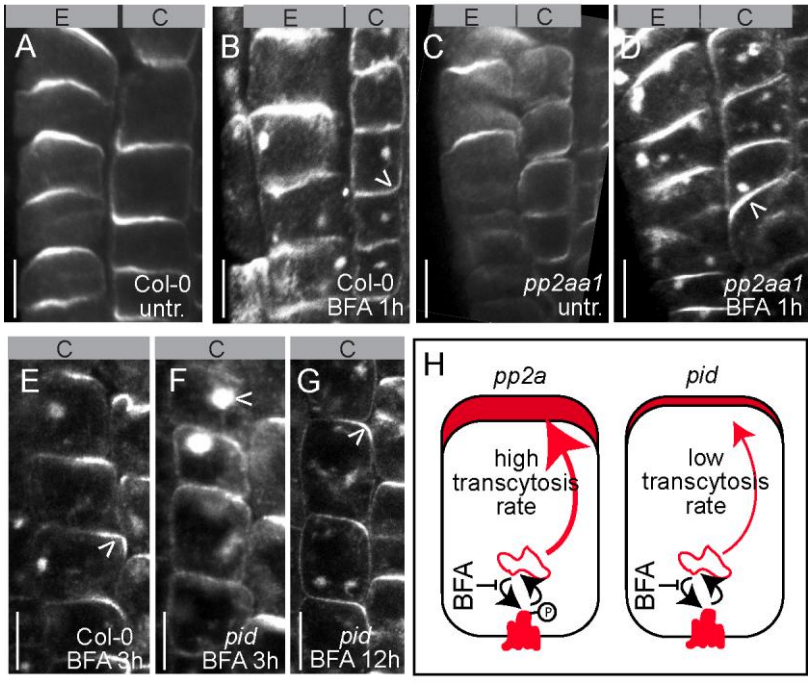

Figure 6. PP2A and PID modulate the BFA-induced transcytosis of PIN proteins
(A) to (D) Wild-type seedlings (A) display only weak basal-to-apical transcytosis of PIN2 in cortex cells after 1 h of BFA [50 µM] treatment (B). Enhanced basal-to-apical transcytosis of PIN2 in cortex cells of *pp2a* mutants (C) after 1 h of BFA (50 µM) treatment (D).
(E) to (G) Preferential apical PIN2 localization in lower cortex cells of wild-type seedlings after 3 h of 50 µM BFA incubation (E). Strong PIN2 accumulation in BFA compartments and reduced basal-to-apical transcytosis of PIN2 in

cortex cells in *pid* mutants (F). PIN2 recruitment to the apical cell side in lower cortex cells after prolonged BFA treatments (12 h) in *pid* mutant background (G).
(H) Scheme depicting altered affinity of PIN proteins to the apical targeting machinery and subsequent PIN transcytosis rate in *pp2aa1* and *pid* mutants.
E, epidermal cell files; C, cortical cell files. Bars = 10 µm.

The PIN Phosphorylation Status Determines the Differential Recruitment to GNOM-dependent or GNOM-independent Pathways

Next, we examined whether reduced PIN recruitment to the GNOM-dependent basal targeting pathway is directly determined by its PID-dependent phosphorylation state. Recently, the phosphorylation sites in PIN1 that are target of PID have been identified and verified with unphosphorylated *PIN1*^{S123A}*-GFP* or phosphorylation-mimicking *PIN1*^{S123E}*-GFP* constructs (Huang et al., 2010). Phosphomimicking PIN1^{S123E}-GFP showed largely BFA-insensitive trafficking (Figures 7E and 7F), suggesting that phosphorylated PIN proteins get recruited to a GNOM-independent pathway. In contrast, non phosphorylated *PIN1*^{S123A}*-GFP* localization remained sensitive to BFA (Figures 7C and 7D). In agreement with the differential recruitment to the GNOM-dependent basal or GNOM-independent apical pathways, PIN mutant proteins mimicking constitutive phosporylation (*PIN1*^{S123E}*-GFP*) or dephosphorylation (*PIN1*^{S123A}*-GFP*) showed a preferential apical or basal localization, respectively (Figures 7C and E) (for detailed analysis, see Huang et al., 2010).

This finding indicates that the PID-dependent PIN phosphorylation state determines the differential PIN recruitment to ARF-GEF-dependent pathways. Unphosphorylated PIN proteins are preferential cargos for the BFA-sensitive ARF-GEF GNOM-dependent basal polar targeting pathway. In contrast, PID-dependent PIN phosphorylation (Michniewicz et al., 2007; Huang et al., 2010) reduces the affinity of PIN proteins to the basal GNOM-dependent recycling pathway, leading to BFA-insensitive apical targeting.

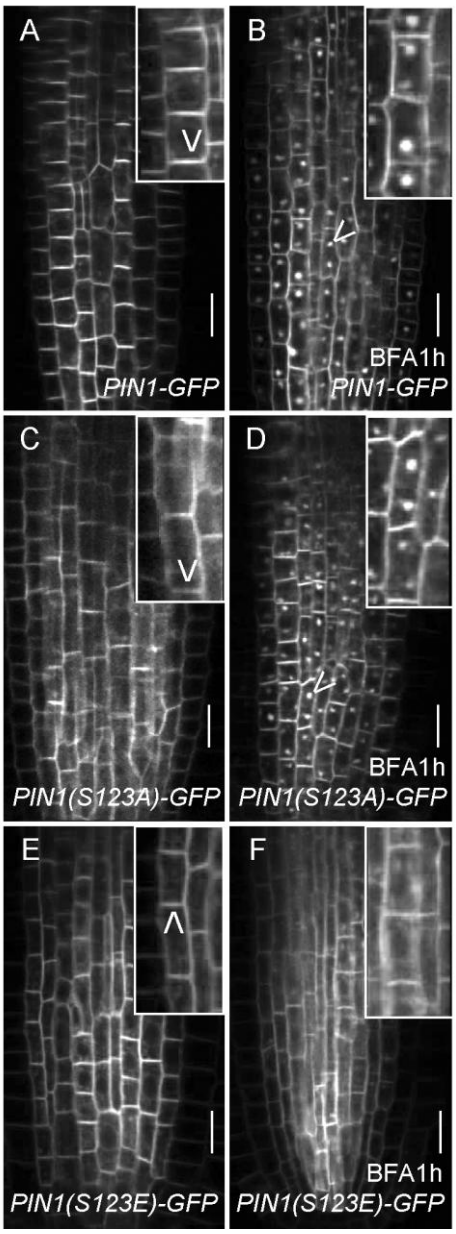

Figure 7. BFA-independent PIN targeting by phosphorylation-based sequence modification
(A) and (B) PIN1-GFP localization in the root (A) is sensitive to BFA treatment, leading to PIN1-GFP accumulation in BFA compartments (B).
(C) and (D) Dephosphorylated PIN *(PIN1^{S123A}-GFP)* targeting in untreated (C) and BFA treated seedlings (D).
(E) and (F) *PIN1^{S123E}-GFP* localisation in untreated (E) and BFA treated seedlings (F), indicating that the phosphorylated PIN proteins preferentially traffic in a BFA-resistant manner.
Bars = 10 µm.

DISCUSSION

PID and GNOM Antagonistically Regulate PIN Polarity and Plant Development

The Ser/Thr kinase PID and the ARF-GEF GNOM are the most prominent regulators of the polar PIN targeting identified to date. PID plays a decisive role in the apical-basal polar PIN targeting and phosphorylates PIN proteins at specific sites (Friml et al., 2004; Michniewicz et al., 2007; Huang et al., 2010). The mechanism by which the PID-dependent PIN phosphorylation regulates the polar PIN delivery and its relation to the GNOM-dependent PIN subcellular trafficking has been elusive so far.

In a remarkable analogy, *PID* gain-of-function and *gnom* loss-of-function lead to the ectopic apical PIN localization in *Arabidopsis* root cells (Friml et al., 2004; Kleine-Vehn et al., 2008a),

resulting in auxin depletion from the root tip and root meristem collapse. In contrast, *pid* loss-of-function and GNOM activity favor basal PIN targeting (Friml et al., 2004; Kleine-Vehn et al., 2008a). In agreement with the subcellular phenotype, the developmental defects in partial *gnom* loss-of-function mutants and *PID* gain-of-function lines were similar, such as lateral root primordia spacing, leaf vascular development, and collapse of the primary root meristem. Furthermore, *PID* overexpression in partial *gnom* loss-of-function mutants induce phenotypes reminiscent of the complete *gnom* loss-of-function, further suggesting that PID might affect GNOM-dependent processes. Our data indicate that GNOM and PID are part of the same mechanism for the polar PIN delivery, because, intriguingly, they interact synergistically with gain-of-function and loss-of-function mutants, implying that they regulate the PIN polarity in an antagonistic manner.

PID Induces PIN Sorting into a GNOM-independent Pathway

Morphological and cellular phenotypes as well as genetic interaction revealed that PID and GNOM are part of the same mechanism that regulates the polar PIN delivery. However, PID does not appear to alter either GNOM localization or its activity. PID kinase gain of function or partial PP2A phosphatase loss of function reduce the BFA sensitivity of the PIN1 localization at the apical plasma membrane, suggesting that PIN phosphorylation promotes its BFA-insensitive, GNOM-independent targeting. This assumption was confirmed by site-directed mutagenesis of PID-targeted phosphorylation sites in PIN1 (Huang et al., 2010), where phosphomimicking versions of PIN1-GFP show a largely BFA-insensitive trafficking. These observations correlate with previous findings that increased PID kinase or decreased PP2A phosphatase activities (Friml et al., 2004; Michniewicz et al., 2007) or phosphorylation-mimicking mutations (Huang et al., 2010) promote the incidence of PIN proteins at the apical polar domain. Consistently, the PID-dependent PIN phosphorylation leads to the PIN protein recruitment into a GNOM-independent trafficking pathway and finally to the apical PIN delivery.

Proposed Model for PID/GNOM-dependent Polar PIN Transcytosis

Polar sorting of cargos as we learned from animal models typically takes place at the endosomal level in so-called sorting endosomes (Farr et al., 2009). However, the PID localization is most pronounced at the plasma membrane, implying that PID does not directly function at the place of the polar PIN sorting. Consequently, PID might not affect the polar targeting of de novo synthesized and, presumably, apolarly secreted PIN proteins (Dhonukshe et al., 2008). We propose that PID regulates the PIN localization upstream of its polar sorting by phosphorylating PIN proteins at the plasma membrane. Following their internalization into endosomes, the phosphorylated PIN proteins have a reduced affinity to the GNOM-dependent basal recycling pathway (Figure 8). As a result, the phosphorylated PIN proteins are recognized and, to a large extent, recruited to the apical GNOM-independent trafficking pathway that still requires ARF1-type proteins (Kleine-Vehn et al., 2008b). This alternative recruitment leads to the basal-to-apical PIN transcytosis (Figure 8). The close PID homologs PID2, WAG1, and WAG2 kinases might similarly contribute to polar PIN resorting during plant development, but the redundancy or specificity of these components still needs to be investigated.

The PID activity could be counteracted by the PP2A phosphatase activity that eventually restores the PIN recruitment to the GNOM-dependent basal recycling pathway. Since PP2AA components can act on multiple, most likely also PIN-unrelated substrates (Zhou et al., 2004) and is broadly subcellularly distributed (Michniewicz et al., 2007), its place and mode of action in PIN polar targeting is still unclear.

The proposed mechanism for PID- and GNOM-dependent polar PIN targeting seems to be functionally important for plant development, because PIN proteins undergo dynamic polarity alterations during various developmental processes, such as gravitropism, lateral root primordium formation, and leaf vascular development (Friml et al., 2002b; Benková et al., 2003; Scarpella et al., 2006; Sauer et al., 2006; Heisler et al., 2005). These processes require both GNOM and PID activity, suggesting that they are both involved in dynamic PIN polarity alterations. We hypothesize that a PID/PP2A-dependent PIN phosphorylation or dephosphorylation might induce rapid PIN polarity changes during plant development via a GNOM-dependent and GNOM-independent transcytosis-like mechanism (Figure 8).

Polar targeting and transcytosis of polar plasma membrane cargos have been extensively studied in animal epithelial cells. A prominent example is albumin that transcytoses from the luminal (apical) to the abluminal (basolateral) sides of the cell (Hu and Minshall, 2009). Intriguingly, GP60, a plasma membrane-located albumin-binding protein, becomes phosphorylated at the plasma membrane

after its binding to albumin (Tiruppathi et al., 1997). Subsequently, a SRC-kinase-dependent signaling cascade initiates the internalization of the GP60/albumin at the apical cell side, leading to its transcytosis and exocytosis at the basolateral cell side (Hu and Minshall, 2009).

The question remains whether the phosphorylation of GP60 in animal cells, in analogy to the PIN phosphorylation in plants, negatively affects the recycling of albumin-bound GP60 back to the apical cell side, subsequently, promoting its translocation to the basolateral side by endosomal resorting. Similarly, it is tempting to speculate that after PID-dependent PIN phosphorylation, a "SRC-like" signaling cascade could also regulate the rate of PIN internalization in plant cells. Hence, future research will unravel whether spatial and temporal PID kinase activity also contributes to other processes, such as the regulation of PIN endocytosis/exocytosis rates at the different cell sides.

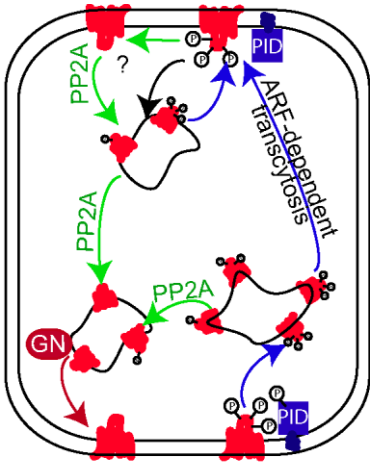

Figure 8. Model of PID and GNOM-dependent intracellular PIN sorting
PID might phosporylate PIN proteins preferentially at the plasma membrane. Phosporylated PIN proteins get internalized into endosomes, but fail to get sorted to the ARF-GEF GNOM-dependent basal recycling pathway. Phosphorylated PIN proteins display an enhanced affinity to a GNOM-independent, but ARF-dependent, apical targeting pathway, eventually leading to basal-to-apical PIN transcytosis. The PP2AA function can counteract the PID-dependent PIN phosphorylation, leading to GNOM-dependent basal recycling of PIN proteins.

EXPERIMENTAL PROCEDURES

Plant Material and Growth Condition

Arabidopsis thaliana (L.) Heyhn. (ecotype Columbia or Landsberg *erecta*) plants and seedlings were grown in growth chambers under long-day conditions (16 h light/8 h darkness) at 23°C. Experiments were carried out on 5-day-old seedlings grown on vertically-oriented plates containing *Arabidopsis* medium (AM) consisting of half-strength Murashige and Skoog (MS) agar, 1% sucrose (pH 5.8). Sedlings were incubated in AM medium supplemented with 50 µM BFA in 24-well cell-culture plates for the indicated time periods. Control treatments contained equal amounts of solvent (dimethylsulfoxide). For in vivo analysis of the development of individual lateral root primordia, 3- to 5-day-old seedlings were transferred on slides with a thin layer of half-strength MS medium with 0.5% agarose, supplemented with naphthaleneacetic acid (NAA) (1 µM; 48 h) and incubated 24-48 h in a humid chamber. For all comparisons, independent experiments were done at least in triplicate with the same significant results. The following mutants and transformants have been described previously: *GNOM*^{M696L}*-MYC; GNOM-MYC* (Geldner et al., 2003); *gnom*^{R5} (Geldner et al., 2004); *DR5rev*$_{Pro}$*:GFP* (Friml et al., 2003)*; PIN1-GFP* (Benková et al., 2003); *pid*^{en197} and *35S*$_{Pro}$*:PID-21* (Benjamins et al., 2001); *pp2aa1*, *pp2aa1 pp2aa3*, and *PID-YFP* (Michniewicz et al., 2007); and *PIN1*^{S123A}*-GFP*, and *PIN1*^{S123E}*-GFP* (Huang et al., 2010).

Expression and Localization Analyses

Whole-mount immunofluorescence preparations were done as described (Friml et al., 2003). Antibodies were diluted as follows: anti-PIN1 (1:2000) (Paciorek et al., 2005), anti-PIN2 (1:2000)

(Abas et al., 2006), anti-GFP (1:300; Molecular Probes, Eugene, OR), anti-ARF1 (1:1000) (Pimpl et al., 2000), and anti-c-myc (1:500; Roche Diagnostics, Brussels, Belgium). FITC- and CY3-conjugated anti-rabbit secondary antibodies (Dianova, Hamburg, Germany) were diluted 1:500, and 1:600, respectively; YFP was visualized in 5% glycerol without fixation (live cell imagining) and analyzed with a confocal laser scanning microscopy (TCS SP2; Leica Microsystems, Wetzlar, Germany) Images were processed in Adobe Photoshop and Illustrator cs2 (Adobe Inc., San Jose, CA). Statistical analyses were done with Office Excell 2003 (Microsoft, Seattle, WA).

Accession Numbers

Sequence data from this article can be found in The Arabidopsis Information Resource (http://www.Arabidopsis.org/) or GenBank/EMBL databases under the following accession numbers: ARF1 (AT1G23490), GNOM (AT1G13980), PID (AT2G34650), PIN1 (AT1G73590), PIN2 (AT5G57090), PP2AA1 (AT1G25490), and PP2AA3 (AT1G13320).

ACKNOWLEDGMENTS

We thank David Robinson for generously donating antibodies-based subcellular markers, Gerd Jürgens for sharing unpublished material, Martine De Cock for help in preparing the manuscript, and the NASC for seed stock supply. This work was supported by grants from the EMBO Young Investigator Program (to J.F.), the Odysseus Programme of the Research Foundation-Flanders (to J.F.), by a Chinese Science Council (CSC) scholarship (to F.H) and the Japanese Society for Plant Sciences (JSPS) (to S.N.). J.K.-V. is indebted to the Friedrich Ebert Stiftung for a personal fellowship.

SUPPLEMENTAL FIGURES

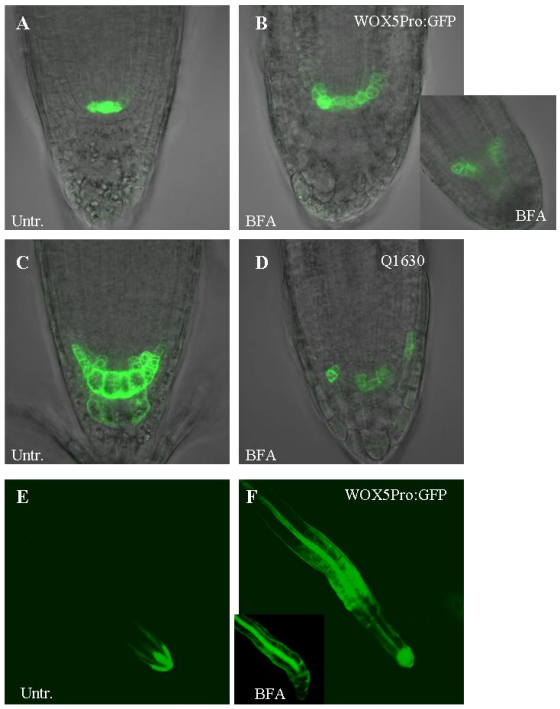

Figure S1. BFA-induced changes in the primary root meristem
(A) and (B) *WOX5Pro:GFP* expression in untreated (A) and BFA germinated (B) seedlings 3 days after germination (DAY). BFA treatment leads to misexpressioin of the quiescent centre (QC) marker *WOX5Pro:GFP*, displaying radial expansion in the endodermis. Inset shows BFA treated *WOX5Pro:GFP* expressing seedlings 4-5 DAY, illustrating ectopic ring of *WOX5Pro:GFP* expression. Asterisks mark the position of the original QC.
(C) and (D) Columella marker *Q1630* expression in untreated (C) and BFA germinated (D) seedlings 3 DAY, reveals BFA-induced misspecification of columella cell lineage.
(E) and (F) depict *DR5revPro:GFP* expression in untreated (A) and BFA germinated (B) seedlings 7 DAY. BFA leads to ectopic DR5 acitivity (see arrowhead) in upper parts of the root. Inset displays collapsing root tip (18 DAY on BFA) that lacks DR5 activity in the very root tip.
(A)-(D) single confocal scans; (E) and (F) fluorescent mircroscopic images.

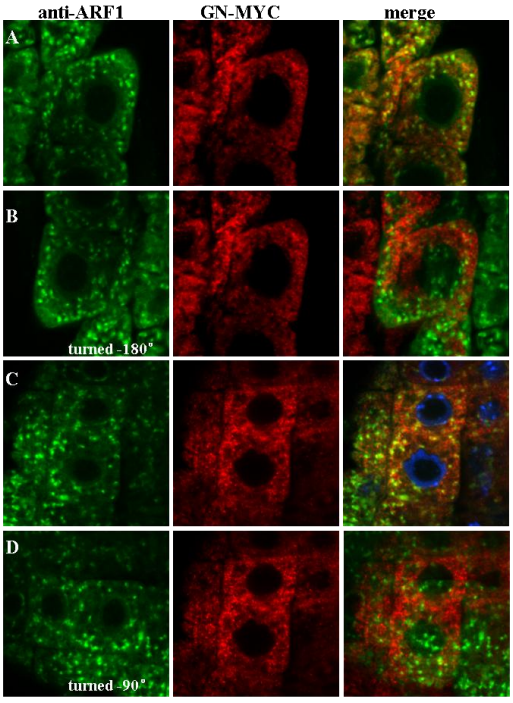

Figure S2. Evaluation of anti-ARF1 and GNOM-MYC colocalization
(A-D) To address potential coincidental overlap of ARF1 and GN-MYC signal we performed commonly used rotation analysis. The rotation of the ARF1 channel for 180° (B) or 90° (D) degree largely abolishes the observed colocalisation (A) and (C), indicating non-coincidental colocalisation of anti-ARF1 and GN-MYC in the original images.

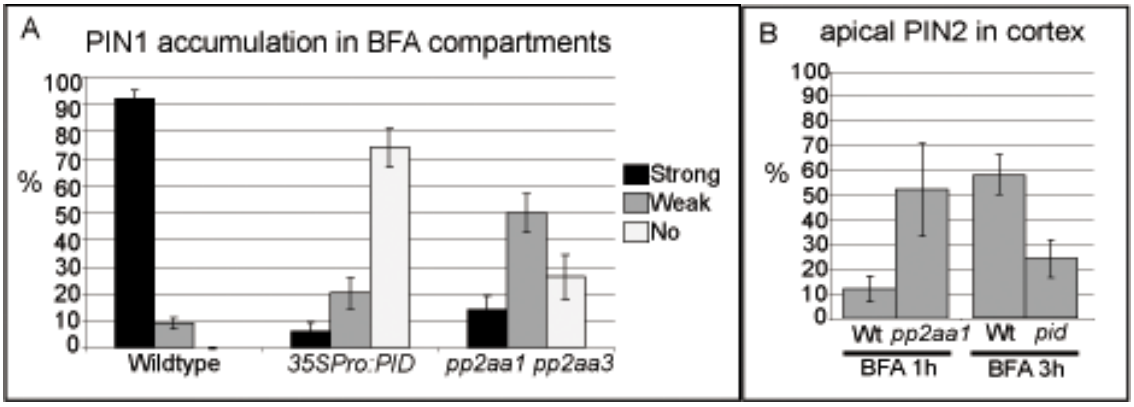

Figure S3. BFA-dependent PIN localization in various mutant backgrounds
(A) The statistical evaluation of the BFA effect on PIN1 localisation in wildtype, *35SPro:PID*, and *pp2aa1 pp2aa3* double mutants. n=8 roots; a total number of at least 408 cells were counted.
(B) Percentage of ectopic, apical PIN2 localisation in lower cortex cells after 1 or 3hours of BFA treatment. Reduced PP2AA activity results in enhanced BFA-dependent basal-to-apical shift, while pid loss-of-function roots show reduced PIN2 basal-to-apical transcytosis. n=8 roots; a total number of at least 112 cells were counted.

CHAPTER 5

Phosphatidylinositol-Induced Ca^{2+} Signaling Regulates Auxin Transport and Cell Polarity

Jing Zhang, Steffen Vanneste, Phillip B. Brewer, Marta Michniewicz, Peter Grones, Jürgen Kleine-Vehn, Christian Löfke, Thomas Teichmann, Agnieszka Bielach, Bernard Cannoot, Klára Hoyerová, Eva Benková, Eva Zažímalová, and Jiří Friml

Modified from Zhang et al., (2010) Manuscript

Author's Contributions: JF initiated the projects; JZ and JF designed experiments; JZ carried out most of the experiments; VS helped in cloning amiRNA constructs; PBB and MM performed the forward genetic screening; PG and BC helped with genotyping; CL and TT measured auxin acropetal transport presented Figure 2G; AB and EB contributed Figure 2C; KH and EZ measured free auxin contents presented Figure S1B; JZ assembled the figures; and JZ, VS, JKV, and JF discussed the resultes; and JZ, VS, and JF wrote the manuscript.

ABSTRACT

Phytohormone auxin acts as an important determinant of plant development. The directional auxin flow within tissues depends on polarly localized PIN auxin transporters. How PIN polarity is regulated throughout development is poorly understood. We identified an inositol polyphosphate 1-phosphatase mutant, *suppressor of PIN1 overexpression* (*supo1*), with elevated $InsP_3$ and Ca^{2+} levels, and altered PIN polarity and auxin transport. Pharmacological and genetic increases of $InsP_3$ or Ca^{2+} levels phenocopy *supo1* including suppression of the *PIN1* gain-of-function phenotype and causes defects in basal PIN localization. In contrast, the decrease of $InsP_3$ levels and Ca^{2+} signaling act antagonistically and targets specifically the apical PIN polarity. $InsP_3$ and Ca^{2+} are evolutionarily conserved secondary messengers involved in various cellular functions, best characterized in stress responses. Our findings implement them as modifiers of cell polarity and polar auxin transport, thus providing a integration point for a wide range of Ca^{2+} signaling-related stimuli into auxin-mediated development.

INTRODUCTION

Development of land plants is characterized by a remarkable capacity towards ever-changing environmental conditions. The asymmetric distribution of the plant signaling molecule auxin within tissues (auxin gradients) is a versatile mechanism providing spatial and temporal coordination for many developmental processes, including adaptive development (Leyser, 2006; Berleth et al., 2007; Benjamins and Scheres, 2008; Mockaitis and Estelle, 2008). Directional auxin transport between cells is a major determinant in the formation of local auxin gradients (Vanneste and Friml, 2009; Grunewald and Friml 2010). Cell-to-cell auxin transport is largely based on the activity of plasma membrane (PM)-resident auxin transporters that include the amino acid permease-like AUXIN RESISTANT1/LIKE AUX (AUX1/LAX) proteins, which mediate auxin influx (Bennett et al., 1996; Yang et al. 2006; Swarup et al., 2008), the PIN-FORMED (PIN) efflux carriers (Luschnig et al., 1998; Petrášek et al., 2006) and the MULTIDRUG RESISTANCE/P-GLYCOPROTEIN (PGP) class of ATP-binding cassette (ABC) auxin transporters (Noh et al., 2001; Geisler et al., 2005; Bandyopadhyay et al., 2007). The asymmetric, subcellular (polar) distribution of PIN proteins provides directionality to the intercellular auxin flow (Friml et al., 2004; Wiśniewska et al., 2006). Alterations in the polarity of PIN proteins in response to endogenous and external signals allow to redirect auxin flow and thus modulate auxin-dependent plant development (Petrášek and Friml, 2009). Despite the importance of PIN polarity regulation for plant development, the underlying regulatory mechanisms are still poorly understood. So far, the only known components regulating the apical (upper cell side) versus basal (lower cell side) PIN distribution are PINOID (PID) Ser/Thr kinase and protein phosphatase 2A (PP2A) that antagonistically mediate PIN phosphorylation of the PIN central hydrophilic loop (Friml et al., 2004; Michniewicz et al. 2007; Huang et al., 2010). PID activity can be regulated by phospholipid signaling (Zegzouti et al., 2006) and PID-interacting proteins which can bind Ca^{2+} (Benjamins et al., 2003), but the relevance of these regulations for auxin transport and auxin-mediated development is unclear.

In all eukaryotes, Ca^{2+} is one of the most ubiquitous second messengers, relaying panoply of signals to downstream intracellular effectors. One of its most interesting features is the speed by which it can modulate processes and signaling cascades. Binding to Ca^{2+} can directly alter biochemical properties and interaction partners of enzymes, transcription factors and other regulatory proteins (DeFalco et al., 2010; Kudla et al., 2010).

Also in plants, Ca^{2+} is involved in numerous cellular functions and is crucial for responses to various biotic and abiotic stimuli (Luan et al., 2002; Yang and Poovaiah, 2003; Kudla et al., 2010), including circadian oscillations (Xu et al., 2007), gravity (Poovaiah et al., 2002), stress responses (Quan et al., 2007), and hormonal signaling (Shishova and Lindberg, 2010). Given its physiological relevance, cytosolic Ca^{2+} concentrations are tightly regulated (White and Broadley, 2003; Hetherington and Brownlee, 2004; DeFalco et al., 2010). A steep gradient of Ca^{2+} between the storage compartments and the cytosol enables instant increases in local Ca^{2+} concentration and activation of associated signaling just by opening a few Ca^{2+} channels. Continuous pumping of Ca^{2+} out of the cytoplasm by ATP-driven Ca^{2+} pumps (Ca^{2+}-ATPases) dissipates the Ca^{2+} signal after a stimulus to a resting concentration (Sze et al., 2000; Hetherington and Brownlee, 2004). The spatio-temporal features of the Ca^{2+} pulse are decoded by various Ca^{2+} binding proteins resulting a suitable physiological output (DeFalco et al., 2010; Kudla et al., 2010).

Given the almost universal role of Ca^{2+} in regulating cellular processes on one hand and the multitude of developmental and physiological roles attributed to auxin on the other hand, the

connections between these signaling mechanisms are surprisingly scarce (Shishova and Lindberg, 2010). Physiological studies linked Ca^{2+} with auxin transport (dela Fuente and Leopold, 1973) and, in particular, gravitropic response (Lee and Evans, 1985; Plieth and Trewavas, 2002; Toyata et al., 2008), but the molecular mechanism underlying the possible influence of Ca^{2+} or other cellular signaling mechanisms and second messengers on auxin transport and auxin-mediated development remains elusive.

Here, we provide a genetic and mechanistic link between Ca^{2+} signaling and the control of cell polarity and PIN-mediated auxin transport .We identified a mutant defective in inositol phosphate 1-phospatase with increased $InsP_3$ and Ca^{2+} levels that rescued PIN gain-of-function phenotype and modified PIN polar targeting, auxin distribution and auxin-mediated development. Our findings imply that $InsP_3$-mediated Ca^{2+} signaling are potential entry-points for various stimuli to influence cell polarity, auxin transport and auxin-mediated development.

RESULTS

Identification of the *Suppressor of PIN1 Overexpression supo1* Mutant

To identify novel regulators of PIN-dependent auxin transport and PIN polar targeting, we performed a forward genetic screen for modulators of *PIN1* overexpression (*35S::PIN1*). *35S::PIN1* seedlings displayed shorter roots, strong agravitropic root growth and higher auxin levels in the root tip presumably because of the ectopic presence of basally localized PIN1 in the epidermal cells of root tips (Petrášek et al., 2006; Mravec et al., 2008). In this screen, we isolated three mutant lines, named *suppressor of PIN1 overexpression* (*supo1* through *supo3*), which harbor second-site mutations restoring gravitropic root growth of *35S::PIN1*.

In *supo1*, the suppression of PIN1 overexpression phenotypes was clearest for the gravitropic response (Figure 1A and 1B). Moreover, *supo1-1* also restored normal auxin levels in contrast to higher levels in *35S::PIN1* root tips as inferred from *DR5::GUS* visualization and direct Indole-3-acetic acid (IAA) measurement (see Figure S1A, B available online). Thus, *supo1* suppresses multiple aspects of PIN1 gain-of-function phenotype, suggesting that *supo1* modifies PIN-mediated auxin transport.

To investigate the genetic interaction between *supo1* and *pin1*, we introduced the *supo1-1* into the *pin1-1* loss-of-function allele, which has characteristic developmental defects in embryogenesis, reflected by mono-, tri- or fused cotyledons (Okada et al., 1991). In the progeny of *pin1-1*+/–, approximately 4% (n=1415) of seedlings had a defective cotyledon formation, whereas only weak patterning defects (1%, n=323) were observed in *supo1-1* plants (Figures 1C and 1D). However, the overall frequency of aberrant cotyledon phenotypes was markedly increased in the progeny of *supo1-1 pin1-1*+/-. Up to 9% (n=1129) of the seedlings had irregular cotyledons and occasionally, some seedlings completely failed to develop cotyledons (Figures 1C and 1D), a feature absent in *pin1* or *supo1-1* single mutant seedlings. These data suggest that *supo1* mutation interferes with PIN function.

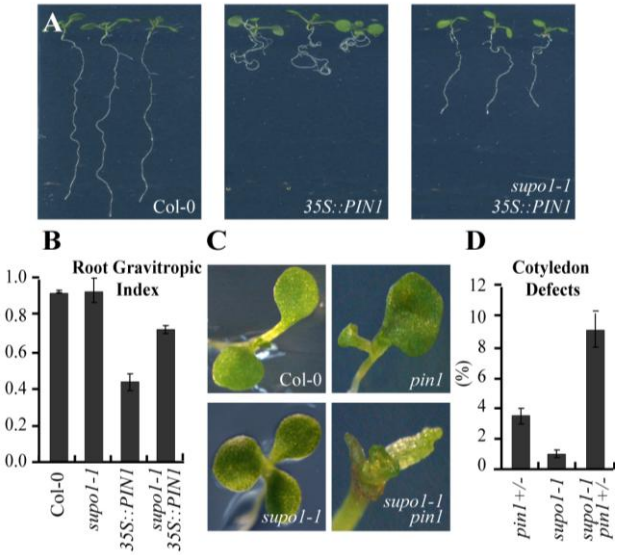

Figure 1. Genetic interaction between *SUPO1* and *PIN1*
(A and B) *SUPO1* suppresses *PIN1* gain-of-function. The *35S::PIN1* agravitropic phenotype is rescued by the *supo1-1* mutation (A); quantification of root gravitropism (B).
(C and D) *SUPO1* enhances the *pin1* loss-of-function. Seedlings lacking cotyledons are occasionally observed in *supo1-1 pin1* double mutants (C); the frequency of defective cotyledon patterning (D).
Error bars are SE.

supo1 is Defective in Auxin-mediated Development

To analyze the role of *SUPO1* in plant development, we segregated the *supo1-1* mutation from the *35S::PIN1* transgene by outcrossing to wild type (Col-0). *supo1* exhibited defected root growth (Figure 2A), and reduced cell division activity in the root meristem as monitored by the mitotic marker *CYCB1;1::DB-GUS* (Figure 2B). In addition, we also observed a delay in lateral root development (Figure 2C), aberrant vertical cell divisions (Figure 2D), disconnected vasculature in cotyledons (*supo1*: 33%, n=40; Col-0: 2%, n=230; Figure 2E), and changes in asymmetric leaf shapes and leaf serration (*supo1*: 47%, n=38; Figure 2F). As some of these phenotypic defects in *supo1* might be caused by defective auxin transport (Benková et al., 2003; Friml et al., 2002a; Scarpella et al., 2006; Tsiantis and Hay, 2003), we directly measured IAA transport in the *supo1* mutant roots and observed that the acropetal IAA transport in *supo1* was elevated as compared to the wild type (Figure 2G). In summary, the *supo1* loss-of-function phenotypes hint at a role for SUPO1 in a broad range of developmental processes; some of which are regulated by auxin transport.

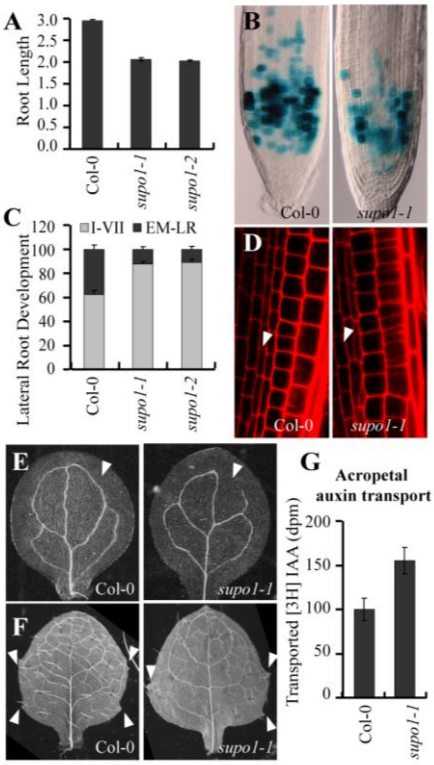

Figure 2. Role of *SUPO1* in the regulation of plant development and auxin transport
(A-F) Morphological defects in *supo1*. Inhibited root elongation (A); decreased cell division in the root meristem visualized by *CYCB1;1::DB-GUS* (B); delayed lateral root development (C); aberrant cell divisions (D); defects in vein patterning (E) and leaf shape (F).
(G) Enhaced acropetal auxin transport in *supo1* roots.
Error bars are SE.

supo1 is a new allele of the inositol polyphosphate 1-phosphatase SAL1

We used recombination mapping by analyzing about 2220 F2 segregants from the cross between the *supo1-1* (Col-0) and Landsberg *erecta*. We mapped *supo1-1* to a 33-kb region on a single BAC clone MBM17 on the right arm of chromosome 5. Through sequencing of candidate genes in the interval we identified a G nucleotide deletion at the position 340bp of the coding sequence. The resulted frame shift created a premature stop codon in the fourth exon of At5g63980 (*SAL1/FRY1/HOS2/ALX8/RON1*) (Figure 3A), encoding a protein with inositol polyphosphate 1-phosphatase and 3'(2'), 5'-bisphosphate nucleotidase activities (Quintero et al., 1996; Xiong et al., 2001, 2004; Gy et al., 2007; Wilson et al., 2009; Robles et al., 2010). Importantly, two T-DNA insertion mutants disrupting this locus, salk_020882 (*supo1-2*) and salk_151367 (*supo1-3*) showed similar phenotypes as seen in *supo1-1* (Figure 2A and 2B; Figure S1D-G) and rescued a gravitropic root growth when crossed with *35S::PIN1* (Figure S1C). The full-length *SUPO1* transcript was not detectable in any of these *supo1* mutant alleles (Figure 3A).

Consistent with a function in $InsP_3$ catabolism, mutant alleles of *supo1*, such as *fry1-1*, display an increase in $InsP_3$ level (Xiong et al., 2001). Therefore, we analyzed the $InsP_3$ contents in the *supo1* alleles in wild type and *35S::PIN1* background confirming that *supo1* mutations confer increased $InsP_3$ levels independent of the presence of the *35S::PIN1* transgene (Figure S2A).

Moreover, N- or C-terminal GFP fusion of *SUPO1* under control of its endogenous promoter (*SUPO1::GFP-SUPO1* and *SUPO1::SUPO1-GFP*) restored *35S::PIN1* root agravitropic phenotype that was suppressed in *supo1-1 35S::PIN1* (data not shown). Independent alleles and mutant complementation demonstrated that a mutation in *SAL1/FRY1/HOS2/ALX8/RON1* gives rise to the *supo1* phenotypes including the suppression of *35S::PIN1* defects.

SUPO1 protein has been reported to have a dual enzymatic activity; inositol polyphosphate 1-phosphatase activities through which it can mediate the catabolism of $InsP_3$, and 3'(2'), 5'-bisphosphate nucleotidase activities (*SAL1/FRY1/HOS2/ALX8/RON1*; Quintero et al., 1996; Xiong et al., 2001, 2004; Wilson et al., 2009; Robles et al., 2010). $InsP_3$ has been implicated in many aspects of plant growth and development, such as abscisic acid (ABA)-regulated processes, including stress response (Sanchez and Chua, 2001; Xiong et al., 2001; Burnette et al., 2003), secondary cell wall and fiber cell development (Zhong et al., 2004), vascular patterning in cotyledons and leaves (Carland and Nelson, 2004), gravitropic response of roots, hypocotyls and inflorescence stems (Perera et al., 2006). As such, SUPO1 function would be pleiotropically required for a broad range of developmental processes; auxin transport-related being only a subset of them.

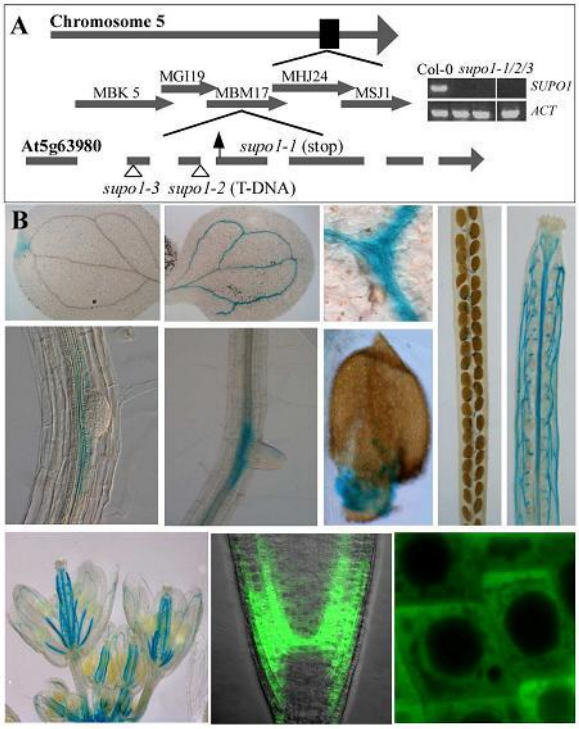

Figure 3. *SUPO1*-encoded Phosphatidylinositol Phosphatase
(A) Map-based cloning of *supo1* mutation. Filled lines and spaces between lines correspond with open reading frames and introns, respectively. The relative position of the stop codon in *supo1-1* is indicated. The T-DNA insertions in

supo1-2 and *supo1-3* are represented by triangles. *SUPO1* mRNA is not detected in the *supo1* alleles by RT-PCR. *Actin* (*ACT*) gene is used as a reference control.
(B) *SUPO1* expression pattern and subcellular localization. The *SUPO1::GUS* reporter construct is expressed in different plant organs and the functional *SUPO1-GFP* fusion reveals a predominantly cytosolic localization.

SUPO1 Expression and Localization

To characterize the action of *SUPO1*, we analyzed its expression and localization. Several independent transgenic lines carrying the transcriptional promoter fusion *SUPO1::GUS* showed consistent expression patterns. In young cotyledons, maximal GUS activity was detected in the tip area (Figure 3B). At later developmental stages, the *SUPO1::GUS* signal became apparent in cotyledon veins (Figure 3B). GUS staining was also observed in root vasculature with enhanced signal in the vicinity of lateral root primordia (Figure 3B). The expression was also detected in seed coats (Figure 3B). In floral organs, the *SUPO1* promoter was active mainly in stems, filaments and throughout vascular strands of carpels, petals and siliques (Figure 3B). In the primary root meristem, the *SUPO1::GUS* signal was stronger in the lateral root cap, columella stem cells, quiescent centre, epidermis, endodermis and cortex of the root meristem (data not shown). The same overall expression pattern was also detected in the transgenics expressing the functional N- or C-terminal GFP fusions as shown for the primary root meristem (Figure 3B). The *SUPO1-GFP* revealed a predominantly cytosolic localization of SUPO1 with a stronger GFP signal beneath the PM (Figure 3B). Thus, both transcriptional and translational fusions revealed a dynamic expression pattern in different tissues and a predominantly cytosolic localization of SUPO1.

Increased levels of $InsP_3$ Mimics *supo1* and Suppress the *PIN1* Overexpression Phenotype

SUPO encodes a bi-functional enzyme, one of its activities related to $InsP_3$ catabolism (Xiong et al., 2001), while the other is related to post-translational gene silencing (Gy et al., 2007). To distinguish between both functions we tested what is the contribution of changed $InsP_3$ levels in *supo1* alleles to the auxin transport-related phenotypes.

First we tested the effectiveness of pharmacological treatments to increase $InsP_3$ levels. The synthetic membrane-permeable $InsP_3$ ester (IP_3) should be a direct source of $InsP_3$ to the cells, whereas the nitric oxide donor sodium nitroprusside (SNP) should indirectly cause an increase in $InsP_3$ levels by stimulating Ptd Ins(4,5)P_2 (Lanteri et al., 2006, 2008; Im et al., 2007). Direct $InsP_3$ measurements validated that these treatments increased endogenous $InsP_3$ levels (Figure S2A).Next, we used these pharmacological manipulations to study the effect of elevated $InsP_3$ levels on *35S::PIN1* root gravitropic responses. Transfer to media supplemented with IP_3 or SNP suppressed to a large extent the agravitropic root growth of *35S::PIN1* (Figure 4A and 4B). Moreover, pharmacologically increasing $InsP_3$ levels also suppressed ectopic auxin accumulation in *35S::PIN1* root tips, as inferred from *DR5rev::GFP* expression (Figures S3A and S3B), mimicking the effects of *supo1*. These data suggested that high $InsP_3$ levels suppress PIN1 gain-of-function phenotypes.

Alternatively, a loss-of-function mutant in the *CVP2* gene, encoding an inositol polyphosphate 5-phosphatase, shows increased $InsP_3$ levels (Carland and Nelson, 2004), without known effects on post-translational gene-silencing. Similar to *supo1, cvp2* also restored the gravitropic response of *35S::PIN1* (Figure 4C), demonstrating that increased $InsP_3$ levels, rather than effects on post-translational gene silencing, suppress PIN1 gain-of-function phenotype.

In summary, these observations show that increased $InsP_3$ underlie the effects of *supo1* mutation on PIN-dependent auxin transport and suggest a role for $InsP_3$-mediated processes in regulating of auxin transport.

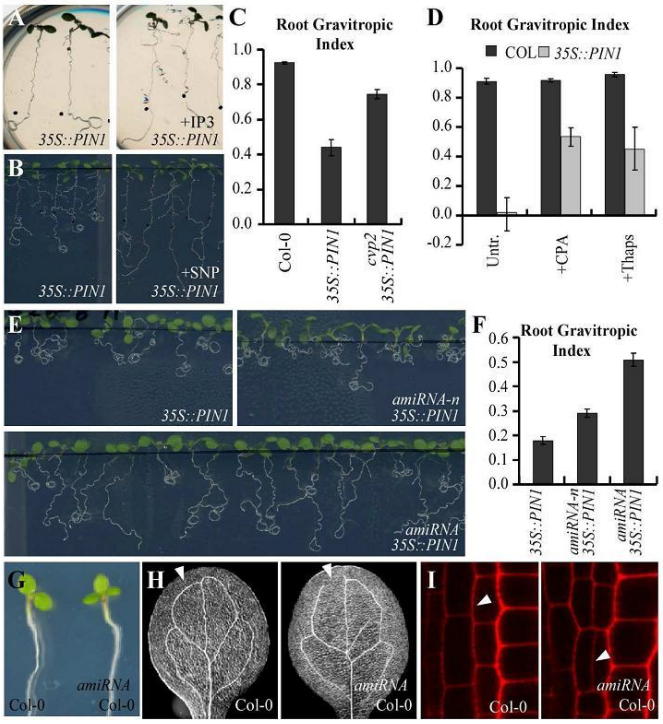

Figure 4. Mimicry of *supo1* auxin-related phenotypes by elevated $InsP_3$ and Ca^{2+} level
(A-C) Effect of increased $InsP_3$ level on root gravitropism. Exogenous application of IP_3 (A) and SNP (B) restores gravitropism of *35S::PIN1*; quantification of *35S::PIN1* root gravitropism partially rescued by *cvp2* mutant (C);
(D-F) Effect of increased Ca^{2+} level on root gravitropism. Quantification of *35S::PIN1* root gravitropism partially restored by exogenous application of CPA and Thaps (D); *amiRNA 35S::PIN1* line has a better gravity response than *35S::PIN1* and *amiRNA-n* (negative control) (E); quantification of root gravitropism (F).
(G-H) Morphological defects in *amiRNA* in wild-type background. Irregular cotyledon numbers (G); discontinued vein pattern (H); aberrant vertical cell division (I).
Error bars are SE.

Suppression of *PIN1* Overexpression Phenotype in *supo1* is tightly correlated with increased Ca^{2+} levels

The mechanism of $InsP_3$ perception and $InsP_3$-mediated Ca^{2+}-release is well known in the animal field (Gilroy et al., 1990; Tang et al., 2007). However, the respective molecular components are not conserved in land plants (Wheeler and Brownlee, 2008). Yet, also in plants $InsP_3$ is known to trigger the release of Ca^{2+} from intracellular stores into the cytoplasm (Gilroy et al., 1990; Blatt et al., 1990; Krinke et al., 2007; Tang et al., 2007). To evaluate whether Ca^{2+} acts downstream of $InsP_3$ to mediate its effects on PIN-dependent auxin transport, we modulated cytosolic Ca^{2+} levels and monitored the effects on *35S::PIN1* growth.

We analyzed the cytosolic Ca^{2+} concentration in the *supo1* alleles in wild type and *35S::PIN1* background using fluorescent Ca^{2+} sensor Indo-1 (Wymer et al., 1997). These experiments show that *supo1* mutations increase cytosolic Ca^{2+}, providing a positive correlation between $InsP_3$ levels and cytosolic Ca^{2+} (Figure S2D and S2E). Generally, the Ca^{2+} concentration in the cytoplasm is controlled by the activities of Ca^{2+} channels that allow Ca^{2+} fluxes into the cytosol and Ca^{2+}-ATPases and Ca^{2+} exchangers that mediate removal of Ca^{2+} from the cytosol into storage sites (Hetherington and Brownlee, 2004; Sze et al., 2000). Therefore, inhibition of Ca^{2+} ATPase activity leads to higher cytosolic Ca^{2+}. Although the molecular targets of Ca^{2+}-ATPase inhibitors cyclopiazonic acid (CPA) and thapsigargin (Thaps) are poorly characterized in plants (Lytton et al., 1991; Liang and Sze, 1998; Moreno et al., 2008; Iwano et al., 2009), they increased intracellular Ca^{2+} levels as visualized by Indo-1 fluorescence (Figure S2B and S2C).

We used these pharmacological manipulations to study effect of increased cytosolic Ca^{2+} on the *35S::PIN1* root gravitropic defect. The CPA and Thaps treatments had little effects on the growth of wild type roots but partially restored gravitropic growth in *35S::PIN1* roots (Figure 4D). Moreover,

application of CPA and Thaps suppressed the *DR5::GUS*-monitored increase of auxin response in the *35S::PIN1* root tips (Figures S3D) mimicking the effect of *supo1* mutation or increased $InsP_3$ levels.

Because these inhibitors are poorly characterized in plants, we aimed to confirm this pharmacological observation genetically. We created transgenic lines with co-overexpression of three artificial microRNA (*amiRNA*) that were constructed to collectively target nine genes encoding Ca^{2+}-ATPases, including *ACA1*, *ACA2*, *ACA4*, *ACA7*, *ACA8*, *ACA9*, *ACA10*, *ACA11* and *ACA13*. Although only the expression of *ACA1*, *ACA4* and *ACA11* was efficiently downregulated (Figure S4A), cytosolic Ca^{2+} levels were increased in the *amiRNA 35S::PIN1* seedlings (Figure S2D and S2E). Notably, in the T2 segregating progeny of *35S::PIN1+/+ amiRNA+/-*, approximately 75% seedlings (n=68) showed rescued gravitropic phenotype (Figures 4E and 4F). These results provided genetic evidence that increased cytosolic Ca^{2+} levels can suppress the effects of *35S::PIN1* on root gravitropism, as seen in *supo1*. This strongly suggests that increased cytosolic Ca^{2+} underlies the effect of *supo1* mutation on PIN-dependent auxin transport and reveals a link between Ca^{2+} signaling and auxin transport.

To further test the effects of increased Ca^{2+} levels on auxin transport, we analyzed *amiRNA* seedlings downregulating Ca^{2+}-ATPases activity in the wild type (Col-0) background (Figures S4B). These plants with increased Ca^{2+} levels (Figure S2F and S2G) displayed various growth defects similar to *supo1* alleles including low frequency of cotyledon formation defects (0.8%, n=235; Figure 4G), disrupted symmetrical cotyledon positioning (2%, n=223; data not shown), discontinuous cotyledon vein patterning (11%, n=153 cotyledons; Figure 4H), and aberrant vertical cell divisions (14%, n=30; Figure 4I) in T2 segregating populations. These observations further strengthened the correlation between the SUPO1 function, cytosolic Ca^{2+} signaling and auxin-mediated plant development.

In summary, these observations show that increased cytosolic Ca^{2+} levels underlie the effects of *supo1* mutation on PIN-dependent auxin transport and suggest a role for Ca^{2+} signaling in regulation of auxin transport.

$InsP_3$-mediated increase of cytosolic Ca^{2+} modulates ectopic basal PIN1 Polarity

How might $InsP_3$ and Ca^{2+} influence the activity of PIN-dependent auxin transport? The polarity of cellular PIN localization is an important determinant of PIN function (Wiśniewska et al., 2006) and the agravitropic *35S::PIN1* phenotype presumably results from the ectopic PIN1 presence at the basal side of epidermis cells, where PIN1 counteracts the action of endogenous PIN2 at the opposite cell side (Petrášek et al., 2006; Mravec et al., 2008). Therefore, we examined the ectopic PIN1 polarity in *supo1 35S::PIN1* roots. The predominantly basal localization of PIN1 in the epidermis of *35S::PIN1* was affected by the *supo1* mutation, as manifested by frequent both basal and apical PIN1 distributions in the same cell (Figures 5A and 5B). Similarly, the number of cells showing both apical and basal epidermal PIN1 in the *cvp2* mutant was also dramatically increased (Figure 5B).

As increased $InsP_3$ levels by external application of IP_3 and SNP mimicked the *supo1* phenotype, we evaluated their effects on PIN1 polarity in the *35S::PIN1* roots. Similarly to the effects of *supo1* and *cvp2*, the number of epidermal cells with "normal" basal PIN1 localization significantly decreased, while that with non-polar PIN1 mainly increased after their treatments (Figures 5A and 5B). The proportion of cells with rearranged PIN1 proteins was comparable to the *supo1* roots (Figure 5B).

Given the strong correlation between SUPO function, $InsP_3$ levels and Ca^{2+}, we manipulated cytosolic Ca^{2+} and examined effects on PIN1 polarity in *35S::PIN1* lines. The exogenously applied CPA and Thaps mimicked the effect of *supo1* on PIN1 polarity, characterized by a strongly reduced basal PIN1 localization and a regular occurrence also at the apical side or entirely non-polar PIN1 distribution (Figures 5A and 5C). Similarly, increasing the cytosolic Ca^{2+} in the *amiRNA 35S::PIN1* lines led to defects in the PIN1 basal localization in the epidermis (Figures 5A and 5C).

Together, these data are consistent with a model in which $InsP_3$ mediates an increase in cytosolic Ca^{2+} which in turn modulates basal polarity of ectopical PIN1 in epidermis, thereby suppressing PIN1 gain-of-function phenotypes in *supo1*.

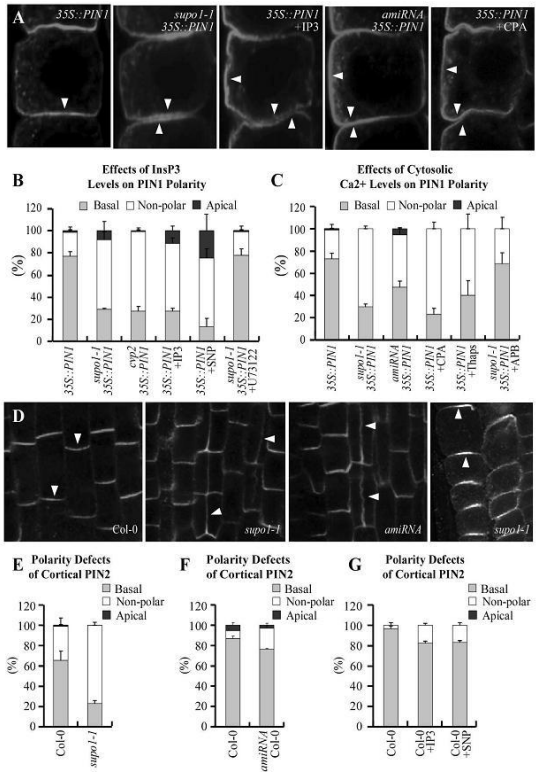

Figure 5. Regulation of basal PIN polarity by elevated $InsP_3$ and Ca^{2+} level
(A-C) Regulation of ectopic PIN polarity by $InsP_3$ and cytosolic Ca^{2+}. Immunolocalization of PIN1 in the epidermis of primary root tips: increase in $InsP_3$ and Ca^{2+} levels affect PIN1 basalization with inducing apical or lateral PIN1(A); quantification of PIN1 polarity defects after manipulation of $InsP_3$ (B) and Ca^{2+} levels (C):*supo1, cvp2* mutation (B) and *amiRNA* transgene (C), and exogenous application of IP_3, SNP (B), CPA, and Thaps (C) affect the basal PIN1 in the epidermis, whereas U73122 (B) and APB (C) counteracts the effects caused by *supo1*, showing predominantly basal PIN1 as in non-treated *35S::PIN1* roots. Cells showing PINs localized simultaneously at either the basal and apical and/or lateral side were considered as non-polar.
(D-G) Regulation of endogenous PIN polarity by $InsP_3$ and cytosolic Ca^{2+}. Immunolocalization of PIN proteins in the primary root tips: lateral PIN1 localizations are induced in *supo1* and *amiRNA*; but apical PIN2 polarity is still normal (D); quantification of cortical PIN2 in the root after immunolocalization: *supo1* (E), *amiRNA* (F), and the treatments of IP_3 and SNP (G) induce more cells with non-polar PIN2.
Arrowheads mark PIN polarity. Error bars are SE.

$InsP_3$-mediated increase of cytosolic Ca^{2+} modulates endogenous basal PIN Polarity

As *supo1*, *cvp2* mutants and seedlings expressing *amiRNA* against Ca^{2+}-ATPases, as well as pharmacological treatments that increase $InsP_3$ and Ca^{2+} levels, had pronounced effects on the basal localization of PIN1 in the *35S::PIN1* roots, we tested their effects on the polarity of endogenous PINs. PIN1 is preferentially distributed at the basal side in endodermis, pericycle and stele cells (Friml et al., 2002a). PIN2, on the other hand, localizes to the apical cell side in epidermis and preferentially to the basal cell side in young cortex cells (Müller et al., 1998; Kleine-Vehn et al., 2008a). In the roots of *supo1*, *cvp2* and *amiRNA* lines, we observed defects in polar PIN1 distribution reflected by frequent occurrence of PIN1 at the lateral cell sides (Figure 5D). The basal PIN2 polarity in the cortex was also much less pronounced, with an increase in the number of cells showing also apical or non-polar PIN2 as compared to the wild type (Figure 5E and 5F). In contrast, apical PIN2 localization in epidermis was not affected in *supo1*, *cvp2* or *amiRNA* roots (Figure 5D; data not shown). Accordingly, pharmacological manipulations had similar effects on the polarity of endogenous PIN proteins. The exogenous applications of compounds elevating $InsP_3$ or cytosolic Ca^{2+} levels mildly induced PIN1 lateralization in the stele cells (SNP: 10%; CPA: 43%; Thaps: 38%; n = 30 roots; data not shown) and reduced the occurrence of basally localized PIN2 protein in the cortex (Figure 5G). Notably, as with genetic manipulations, increased $InsP_3$ or Ca^{2+} levels had no impact on the apical PIN2 (data not shown).

These results show that genetic and pharmacological increase in $InsP_3$-mediated cytosolic Ca^{2+}

affect preferentially the basal localization of PIN1 in the stele and PIN2 in the cortex cells but not the apical localization of PIN2 in the epidermis cells. This is also in accordance with absence of defects in basipetal auxin transport and gravitropic root growth in the *supo1* mutant roots as these processes require preferentially apically localized PIN2 in epidermis.

Decreased Levels of $InsP_3$ and Cytosolic Ca^{2+} Counteract Effects of *supo1* and Modulates Apical PIN Polarity

Our observations established that increased levels of $InsP_3$ and cytosolic Ca^{2+} rescue defects of PIN1 gain-of-function lines and modulates auxin transport and auxin distribution-mediated development. These effects correlate with and can be explained by $InsP_3$-mediated cytosolic Ca^{2+}, which specifically affects the basal localization of PIN proteins.

As a complementary approach, we artificially decreased $InsP_3$ and cytosolic Ca^{2+} levels by the pharmacological means using U73122, an established inhibitor of PLC activity that decreases $InsP_3$ (Cousson, 2003), Ca^{2+} channel blockers 2-aminoethoxydiphenylborane (2-APB; Engstrom et al 2002) and $LaCl_3$ (Lanteri et al., 2006), and Ca^{2+} chelator EGTA (Figure S2B and S2C). The treatments reduced the gravitropic growth of *supo1 35S::PIN1*, while only weak effects observed from wild type (Figure S5A). Moreover, their effects on the *DR5* distribution were opposite to that of the *supo1* mutation, as manifested by suppression of the increased and decreased *DR5* expression respectively in *supo1* and *supo1 35S::PIN1* by U73122, 2-APB, and $LaCl_3$ (Figure S5B and S5C). Treatments with U73122 and 2-APB also effectively counteracted the *supo1*-mediated depolarization of ectopically expressed PIN1 and resulting in a largely "normal" basal PIN1 localization (Figure 5B and 5C). These results suggested that decreased $InsP_3$ and Ca^{2+} levels counteract the effects of *supo1* on auxin transport-related processes as well as on basal PIN polarity.

Next, we analyzed the effects on endogenous PIN polarity. In contrast to the increase of $InsP_3$ and cytosolic Ca^{2+} levels, their decrease after application of U73122, $LaCl_3$, and EGTA, specifically affected the apical localization of PIN2 and led to a largely non-polar PIN2 localization in the epidermis (Figures 6A). To evaluate these polarity defects quantitatively, we scored the number of cells showing different PIN distribution as done in top panel (Figure 5). Indeed, non-polar PM localization of PIN2 was enhanced after these treatments (Figure 6B). The observations were further confirmed by an alternative quantification, in which we measured the ratio between PIN2 fluorescence intensity at the outer lateral and the apical membrane in epidermis cells (Figure 6C).

Notably, despite the pronounced disruptions of PIN2 apical targeting, we did not detect any defect in the basal PIN1 localization in the stele and PIN2 in the cortex cells (data not shown). Our data showed that endogenous or exogenous manipulations of $InsP_3$-mediated Ca^{2+} signaling correlate with defects in PIN polarity. In general, these results suggested that high $InsP_3$ and Ca^{2+} levels preferentially affect the basal targeting of PIN proteins, whereas low levels interfere preferentially with the apical targeting. Notably, the manipulations with $InsP_3$ and Ca^{2+} caused a depolarization rather than an inversion of polarity.

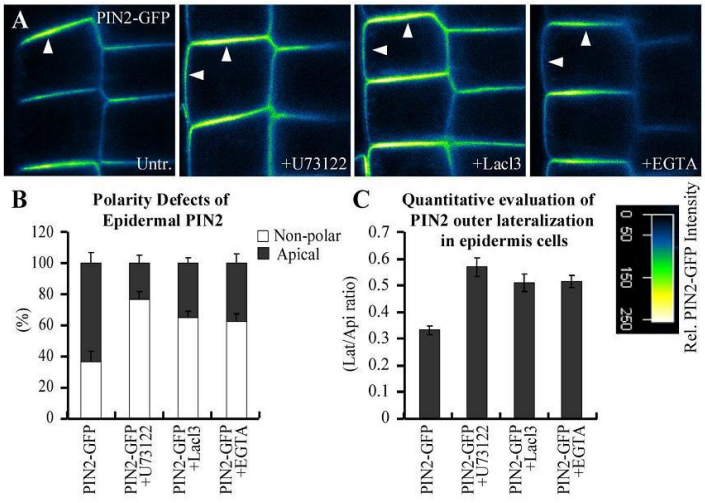

Figure 6. Regulation of apical PIN polarity by attenuated $InsP_3$ and Ca^{2+} level

(A) Live images of GFP-tagged PIN2 in the epidermis of wild-type roots. Supplementations of U73122, $LaCl_3$ and EGTA lead to a non-polar manner of PIN2.
(B and C) Quantification of apical PIN2 polarity defects. The numbers of cells showing different PINs are scored in (B); the quotients between mean fluorescence intensity of the outer lateral and apical membrane in epidermis cells are calculated in (C).
Arrowheads mark PIN polarity. Error bars are SE.

$InsP_3$-mediated cytosolic Ca^{2+} Acts on PID-related Mechanism of PIN Polarity Regulation

Next, we addressed the mechanism by which $InsP_3$-mediated Ca^{2+} could affect PIN polar targeting. PIN polar localization and its changes are related to the constitutive, endocytic recycling of PIN proteins (Kleine-Vehn et al., 2008b; Dhonukshe et al., 2008). Indeed, pharmacological manipulations of $InsP_3$ or Ca^{2+} levels reversibly affected trafficking of PIN2 PM localization as demonstrated by increased intracellular accumulations of PIN2-GFP in the cells (Figure S6; also see Xu et al., accompanying manuscript).

A candidate target of the $InsP_3$-mediated cytosolic Ca^{2+} regulation is the protein kinase PINOID (PID) that is negatively regulated by Ca^{2+} (Benjamins et al., 2003; Zegzouti et al., 2006). PID is an important regulator of auxin transport and a determinant of PIN polar targeting as well as PIN endocytic recycling (Benjamins et al., 2001; Friml et al., 2004; Michniewicz et al., 2007; Kleine-Vehn et al., 2009; Dhonukshe et al., 2010). To determine whether observed Ca^{2+}-mediated regulations of PIN polarity are related to PID action, we assessed effects of Ca^{2+}-interfering drugs on the root collapse of *PID* gain-of-function (*35S::PID*) seedlings. Interestingly, the presence of compounds elevating $InsP_3$ or cytosolic Ca^{2+} delayed the *35S::PID*-mediated root collapse, whereas the treatments decreasing cytosolic Ca^{2+} contents rather enhanced the collapse (Figure 7A; Benjamins et al., 2003). Next, we tested the *pid* loss-of-function line *pid wag1 wag2* that displays a completely disrupted cotyledon formation (Dhonukshe et al., 2010). In the F2 segregating progeny, the frequencies of the seedlings lacking cotyledons were increased approximately 2-folds in *supo1* or *cvp2* crosses as compared with the wild-type cross (Figure 7B). Accordingly, SNP and Thaps treatments regularly induced basal localization for endogenous PIN2 in the young cortex cells in *35S::PID* (Figure S7A). In contrast, chelating Ca^{2+} by EGTA led to a gradual basal-to-apical PIN2 polarity in young epidermal cells of *pid wag1 wag2* roots (Figure S7B and S7C).

These observations put forward a scenario that $InsP_3$-mediated Ca^{2+} levels negatively regulate the PID kinase activity, and might thus contribute to the determination of localization of the PIN proteins.

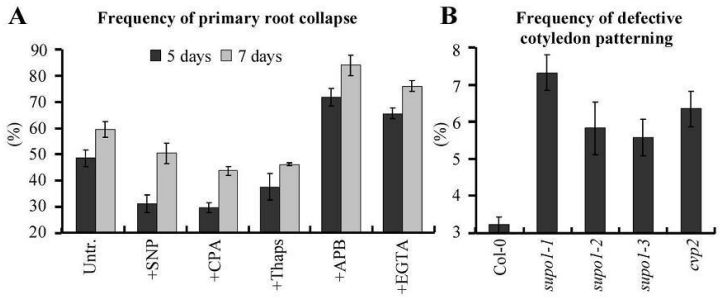

Figure 7. Modulation of PID-related $InsP_3$ and Ca^{2+} signaling on PIN polarity
(A) Quantification of *35S::PID*-mediated primary root collapse in 5- and 7-day-old seedlings.
The collapses are delayed by SNP, CPA, and Thaps, but enhanced by APB and EGTA.
(B) Quantification of defective cotyledon patterning in *pid wag1 wag2* seedlings. The failure to make cotyledon in F2 segregating progeny is increased in *supo1* and *cvp2* alleles.

DISCUSSION

$InsP_3$-dependent Ca^{2+} Signaling Mediates PIN-dependent Auxin Distribution

The transport-mediated auxin gradients within tissues represent a plant-specific mechanism to regulate basic developmental processes, such as embryogenesis (Friml et al., 2003; Geldner et al., 2004), organogenesis (Benková et al., 2003) and vascular tissue formation (Scarpella et al., 2006) as well as

adaptive development in response to environmental influences such as tissue regeneration after wounding (Xu et al., 2006) or tropisms (Chen et al., 1998; Luschnig et al., 1998; Müller et al., 1998; Friml et al., 2002b). The important factors in auxin transport are polarly localized PIN proteins that mediate directionality of the auxin flow between cells (Wiśniewska et al., 2006). On the other hand, fine-tuning of many basic cellular processes depends on Ca^{2+} signaling, which can be modulated by a multitude of signals, among others $InsP_3$ (White and Broadley, 2003; Kudla et al., 2010).

Our experimental results link the plant-specific mechanism of intercellular auxin transport and the evolutionarily conserved second messengers $InsP_3$ and Ca^{2+}. The initial observation came from the isolation of the *supo1* mutant defective in phosphatidylinositol phosphatase from a screen for mutants suppressing agravitropic growth in *PIN1* gain-of-function alleles. The *supo1* shows a number of defects typical for auxin transport-related mutants (eg. disconnected vasculature) and also, importantly, changes in auxin distribution. Multiple independent genetic and pharmacological manipulations demonstrated that increased levels of $InsP_3$ in the *supo1* mutant are responsible for the auxin transport-related defects, including the rescue of the *PIN1* gain-of-function agravitropic phenotype. These results linked $InsP_3$-related signaling to the PIN action in auxin transport.

A prominent downstream event of $InsP_3$ action is regulation of cytosolic Ca^{2+} levels (Gilroy et al., 1990; Tang et al., 2007) and thus Ca^{2+} signaling. Indeed, genetic and pharmacological manipulations of cytosolic Ca^{2+} levels confirmed that $InsP_3$-dependent Ca^{2+} signaling mediates the auxin transport-related defects of *supo1*. As expected, given the multiple cellular roles of phosphatidylinositols and Ca^{2+}, these regulatory circuits are also involved in other processes besides auxin transport as demonstrated by the identification of multiple *supo1* alleles in different genetic screens, e.g., focused on drought tolerance (Wilson et al., 2009) or ABA signaling (Xiong et al., 2001). Nonetheless, the remarkable rescue of the *PIN1* gain-of-function phenotype as well as other auxin-related phenotypes after manipulations of Ca^{2+} and $InsP_3$ levels establishes that $InsP_3$-mediated Ca^{2+} signaling is linked to the regulation of PIN activity, auxin transport and auxin-dependent development. As Ca^{2+} is one of the central second messengers in eukaryotic cells, these findings provide a mechanistic framework for multiple cellular processes and signals to modulate auxin gradient-mediated development via Ca^{2+} signaling.

$InsP_3$-dependent Ca^{2+} Signaling Mediates Apical-basal PIN Polarity

The PIN proteins have a dual role in mediating auxin distribution: they have auxin transport capability (Petrášek et al., 2006) and they determine the directionality of the auxin flow on account of their subcellular, polar localization (Wiśniewska et al., 2006). The PIN localizations in the *supo1* mutant and after the genetic and pharmacological manipulations with $InsP_3$ levels or cytosolic Ca^{2+} levels showed that these processes have impacts both on the apical and basal polarities of PIN localization. Increasing $InsP_3$ levels or activating cytosolic Ca^{2+} signaling has a preferential impact on targeting of PINs to the lower cell side, whereas inhibiting cytosolic Ca^{2+} signaling preferentially affected the apical PIN targeting. These observations suggested that cytosolic Ca^{2+} levels might specifically affect the basal versus apical decision of the PIN polar targeting. Modulation of the apical-basal PIN targeting can therefore explain the rescue of the *35S::PIN1* agravitropic growth and other observed auxin-related developmental defects. The molecular basis of the *35S::PIN1* agravitropism is the ectopic presence of the PIN1 at the basal side of epidermal cells, where it counteracts the PIN2 action at the apical side of cells in mediating the upward auxin flow (Mravec et al., 2008). Thus, interference with the basal PIN1 polarization mediated by $InsP_3$-induced Ca^{2+} in the epidermis allows the restoration of the PIN2-mediated flow, which is necessary for gravitropic root growth, whereas inhibition of Ca^{2+} signaling counteracts the apicalization of PIN1 in *supo1* mutant and prevents gravitropism rescue. Accordingly, the effects on basally localized PIN proteins can account for the defects in auxin distribution and auxin-mediated development.

The important remaining question relates to the mechanism by which the Ca^{2+} signaling regulates the apical-basal PIN polarity. The decision about apical-basal PIN targeting depends on PIN phosphorylation that is mediated by the antagonistic action of PID kinase and PP2A phosphatase (Friml et al., 2004; Michniewicz et al., 2007; Huang et al., 2010). Interestingly, PID activity can be regulated by phospholipid signaling (Zegzouti et al., 2006) and PID-interacting proteins that can bind Ca^{2+} (Benjamins et al., 2003). The relevance of these regulations for auxin transport and auxin-mediated development is unclear, but they provide a potential entry point for Ca^{2+} signaling on the apical-basal polarity.

EXPERIMENTAL PROCEDURES

Materials

35S::PIN1 (Benková et al., 2003); *pin1* (*pin1-1*) (Okada et al., 1991); *CYCB1;1::DB-GUS* (Colón-Carmona et al., 1999); *DR5rev::GFP* (Friml et al., 2003); *DR5::GUS* (Ulmasov et al., 1997); *cvp2* (Carland and Nelson, 2004); *PIN2::PIN2:GFP* (Xu and Scheres, 2005); *35S::PID* (Benjamins et al., 2001); and *pid wag1 wag2* (Dhonukshe et al., 2010) had been described previously. The insertion mutant lines *supo1-2* (SALK_020882) and *supo1-3* (salk_151367) were obtained from NASC. Insertion sites were verified, homozygous lines selected and the absence of the *SUPO1* transcript shown by RT-PCR.

The *SUPO1 promoter::GUS* fusion was generated with approximately 2 kb of the At5g63980 5'UTRs. The promoter fragments were amplified from genomic DNA with the following primer combinations containing the *attB* recombination sites (underlined): 5'-GGGGACAAGTTTGTACAAAAAAGCAGGCTTATTTCAGGAACAAAACAGAGC-3' and 5'-GGGGACCACTTTGTACAAGAAAGCTGGGTATCGCTTTTCAAGAAGATAAATATAT-3' for *SUPO1*. The fragments were finally cloned into the pKGWFS7.1 Gateway destination vector. The *SUPO1-GFP* C-terminal translational fusion was constructed by cloning separately the promoter and the whole genomic coding region of the *SUPO1* gene with the following primer combinations: 5'-GGGGACAACTTTGTATAGAAAAGTTGCTTTTCAGGAACAAAACAGAGCTATTC-3' and 5'-GGGGACTGCTTTTTTGTACAAACTTGCTCGCTTTTCAAGAAGATAAATATAT-3' for the promoter; 5'-GGGGACAGCTTTCTTGTACAAAGTGGCTATGATGTCTATAAATTGTTTTCG-3' and 5'-GGGGACAACTTTGTATAATAAAGTTGCTCAGAGAGCTGAAGCTTTCTC-3' for the coding region. The resulting entry clones combined with a clone of the GFP tag pEN-L1-F-L2, 0 were subsequently cloned into the Gateway destination vector pK7m34GW and its functionality was confirmed by transformation into the *supo1* mutant in the *35S::PIN1* background. The *GFP-SUPO1* N-terminal translational fusion was engineered by amplification of the *SUPO1* genomic fragment including the 2-kb promoter region and by cloning to the Gateway vector pK7FWG. The oligonucleotides used for PCR were: 5'-GGGGACAAGTTTGTACAAAAAAGCAGGCTTATTTCAGGAACAAAACAGAGC-3' and 5'-GGGGACCACTTTGTACAAGAAAGCTGGGTAGAGAGCTGAAGCTTTCTCTTGC-3'. The gain-of-function *SUPO1* construct was generated by cloning the complete genomic coding region with the primers: 5'-GGGGACAAGTTTGTACAAAAAAGCAGGCTTAATGATGTCTATAAATTGTTTTCG-3' and 5'-GGGGACCACTTTGTACAAGAAAGCTGGGTAGAGAGCTGAAGCTTTCTCTTGC-3'. The resulting fragment was finally cloned into the Gateway destination vector pK7FWG2, 0. The obtained constructs were transformed into the *Arabidopsis thaliana* wild type (ecotype Col-0) and the *supo1 35S::PIN1* by the standard floral dip method (Clough and Bent, 1998).

amiRNAs were engineered as described (Schwab et al., 2006) and placed under the control of the CaMV35S promoter. Three independent amiRNA fragments, miRNA-A, miRNA-B and miRNA-C, were initially generated with the following primer combinations for miRNA-A: ACA_A_I, 5'-GATCCATTATCATGTTAACCCACTCTCTCTTTTGTATTCC-3'; ACA_A_II, 5'-GAGTGGGTTAACATGATAATGGATCAAAGAGAATCAATGA-3'; ACA_A_III, 5'-GAGTAGGTTAACATGTTAATGGTTCACAGGTCGTGATATG-3'; and ACA_A_IV, 5'-GAACCATTAACATGTTAACCTACTCTACATATATATTCCT-3'. For miRNA-B: ACA_B_I, 5'-GATAGTTGTCATCCAAGATGATATCTCTCTTTTGTATTCC-3'; ACA_B_II, 5'-GATATCATCTTGGATGACAACTATCAAAGAGAATCAATGA-3'; ACA_B_III, 5'-GATACCATCTTGGATCACAACTTTCACAGGTCGTGATATG-3'; and ACA_B_IV: 5'-GAAAGTTGTGATCCAAGATGGTATCTACATATATATTCCT-3'. For miRNA-C; ACA_C_I, 5'-GATATGCACCAAGTGTGTCCGTGTCTCTCTTTTGTATTCC-3'; ACA_C_II, 5'-GACACGGACACACTTGGTGCATATCAAAGAGAATCAATGA-3'; ACA_C_III, 5'-GACAAGGACACACTTCGTGCATTTCACAGGTCGTGATATG-3'; and ACA_C_IV, 5'-GAAATGCACGAAGTGTGTCCTTGTCTACATATATATTCCT-3'. The predicted miRNA targets for amiRNA-A were AT1G27770 (*ACA1*), AT4G37640 (*ACA2*), AT2G41560 (*ACA4*), AT2G22950 (*ACA7*), and AT3G57330 (*ACA11*); for amiRNA-B, AT5G57110 (*ACA8*), AT3G21180 (*ACA9*), and AT4G29900 (*ACA10*); and for amiRNA-C, AT2G41560 (*ACA4*), AT3G57330 (*ACA11*), and AT3G22910 (*ACA13*). The obtained fragments of miRNA-A, miRNA-B and miRNA-C were subsequently constructed with the *attB* recombination sites by PCR amplification with the following primer combinations; attB4F, 5'-GGGGACAACTTTGTATAGAAAAGTTGGACCCCAAACACACGCTCGGACGC-3' and attB3R,

5’-GGGGACAACTTTGTATAATAAAGTTGTCCCCATGGCGATGCCTTAAAT-3’; attB1F, 5’-GGGGACAAGTTTGTACAAAAAAGCAGGCTGCCCCCAAACACACGCTCGGACGC-3’ and attB2R, 5’-GGGGACCACTTTGTACAAGAAAGCTGGGTCCCCCATGGCGATGCCTTAAAT-3’; attB6F, 5’-GGGGCAACTTTGTATTAAAAAGTTGCCCCAAACACACGCTCGGACGC-3’and attB5R: 5’-GGGGACAACTTTGTATACAAAAGTTGTGCCCCATGGCGATGCCTTAAAT-3’. The resulting three miRNA-A, miRNA-B and miRNA-C fragments were recombined simultaneously in the Gateway cassette vector pK7m34GW2-8m21GW3-9m56GW4 (Karimi et al., 2007) and obtained *amiRNA* construct was transformed into the *35S::PIN1* lines.

Drug Applications and Experimental Conditions

Arabidopsis seedlings and plants were grown as described (Friml et al., 2002a; Himanen et al., 2002). For details of the experimental conditions of drug applications, see Supplemental Information.

Exogenous drugs were applied by incubating seedlings in solid or liquid half-strength Murashige and Skoog (MS) medium supplemented with IP_3 (40 mM stock in Pluronic solution in DMSO) (40/80 µM), sodium nitroprusside (SNP) (50 mM stock in H_2O) (5/10 µM), U73122 (20 mM stock in DMSO) (5 µM), Cyclopiazonic acid (CPA) (4 mM stock in DMSO)(5/10 µM), Thapsigargin (Thaps) (2 mM stock in DMSO) (5/10 µM), 2-aminoethoxydiphenylboraneand (2-APB) (40 mM stock in DMSO) (10 µM), $LaCl_3$ (500 mM stock in H_2O) (600 µM), or EGTA (500 mM stock in H_2O) (500 mM). Control treatments contained an equivalent amount of solvent.

For the gravitropism assay, six-day-old seedlings grown vertically on regular MS medium were transferred to the solid medium supplemented with compounds and the positions of the root tips were marked. Downward growth was recorded from the marked point and was evaluated by a vertical growth index (VGI) (Grabov et al., 2005). ImageJ software was used for quantification (rsbweb.nih.gov/ij/download.html). Results are presented as means with standard errors. For *DR5* activity induction and PIN polarity relocation, long-term treatments of five-day-old seedlings were carried out in liquid medium (**>** 16 h). For all the assays in *35S::PID* and *pid wag1 wag2*, durgs were supplemented since the seeds germination. If alternative concentrations are mentioned, always relative lower one was used for gravitropism or *PID*-related assays. Only manipulation of IP_3 on gravitropism was done with 5 roots for each independent experiment, whereas for the other treatments, 10-30 roots were analyzed each time. For all comparisons, independent experiments were done in triplicate and always showed similar significant results. Representative data are shown.

Lateral Root Phenotype Analyses and GUS Staining

Lateral root initiation, developmental stage progression analyses and GUS staining were done as described (Benková et al., 2003).

Free IAA measurements

Shoots and roots (30 pieces each) of 6-day-old Arabidopsis seedlings grown on vertical plates were separated and collected in 700 µl or 300 µl methanol, respectively. After overnight extraction at -20°C, the tissues were separated by centrifugation (10,000 g) and extracts were evaporated to dryness. Free IAA determination was performed as described (Vandenbussche et al., 2010).

Auxin Transport Assays

Acropetal auxin transport was measured in 8-d-old plants after the modified method of Rashotte et al. (2000). Warm agar at 1,5 % (v/v) was mixed with 200 nM 3-[5(n)-^{3}H]IAA (26 Ci/mmol; Amersham), 100 nM cold IAA and DMSO at a final concentration of 0,2 % (v/v). A narrow stem glass transfer pipettes were used to excel small cylinders out of the hardened agar mixture. This was applied at the junction between the root and hypocotyl. The IAA transport was measured in the vertically oriented plants after 18 h in the dark (minimize IAA degradation) at 22 °C. First, abolish the apical 1 cm from the [^{3}H]IAA source, then harvest the rest segment to the root tip. Each independent root sample was placed into 10 mL of scintillation fluid and 1 mL of water. Then the radioactivity was measured for 10 min using a scintillation counter (model Tri-Carb 2800TR, Perkin Elmer, Waltham, MA).

Measurement of $InsP_3$ Content

5-day-old seedlings were used for the measurement of $InsP_3$ contents. Two hundred milligrams of fresh intact seedlings were harvested after being rinsed three times in H_2O, and then immediately frozen in liquid nitrogen. After being ground in liquid nitrogen, the samples were extracted with 20 % cold perchloric acid and supernatants collected after centrifugation at 2000 *g* for 15 min at 4 °C. The supernatants were neutralized to pH 7.5 with KOH, and then the $InsP_3$ level was measured using Inositol-1,4,5-Trisphosphate [^{3}H] Radioreceptor Assay Kit following manufacturer's instructions (PerkinElmer Life Sciences). The final $InsP_3$ contents in the samples were interpolated from a standard curve generated with known amounts of standard $InsP_3$. The independent assay experiments were repeated twice, and each measurement was performed in triplicate.

Measurement of cytosolic Ca^{2+} levels

Cytosolic Ca^{2+} was measured according to Legue et al. (1997) and Wymer et al. (1997). The intact seedlings were incubated in the Indo-1 solution (20 mM, Invitrogen) under darkness for 1 h. After being rinsed three times with liquid MS medium, seedlings were placed on a Zeiss confocal laser scanning microscope for fluorescence imaging. The distribution of Ca^{2+} was imaged from the root hairs and Ca^{2+} levels were pseudocolored according to the scale. As a quantitative support, mean fluorescence intensity at the tip of root hairs was measured using ImageJ software.

Map-based Cloning of *SUPO1*

To genetically map the *SUPO1* gene, we followed the segregation of the mutant phenotype in the F2 population of the cross between *supo1* (Col-0) and Landsberg *erecta* (Ler). Genetic analysis with 60 F2 segregants revealed the *supo1* mutant phenotype was initially linked to the terminal region of right arm of the chromosome 5. The linkage was narrowed down to a region between the SSLP (simple sequence length polymorphism) markers MQB2 and MUB3 by analyzing 560 F2 individuals. Final fine-mapping of 1600 F2 individuals further delimited a target region of 33 kb flanked by the CAPS (cleaved amplified polymorphic sequence) markers MBM17-Tas1 and MBM17-Bsp1407I on a single bacterial artificial chromosome (BAC) clone MBM17, which delineated six candidate genes. Genomic DNA from Ler and *supo1* mutant plants was extracted, and the six genes were amplified separately by PCR with appropriate primers. These products were sequenced directly and compared to determine the mutation site.

In Situ Expression and Localization Analysis

Whole-mount immunolocalization was performed as described (Friml et al., 2003; Sauer et al., 2006). Antibodies were diluted as follows: 1:1000 for rabbit anti-PIN1 (Paciorek et al., 2005); 1:1000 for rabbit anti-PIN2 (generously provided by C. Luschnig); and 1:600 for CY3-(Sigma) and Alex-(Invitrogen) conjugated anti-rabbit secondary antibodies. For each genotype or treatment, at least three independent experiments were performed, at least 10 roots in total were analyzed, and representative images are presented. For *in vivo* GFP inspection, five-day-old seedlings were mounted in the liquid MS medium containing relevant drugs without fixation for live-cell imaging. All the fluorescence signals were evaluated on a Leica TCS SP2 and Zeiss LSM 5 DUO confocal laser scanning microscope. The same microscope settings were always used for each independent experiment and pixel intensities were taken into account when comparing the images between control and mutants. Images were finally processed in Adobe Photoshop 7.0 and Adobe Illustrator 8.0.

Microscopy

Details regarding immunological staining, antibodies and dilutions can be found in Supplemental information. GFP samples were scanned without fixation. Confocal imaging was performed on a Leica TCS SP2 and Zeiss LSM 5 DUO confocal microscopes.

Quantitative analysis of PIN relocation

The statistical evaluations of PIN relocation in Figure 5 and Figure 6A were done by scoring the number of cells showing different PIN polarity. Their distributed percentages are present in the figures.

For Figure 6B, the mean fluorescence intensity of PIN2 signal at the outer lateral and the apical membrane of epidermis cells were measured using ImageJ software. The ratios between lateral and apical value were calculated and presented in the figure. Only median scans were analyzed for these quantitative evaluations and for each treatment at least 50 epidermal or cortical cells were analyzed. Results are presented as means with standard errors.

ACKNOWLEDGEMENTS

We are very grateful to M. De Cock for help in preparing the manuscript. We thank the Labor für Radioisotope (LARI) for support. This work was supported by grants from the Research Foundation-Flanders (Odysseus) (to JF), the European Union FP7-ERC-Starting Grant (ERC-2007-Stg-207362-HCPO) (to EB), a long-term fellowship from the European Molecular Biology Organization (ATLF142-2007) and a postdoctoral fellowship of the Research Foundation Flanders (to SV).

SUPPLEMENTAL FIGURES

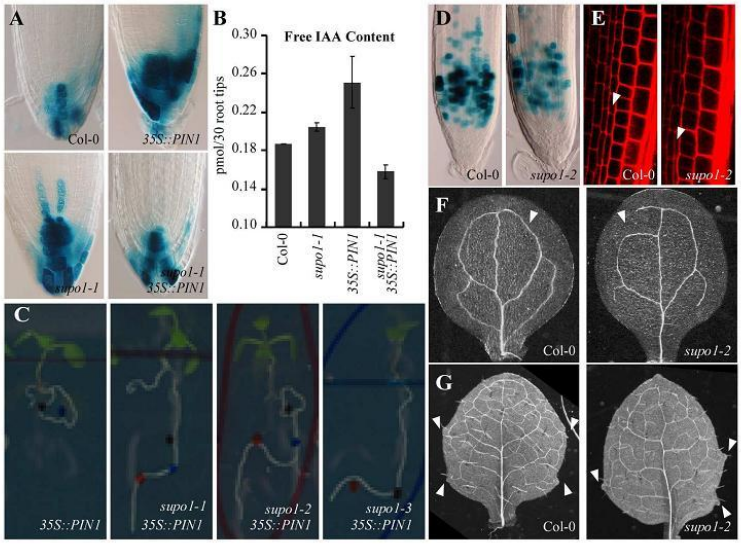

Figure S1. Role of *SUPO1* in the suppression PIN1 gain-of-function and regulation of plant development.
(A and B) Auxin distribution defects in *supo1-1*. *DR5::GUS* activity in the root meristem is higher in the *supo1-1* mutant than that of the wild type, but increased *DR5* activity originally seen in root tips of *35S::PIN1* is attenuated in *supo1-1* (A); *supo1-1* mutant has higher endogenous free IAA than the wild type, whereas *supo1 35S::PIN1* has lower IAA level in the root tips than *35S::PIN1* (B).
(C) Suppression of *35S::PIN1* agravitropic root growth by *supo1* alleles (*supo1-1*, *supo1-2* and *supo1-3*).
(D-G) Morphological defects in *supo1-2*. Decreased cell division in the root meristem visualized by *CYCB1;1::DB-GUS* (D); aberrant cell divisions (E); defects in vein patterning (34%, n=56; F) and leaf shape (42%, n=52; G).
Error bars are SE.

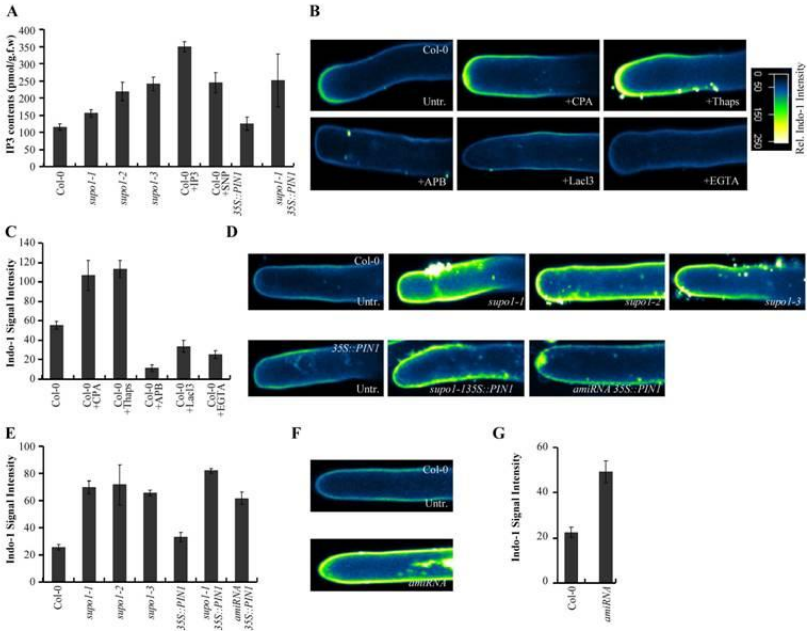

Figure S2. Measurement of status of $InsP_3$ and cytosolic Ca^{2+}
(A) Changes of $InsP_3$ contents. The increased levels of $InsP_3$ in *supo1* alleles and wild type in response to IP_3 and SNP treatments are present. $InsP_3$ was measured using a receptor-binding assay as described in the Experimental Procedures.
(B and C) Changes of cytosolic Ca^{2+} contents in response to various treatments. Image analysis was performed by UV confocal ratio on root hairs loaded with the fluorescent Ca^{2+} sensor Indo-1. Intercellular Ca^{2+} levels are color coded according to the inset scale (B); quantification of the fluorescence intensity at the tips of root hairs (C).
(D-G) Changes of cytosolic Ca^{2+} contents in *supo1* and *amiRNA* genotypes in wild type and *35S::PIN1* background.

Intercellular Ca^{2+} levels are color coded according to the inset scale (D and F); quantification of the fluorescence intensity at the tips of root hairs (E and G).
Error bars are SE.

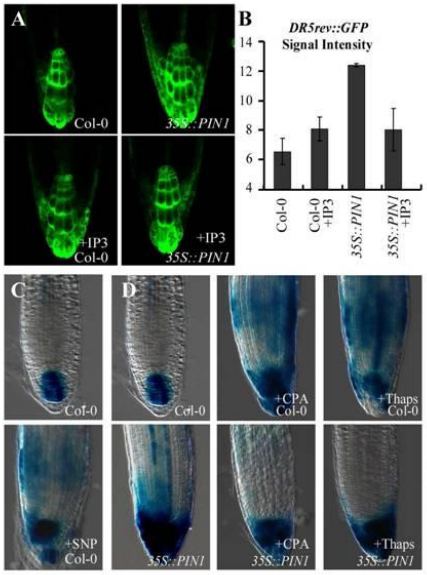

Figure S3. Role of elevated $InsP_3$ and cytosolic Ca^{2+} levels on auxin distribution
(A-C) Effect of manipulation of $InsP_3$ level on auxin distribution. Treatment with IP_3 broadens the *DR5rev::GFP* expression with signals detected also in outer cell layers, the lateral root cap, and the epidermis, but increased *DR5* signals in *35S::PIN1* roots are suppressed by IP_3 (A); quantification of the GFP fluorescence intensity (B); application of SNP also increases *DR5::GUS* activity in the wild type (C).
(D) Effect of manipulation of Ca^{2+} level on auxin distribution. Exogenous applications of CPA and Thaps increase *DR5* response in the roots of wild type and suppresses it in *35S::PIN1*.
Error bars are SE.

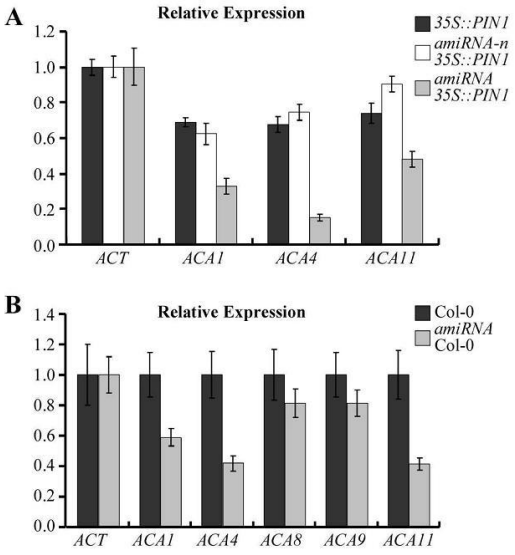

Figure S4. Quantitative RT-PCR analysis on the genes targeted by the *amiRNA* transgenes
(A) Relative gene expression in *amiRNA 35S::PIN1* line. The expression of *ACA1*, *ACA4* and *ACA11* is downregulated; *Actin* (*ACT*) gene is used as a reference control.
(B) Relative gene expression in *amiRNA* in wild-type background. The expression of *ACA1*, *ACA4*, *ACA8*, *ACA9* and *ACA11* is downregulated; *Actin* (*ACT*) gene is used as a reference control.
Error bars are SE.

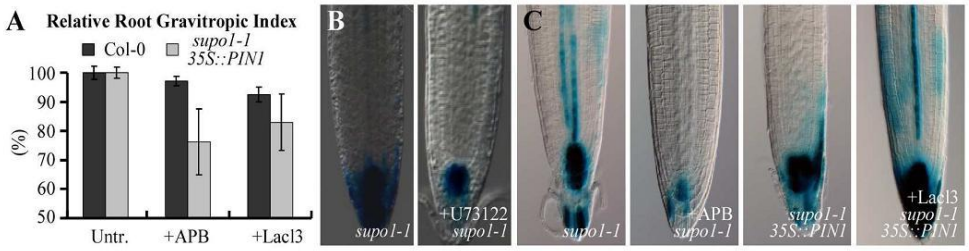

Figure S5. Role of attenuated $InsP_3$ and cytosolic Ca^{2+} levels on root gravitropism and auxin distribution
(A) Effect of decreased Ca^{2+} levels on root gravitropism. Treatments of APB and $LaCl_3$ cause more agravitropic root growth in *supo1 35S::PIN1*.
(B) Effect of decreased $InsP_3$ levels on auxin distribution. U73122 treatment counteracts the effect of *supo1* on the increase of *DR5* auxin response.
(C) Effect of decreased Ca^{2+} levels on auxin distribution. *DR5* activity in *supo1* is decreased by APB, but increased particularly by $LaCl_3$ in *supo1 35S::PIN1*.
Error bars are SE.

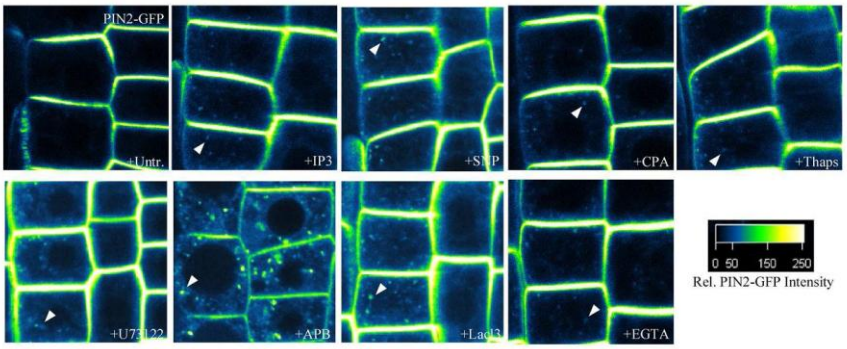

Figure S6. Regulation of PIN2 trafficking by $InsP_3$ and Ca^{2+} signalling
All the pharmacological manipulations induce intercellular accumulation of GFP-tagged PIN2 protein. PIN2 signal intensities are color coded according to the inset scale.

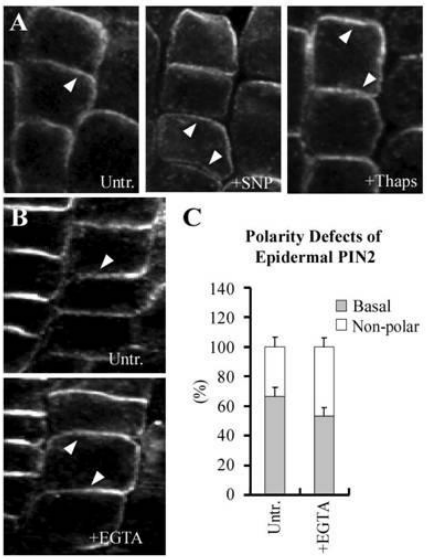

Figure S7. PID-related regulation of $InsP_3$ and Ca^{2+} signaling on PIN polarity
(A) Immunolocalization of PIN2 in the cortex of *35S::PID* roots. Supplementation of SNP and Thaps mildly induce basally localized PIN2.
(B and C) Immunolocalization of PIN2 in the epidermis of *pid wag1 wag2* roots. EGTA treatment causes a gradual basal-to-apical shift of PIN2 in young epidermis cells (B); quantification of defective epidermal PIN2 (C).
Arrowheads mark PIN polarity. Error bars are SE.

CHAPTER 6

Concluding Remarks

CONCLUSIONS AND FUTURE DIRECTIONS

The intracellular flow of auxin from young apical tissues from where it is synthesized to the place of its action is mediated by the directional, cell-to-cell delivery system known as PAT. The main components driving PAT are PIN auxin efflux carriers, which asymmetrically localized at PM. The polar localization of PIN protein at the level of single cell correlates well with the directionality of auxin flow. The extensive data have indicated that PIN polarity is controlled by a complex network of molecular cell autonomous components, which integrates external and internal cues at the single cell level. However, the question of how the polar subcellular localizations of PIN proteins are controlled is still not well understood. Thus, identifying the mechanisms underling the PIN polar targeting was the main task of this Ph.D study.

In this thesis, we demonstrated that the level of reversible phosphorylation mediated by PINOID kinase and PP2A phosphatase regulates PIN polarity and thus auxin transport and auxin-related developmental processes. We also indentified an evolutionarily conserved phosphorylation site within the PIN1 hydrophylic loop, which is required and sufficient for proper polar PIN localization. We further proposed an underlying mechanism of how GNOM ARF GEF-independent recycling pathway is involved in the phosphorylation-based modulation of PIN polar delivery. Nevertheless, many questions are still needed to be answered. For instance, how do the cellular mechanisms distinguish phosphorylated over non-phosphorylated PIN proteins before recruiting it to apical or basal polar trafficking pathways; what are the upstream components in the phosphorylation cascade; what are the downstream elements acting after PIN phoshorylation; and beside PID, can other AGC kinases regulate PIN activity? These research questions will be the next challenges for the coming years.

One of surprising findings of the thesis is that the $InsP_3$-mediated Ca^{2+} signaling is linked to the regulation of PIN activity, auxin transport and auxin-dependent development. *supo1* mutant was identified as a suppressor of *PIN1* gain-of-function agravitropic root growth from a forward genetic screen. *supo1* mutation encodes an inositol phosphatase which is involved in the metabolism of $InsP_3$. Multiple independent genetic and pharmacological manipulations demonstrated that the role of $InsP_3$-mediated Ca^{2+} in the decision of PIN polar delivery. The remaining question related to the mechanism by which the Ca^{2+} signaling regulates the apical-basal PIN polarity remains elusive. Ca^{2+} signaling negatively regulate PID activity and PID can mediate basal-apical PIN localization. Although it is clarified that regulation of PIN polarity by Ca^{2+} is PID kinase-related, how the model exactly works is still not known. In order to indentify the downstream component involved in the regulation of Ca^{2+} signaling on PIN localization, we would probably design another forward genetic screen for a suppressor of *supo1 35S::PIN1* gravitropic root growth.

AUTHOR'S CONTRIBUTIONS TO THE MANUSCRIPTS

Michniewicz M, Zago MK, Abas L, Weijers D, Schweighofer A, Meskiene I, Heisler MG, Ohno C, Zhang J, Huang F, Schwab R, Weigel D, Meyerowitz EM, Luschnig C, Offringa R, Friml J. (2007). Antagonistic Regulation of PIN Phosphorylation by PP2A and PINOID Directs Auxin Flux. Cell 130, 1044-1056.

JZ performed experiments presented in Figure 5G-I.

Zhang J, Nodzynski T, Pencík A, Rolcík J, Friml J. (2010). PIN phosphorylation is sufficient to mediate PIN polarity and direct auxin transport. Proc Natl Acad Sci USA. 107, 918-922.

JF initiated the projects; JZ and JF designed experiments; JZ carried out most of the experiments; NT performed experiments presented in Figure 4D and Figure S3; PA and RJ contributed Figure 3C; JZ assembled the figures; and JZ and JF discussed the resultes and wrote the manuscript.

Kleine-Vehn J, Huang F, Naramoto S, Zhang J, Michniewicz M, Offringa R, Friml J. (2009). PIN auxin efflux carrier polarity is regulated by PINOID kinase-mediated recruitment into GNOM-independent trafficking in Arabidopsis. Plant Cell 21, 3839-3849.

JZ performed experiments presented in Figure 1.

Zhang J, Vanneste S, Brewer PB., Michniewicz M, Grones P, Kleine-Vehn J, Löfke C, Teichmann T, Bielach A, Cannoot B, Hoyerová K, Benková E, Zažímalová E, Friml J. (2010). Phosphatidylinositol phosphatase links calcium signaling with auxin transport and cell polarity. Developmental Cell, Submitted.

JF initiated the projects; JZ and JF designed experiments; JZ carried out most of the experiments; VS helped in cloning amiRNA constructs; PBB and MM performed the forward genetic screening; PG and BC helped with genotyping; CL and TT measured auxin acropetal transport presented Figure 2G; AB and EB contributed Figure 2C; KH and EZ measured free auxin contents presented Figure S1B; JZ assembled the figures; and JZ, VS, JKV, and JF discussed the resultes; and JZ, VS, and JF wrote the manuscript.

FREQUENTLY USED ABBREVIATIONS

ABA	Abscisic acid
APB	Aminoethoxydiphenylborane
ARF	Adenosyl ribosylation factor
BFA	Brefeldin A
bp	Base pair
Ca^{2+}-ATPases	ATP-driven pumps
Col-0	Columbia-0
CPA	Cyclopiazonic acid
CVP2	Cotyledon vascular pattern2
DMSO	Dimethylsulfoxide
DRM	Detergent-resistant microdomains
ER	Endoplasmatic reticulum
EryB	Erythrosin B
GC/MS	Gas chromatography/mass spectroscopy
GEF	Guanine nucleotide exchange factor
GFP	Green Fluorescent protein
GUS	β-Glucuronidase
HA	Hemagglutinin
HL	Hydrophilic loop
IAA	Indolacetic acid
$InsP_3$	Inositol 1,4,5-trisphosphate
LatB	Latrunculin B
MBP	Myelin Basic Protein
MS	Murashige and shoog
NPA	1-N-naphtylphtalamic acid
PAT	Polar auxin transport
PGP	Mulutidrug resistance/P glycoprotein
PI3K	Phosphatidylinositol-3-kinase
PID	PINOID
PIN	PIN-FORMED
PLC	Phospholipase C
PM	Plasma membrane
PP2A	Protein phosphatase 2A
RCN	Root curl on NPA
SNP	Sodium nitroprusside
SNX	SORTING NEXIN
SUPO1	Suppressor of PIN1 overexpression
Thaps	Thapsigargin
VPS	Vacuolar protein sorting
YFP	Yellow fluorescent protein

CURRICULUM VITAE

Jing Zhang was born on 28 January 1983 in Shanxi, China. Since 2002, having finished first two years study of Bachelor programme in Plant Biotechnology at China Agriculture University, she joined in the same programme at Larenstein University in the Netherlands, where she obtained a Bachelor degree in 2004. The two-year experience as a visiting student convinced her to pursuit a Master of Science degree. Therefore, from 2004 to 2006, she participated in a Master programme of plant biotechnology at the Wageningen University, and did research on the identification and characterization of *Arabidopsis* germination stimulants of *Orobanche ramose* under the supervision of Professor Harro Bouwmeester. Her success in master study had led to a Ph.D study on a project of "phosphorylation-mediated regulation of cell polarity and auxin transport in plants" under supervision of Professor Jiri Friml from October 2006 in Department of Plant Systems Biology, Gent University, Belgium. This thesis is the product of her four years Ph.D research, which was financed by the Odysseus program of the Research Foundation-Flanders.

PUBLICATIONS

Zhang J, Nodzynski T, Pencík A, Rolcík J, Friml J (2010). PIN phosphorylation is sufficient to mediate PIN polarity and direct auxin transport. ***Proc Natl Acad Sci USA. 107, 918-922.***

Zhang J, Vanneste S, Brewer PB., Michniewicz M, Bielach A, Hoyerová K, Kleine-Vehn J, Benková E, Zažímalová E, Friml J. (2010). Phosphatidylinositol phosphatase links calcium signaling with auxin transport and cell polarity. ***Developmental Cell, Submitted.***

Robert S, Kleine-Vehn J, Barbez E, Sauer M, Paciorek T, Baster P, Vanneste S, **Zhang J**, Simon S, Čovanová M, Hayashi K, Dhonukshe P, Yang Z, Bednarek SY, Jones AM, Luschnig C, Aniento F, Zažímalová E, Friml J. (2010) ABP1 mediates auxin inhibition of clathrin-dependent endocytosis in Arabidopsis. ***Cell 143, 111-121.***

Hazak O, Bloch D, Poraty L, Sternberg H, **Zhang J**, Friml J, Yalovsky S. (2010). A rho scaffold integrates the secretory system with feedback mechanisms in regulation of auxin distribution. ***PLoS Biol 8, e1000282.***

Kleine-Vehn J, Huang F, Naramoto S, **Zhang J**, Michniewicz M, Offringa R, Friml J. (2009). PIN auxin efflux carrier polarity is regulated by PINOID kinase-mediated recruitment into GNOM-independent trafficking in Arabidopsis. ***Plant Cell 21, 3839-3849.***

Mravec J, Skůpa P, Bailly A, Hoyerová K, Krecek P, Bielach A, Petrásek J, **Zhang J**, Gaykova V, Stierhof YD, Dobrev PI, Schwarzerová K, Rolcík J, Seifertová D, Luschnig C, Benková E, Zazímalová E, Geisler M, Friml J. (2009). Subcellular homeostasis of phytohormone auxin is mediated by the ER-localized PIN5 transporter. ***Nature 459, 1136-1140.***

Michniewicz M, Zago MK, Abas L, Weijers D, Schweighofer A, Meskiene I, Heisler MG, Ohno C, **Zhang J**, Huang F, Schwab R, Weigel D, Meyerowitz EM, Luschnig C, Offringa R, Friml J (2007). Antagonistic Regulation of PIN Phosphorylation by PP2A and PINOID Directs Auxin Flux. ***Cell 130, 1044-1056.***

ACKNOWLEDGEMENTS

My overseas study in European started eight years ago when I was a naive girl, full of dreams but no exact direction. I am grateful to everyone who has helped me to find my own way and to achieve this milestone in my life journey. Please forgive me if I forget to mention your name. You are in my heart anyway!

The story started from my bachelor study, the first person I want to acknowledge is my supervisor Frans H.A.Wilms, who had guided me to knock on the door of plant biotechnology. I also thank my daily supervisor Harro Bouwmeester and Zhongkui Sun for guidance and suggestions during my master thesis. I appreciate your patience with my limited experience in the lab at the beginning. I cannot thank you enough for your kindness and support over the years.

Three months before I finished my master thesis, Jiri Friml proposed to me this PhD project under the supervision of himself. Jiri, I am grateful that you chose me for this position. Your profound knowledge, your brilliant ideas, and your excellent experience in teaching and supervising made discussions with you so insightful, and your enthusiasm and passion on the research also deeply impressed me, which will have a great impact in my further career. I have truly learned a lot from you after each discussion and interpretation with you. There would have been no guarantee of the academic quality of this dissertation, without your critical and detailed comments on the design, analysis and writing. Thank you very much for everything you did for me, and for your constant support.

I must say that I enjoyed life in the PSB very much, especially the nice international and scientific atmosphere here. Actually, my stay at PSB located mainly at the Auxin Lab, a big family-like group. I will never forget the group members who make my daily life beautiful. So my deep acknowledgements go to all the people in the Auxin group (ex-colleague: Jozef, Stéphanie, Hiro and saeko; current colleague: Jürgen, Steffen, Satoshi, Helene, ZhaoJun, Wim, Sibylle, Yunlong, Xu, Niloufer, Lukasz, Marta, Tomek, Elena, Ricardo, Elke, Pawel, Urszula, Peter, Hana, Krzysztof, Bernard and Mugurel). You are not only my colleagues but also my friends who can share my happiness and sadness at any time. Above all this, I would like to especially thank Jürgen and Steffen, you guys are always there for me whenever I need a discussion or help. My special heartfelt thanks are also to the help from Hana and Peter. Eva and Agnieszka have been one of our nice collaborators, my gratitude land on their willingness to help and their significant contributions.

Work discussion in the joint cell biology groups every Tuesday morning was an important part of my PhD life. Thanking all the participants for sharing information, ideas and suggestions.

Although I have stayed abroad for long time, I am not root detached. I would send my thanks to all my Chinese friends in PSB. My dear lunch-mates, ZhaoJun, HuiYu, Yunlong, Xu, DaLong, Wei, GuangLing, Bing and YaoYao, it was my great pleasure to meet you and to share lunch time with you. I must specially mention a friend, who had polished my life with joy and colors: Niu, my lovely room-mate. You are such a sunny girl and I really enjoyed time we spend together. Our friendship is my treasures forever.

I am a lucky person. Besides all above, the love from parents, parents in law, sister, brother and all the relatives in the family is the key reason of building-up my positive attitude. Dad and Mom, You are all the time supporting me whenever I need. I am in great debt of you for your love.

我是一个特别幸运的人。我的幸运除了上述的所有际遇外，我的家人们（爸爸妈妈，公公婆婆，妹妹，弟弟以及亲戚们）对我无限的关爱是让我拥有乐观个性的关键。我最亲最亲的爸爸妈妈，谢谢你们这么多年来对我无微不至的关怀，是你们用博大的胸怀与深沉的爱包容了我的一切优点与缺点。还有公公婆婆，谢谢你们一直以来对我默默的支持，是你们用宽容和理解坚定了我在外求学的决心。再次感谢家人，你们是我感情的寄托，是我心灵的港湾，我爱你们。

There may be many regrets and failures in my thesis and also in my personal life, but I would never regret to marry Wu Feng. Although we are temporarily spaced, I never feel there is a distance between us. Without your love, understanding, supporting, and encouragement over years, I would have never come to this academic point. I am grateful for the special love you show in different ways. Feng, you know how pride I am of you, because of your charming personality, responsible attitude, and successful career. My wish is to hold your hands and grow old together.

REFERENCES

Abas, L., Benjamins, R., Malenica, N., Paciorek, T., Wiśniewska, J., Moulinier-Anzola, J.C., Sieberer, T., Friml, J., and Luschnig, C. (2006). Intracellular trafficking and proteolysis of the Arabidopsis auxin-efflux facilitator PIN2 are involved in root gravitropism. Nat. Cell Biol. 8, 249-256.

Bandyopadhyay, A., Blakeslee, J.J., Lee, O.R., Mravec, J., Sauer, M., Titapiwatanakun, B., Makam, S.N., Bouchard, R., Geisler, M., Martinoia, E., et al. (2007). Interactions of PIN and PGP auxin transport mechanisms. Biochem. Soc. Trans. 35, 137-141.

Bartel, B., LeClere, S., Magidin, M., and Zolmann, B.K. (2001) Inputs to the active indole-3-aceticacid pool: de novo synthesis, conjugate hydrolysis, and indole-3-butyric acid β-oxidation. J. Plant Growth Regul. 20, 198-216.

Benjamins, R., Quint, A., Weijers, D., Hooykaas, P., and Offringa, R. (2001). The PINOID protein kinase regulates organ development in Arabidopsis by enhancing polar auxin transport. Development 128, 4057-4067.

Benjamins, R., Ampudia, C.S., Hooykaas, P.J., and Offringa, R. (2003). PINOID-mediated signaling involves calcium-binding proteins. Plant Physiol. 132, 1623-1630.

Benjamins, R., and Scheres, B. (2008). Auxin: the looping star in plant development. Annu. Rev. Plant Biol. 59, 443-465.

Benková, E., Michniewicz, M., Sauer, M., Teichmann, T., Seifertova, D., Jurgens, G., and Friml, J. (2003). Local, efflux-dependent auxin gradients as a common module for plant organ formation. Cell 115, 591-602.

Bennett, S.R.M., Alvarez, J., Bossinger, G., and Smyth, D.R. (1995). Morphogenesis in pinoid mutants of Arabidopsis thaliana. Plant J. 8, 505-520.

Bennett, M.J., Marchant, A., Green, H.G., May, S.T., Ward, S.P., Millner, P.A., Walker, A.R., Schulz, B., Feldmann, K.A. (1996) Arabidopsis AUX1 gene: a permease-like regulator of root gravitropism. Science 273, 948-950.

Benschop, J.J., Mohammed, S., O'flaherty, M., Heck, A.J., Slijper, M., and Menke, F.L. (2007). Quantitative phospho-proteomics of early elicitor signalling in Arabidopsis. Mol. Cell. Proteomics 6, 1198-1214.

Berleth, T., Scarpella, E., and Prusinkiewicz, P. (2007). Towards the systems biology of auxin-transport-mediated patterning. Trends Plant Sci. 12, 151-159.

Berridge, M.J. (2009). Inositol trisphosphate and calcium signalling mechanisms. Biochim. Biophys. Acta 1793, 933-940.

Blakeslee, J.J., Bandyopadhyay, A., Lee, O.R., Mravec, J., Titapiwatanakun, B., Sauer, M., Makam, S.N., Cheng, Y., Bouchard, R., Adamec, J., et al. (2007). Interactions among PIN-FORMED and P-glycoprotein auxin transporters in Arabidopsis. Plant Cell 19, 131-147.

Blilou, I., Xu, J., Wildwater, M., Willemsen, V., Paponov, I., Friml, J., Heidstra, R., Aida, M., Palme, K., and Scheres, B. (2005). The PIN auxin efflux facilitator network controls growth and patterning in Arabidopsis roots. Nature 443, 39-44.

Burnette, R.N., Gunesekera, B.M., and Gillaspy, G.E. (2003). An Arabidopsis inositol 5-phosphatase gain-of-function alters abscisic acid signaling. Plant Physiol. 132, 1011-1019.

Cambridge, A., and Morris, D. (1996). Transfer of exogenous auxin from the phloem to the polar auxin transport pathway in pea (Pisum sativum L.). Planta 199, 583-588.

Carland, F.M., and Nelson, T. (2004). COTYLEDON VASCULAR PATTERN2-mediated inositol (1,4,5) triphosphate signal transduction is essential for closed venation patterns of Arabidopsis foliar organs. Plant Cell 16, 1263-1275.

Casanova, J.E., Breitfeld, P.P., Ross, S.A., and Mostov, K.E. (1990). Phosphorylation of the polymeric immunoglobulin receptor required for its efficient transcytosis. Science 248, 742-745.

Casimiro, I., Marchant, A., Bhalerao, R.P., Beeckman, T., Dhooge, S., Swarup, R., Graham, N., Inzé, D., Sandberg, G., Casero, P.J., et al. (2001). Auxin transport promotes Arabidopsis lateral root initiation. Plant Cell 13, 843-852.

Chalmers, A.D., Pambos, M., Mason, J., Lang, S., Wylie, C., and Papalopulu, N. (2005). aPKC, Crumbs3 and Lgl2 control apicobasal polarity in early vertebrate development. Development 132, 977-986.

Chen, R., Hilson, P., Sedbrook, J., Rosen, E., Caspar, T., and Masson, P. (1998). The Arabidopsis thaliana AGRAVITROPIC1 gene encodes a component of the polar-auxin-transport efflux carrier. Proc. Natl. Acad. Sci. USA 95, 15112-15117.

Cheng, Y., Qin, G., Dai, X., and Zhao, Y. (2008) NPY genes and AGC kinases define two key steps in auxin-mediated organogenesis in Arabidopsis. Proc Natl Acad Sci USA 105, 21017-21022.

Christensen, S.K., Dagenais, N., Chory, J., and Weigel, D. (2000). Regulation of auxin response by the protein kinase PINOID. Cell 100, 469-478.

Chow, C.-M., Neto, H., Foucart, C., and Moore, I. (2008). Rab-A2 and Rab-A3 GTPases define a *trans*-Golgi endosomal membrane domain in *Arabidopsis* that contributes substantially to the cell plate. Plant Cell 20, 101-123.

Colón-Carmona, A., You, R., Haimovitch-Gal, T., and Doerner, P. (1999). Spatio-temporal analysis of mitotic activity with a labile cyclin-GUS fusion protein. Plant J. 20, 503-508.

Cousson, A. (2003). Two potential Ca2+-mobilising processes depend on the abscisic acid concentration and growth temperature in the Arabidopsis stomatal guard cell. J. Plant Physiol. 160, 493-501.

Darwin, C., and Darwin, F. (1881). The power of movement in plants. (German translation:Das Bewegungsvermögen der Pflanze). Darwins gesammelte Werke, Vol.13.Schweizer-bart'sche Verlagsbuchhandlung, Stuttgart.

daSilva, L.L.P., Taylor, J.P., Hadlington, J.L., Hanton, S.L., Snowden, C.J., Fox, S.J., Foresti, O., Brandizzi, F., and Denecke, J. (2005). Receptor salvage from the prevacuolar compartment is essential for efficient vacuolar protein targeting. Plant Cell 17, 132-148.

Davis, P. J. (2004). Plant Hormones: Biosynthesis, Signal Transduction, Action! (Dordrecht, The Netherlands: Kluwer Academic Publishers).

DeFalco, T.A., Bender, K.W., and Snedden, W.A. (2010). Breaking the code: Ca2+ sensors in plant signalling. Biochem J. 425, 27-40.

dela Fuente, R.K., and Leopold, A.C. (1973). A role for calcium in auxin transport. Plant Physiol. 51, 845-847.

Dhonukshe, P., Kleine-Vehn, J., Friml, J. (2005). Cell polarity, auxin transport, and cytoskeleton-mediated division planes: who comes first? Protoplasma 226, 67-73.

Dhonukshe, P., Aniento, F., Hwang, I., Robinson, D., Mravec, J., Stierhof, Y.-D., and Friml, J. (2007). Clathrin-mediated constitutive endocytosis of PIN auxin efflux carriers in Arabidopsis. Curr. Biol. 17, 520-527.

Dhonukshe, P., Tanaka, H., Goh, T., Ebine, K., Mähönen, A.P., Prasad, K., Blilou, I., Geldner, N., Xu, J., Uemura, T., et al. (2008). Generation of cell polarity in plants links endocytosis, auxin distribution and cell fate decisions. Nature 456, 962-966.

Dhonukshe, P. (2009). Cell polarity in plants: Linking PIN polarity generation mechanisms to morphogenic auxin gradients. Commun Integr Biol. 2, 184-90.

Donaldson, J.G., and Jackson, C.L. (2000). Regulators and effectors of the ARF GTPases. Curr. Opin. Cell Biol. 12, 475-482.

Eshed, Y., Baum, S.F., Perea, J.V., Bowman, J.L. (2001). Establishment of polarity in lateral organs of plants. Curr. Biol. 11, 1251-60.

Farr, G.A., Hull, M., Mellman, I., and Caplan, M.J. (2009). Membrane proteins follow multiple pathways to the basolateral cell surface in polarized epithelial cells. J. Cell Biol. 186, 269-282.

Friml, J., Benková, E., Blilou, I., Wiśniewska, J., Hamann, T., Ljung, K., Woody, S., Sandberg, G., Scheres, B., Jurgens, G., et al. (2002a). AtPIN4 mediates sink-driven auxin gradients and root patterning in Arabidopsis. Cell 108, 661-673.

Friml, J., Wiśniewska, J., Benková, E., Mendgen, K., and Palme, K. (2002b). Lateral relocation of auxin efflux regulator PIN3 mediates tropism in Arabidopsis. Nature 415, 806-809.

Friml, J., and Palme, K. (2002c). Polar auxin transport--old questions and new concepts? Plant Mol Biol. 49, 273-284.

Friml, J., Vieten, A., Sauer, M., Weijers, D., Schwarz, H., Hamann, T., Offringa, R., and Jurgens, G. (2003a). Efflux-dependent auxin gradients establish the apical-basal axis of Arabidopsis. Nature 426, 147-153.

Friml, J. (2003b). Auxin transport-shaping the plant. Curr. Opin. Plant Biol. 6, 7-12.

Friml, J., Benková, E., Mayer, U., Palme, K., and Muster, G. (2003c) Automated whole mount localisation techniques for plant seedlings. Plant J. 34, 115-124.

Friml, J., Yang, X., Michniewicz, M., Weijers, D., Quint, A., Tietz, O., Benjamins, R., Ouwerkerk, P.B., Ljung, K., Sandberg, G., et al. (2004). A PINOID-dependent binary switch in apical-basal PIN polar targeting directs auxin efflux. Science 306, 862-865.

Gälweiler, L., Guan, C., Müller, A., Wisman, E., Mendgen, K., Yephremov, A., and Palme, K. (1998). Regulation of polar auxin transport by AtPIN1 in Arabidopsis vascular tissue. Science 282,

2226-2230.
Garbers, Ch., DeLong, A., Deruére, J., Bernasconi, P., and Söll, D. (1996). A mutation in protein phosphatase 2A regulatory subunit A affects auxin transport in Arabidopsis. EMBO J. 15, 2115-2124.
Geisler, M., Blakeslee, J.J., Bouchard, R., Lee, O.R., Vincenzetti, V., Bandyopadhyay, A., Titapiwatanakun, B., Peer, W.A., Bailly, A., Richards, E.L., et al. (2005) Cellular efflux of auxin catalyzed by the Arabidopsis MDR/PGP transporter AtPGP1. Plant J. 44, 179-194.
Geldner, N., Friml, J., Stierhof, Y.-D., Jürgens, G., and Palme, K. (2001). Auxin transport inhibitors block PIN1 cycling and vesicle trafficking. Nature 413, 425-428.
Geldner, N., Anders, N., Wolters, H., Keicher, J., Kornberger, W., Muller, P., Delbarre, A., Ueda, T., Nakano, A., and Jürgens, G. (2003). The *Arabidopsis* GNOM ARF-GEF mediates endosomal recycling, auxin transport, and auxin-dependent plant growth. Cell 112, 219-230.
Geldner, N., Richter, S., Vieten, A., Marquardt, S., Torres-Ruiz, R.A., Mayer, U., and Jürgens, G. (2004). Partial loss-of-function alleles reveal a role for *GNOM* in auxin transport-related, post-embryonic development of *Arabidopsis*. Development 131, 389-400.
Gilroy, S., Read, N.D., and Trewavas, A.J. (1990). Elevation of cytoplasmic calcium by caged calcium or caged inositol triphosphate initiates stomatal closure. Nature 346, 769-771.
Grabov, A., Ashley, M.K., Rigas, S., Hatzopoulos, P., Dolan, L., and Vicente-Agullo, F. (2005) Morphometric analysis of root shape. New Phytol. 165, 641-651.
Grebe, M., Xu, J., Mobius, W., Ueda, T., Nakano, A., Geuze, H.J., Rook, M.B., and Scheres, B. (2003). Arabidopsis sterol endocytosis involves actin-mediated trafficking via ARA6-positive early endosomes. Curr Biol. 13, 1378-1387.
Hamann, T., Benkova, E., Baurle, I., Kientz, M. and Jurgens, G. (2002). The Arabidopsis BODENLOS gene encodes an auxin response protein inhibiting MONOPTEROS-mediated embryo patterning. Genes Dev. 16, 1610-1615.
Hardtke, C.S., and Berleth, T. (1998). The Arabidopsis gene MONOPTEROS encodes a transcription factor mediating embryo axis formation and vascular development. EMBO J. 17, 1405-1411.
Hawkins, J., Zheng, S., Frantz, B., and LoGrasso, P. (2000) p38 map kinase substrate specificity differs greatly for protein and peptide substrates. Arch. Biochem Biophys. 382, 310-313.
Heisler, M.G., Ohno, C., Das, P., Sieber, P., Reddy, G.V., Long, J.A., and Meyerowitz, E.M. (2005). Patterns of auxin transport and gene expression during primordium development revealed by live imaging of the *Arabidopsis* inflorescence meristem. Curr. Biol. 15, 1899-1911.
Hellens, R.P., Edwards, E.A., Leyland, N.R., Bean, S. and Mullineaux, P.M. (2000) "pGreen: a versatile and flexible binary Ti vector for Agrobacterium mediated plant transformation", Plant Mol. Bio. 42, 819-832.
Himanen, K., Boucheron, E., Vanneste, S., de Almeida Engler, J., Inzé, D., and Beeckman, T. (2002). Auxin-mediated cell cycle activation during early lateral root initiation. Plant Cell 14, 2339-2351.
Hu, G., and Minshall, R.D. (2009). Regulation of transendothelial permeability by *Src* kinase. Microvasc. Res. 77, 21-25.
Huang, F., Zago, M.K., van Marion, A., Galván-Ampudia, C.S., and Offringa, R. (2009) Phosphorylation of conserved PIN motifs by PINOID controls Arabidopsis PIN1 polar targeting. Plant Cell 22, 1129-1142.
Im, Y.J., Perera, I.Y., Brglez, I., Davis, A.J., Stevenson-Paulik, J., Phillippy, B.Q., Johannes, E., Allen, N.S., and Boss, W.F. (2007). Increasing plasma membrane phosphatidylinositol(4,5)bisphosphate biosynthesis increases phosphoinositide metabolism in Nicotiana tabacum. Plant Cell 19, 1603-1616.
Jaillais, Y., Fobis-Loisy, I., Miège, C., Rollin, C., and Gaude, T. (2006). AtSNX1 defines an endosome for auxin-carrier trafficking in Arabidopsis. Nature 443, 106-109.
Jaillais, Y., Santambrogio, M., Rozier, F., Fobis-Loisy, I., Miège, C., and Gaude, T. (2007). The retromer protein VPS29 links cell polarity and organ initiation in plants. Cell 130, 1057-1070.
Jaillais, Y., Fobis-Loisy, I., Miège, C., and Gaude, T. (2008). Evidence for a sorting endosome in Arabidopsis root cells. Plant J. 53, 237-247.
Janssens, V., and Goris, J. (2001). Protein phosphatase 2A: a highly regulated family of serine/threonine phosphatases implicated in cell growth and signalling. Biochem. J. 353, 417-439.
Kallunki, T., Deng, T., Hibi, M., and Karin, M. (1996) c-Jun can recruit JNK to phosphorylate dimerization partners via specific docking interactions. Cell 87, 929-939.

Karlova, R., Boeren, S., Russinova, E., Aker, J., Vervoort, J., and de Vries, S.C. (2006). The Arabidopsis SOMATIC EMBRYOGENESIS RECEPTOR-LIKE KINASE1 protein complex includes BRASSINOSTE- ROID-INSENSITIVE1. Plant Cell 18, 626-638.

Kepinski, S., and Leyser, O. (2005) Plant development: auxin in loops. Curr Biol 15:R208-R210.

Kleine-Vehn, J., and Friml, J. (2008). Polar targeting and endocytic recycling in auxin-dependent plant development. Annu. Rev. Cell Dev. Biol. 24, 447-473.

Kleine-Vehn, J., Dhonukshe, P., Sauer, M., Brewer, P., Wiśniewka, J., Paciorek, T., Benková, E., and Friml, J. (2008a). ARF GEF-dependent transcytosis and polar delivery of PIN auxin carriers in *Arabidopsis*. Curr. Biol. 18, 526-531.

Kleine-Vehn, J., Langowski, L., Wiśniewska, J., Dhonukshe, P., Brewer, P.B., and Friml, J. (2008b). Cellular and molecular requirements for polar PIN targeting and transcytosis in plants. Mol. Plant 1, 1056-1066.

Kleine-Vehn, J., Leitner, J., Zwiewka, M., Sauer, M., Abas, L., Luschnig, C., and Friml, J. (2008c). Differential degradation of PIN2 auxin efflux carrier by retromer-dependent vacuolar targeting. Proc. Natl. Acad. Sci. USA 105, 17812-17817.

Kleine-Vehn, J., Huang, F., Naramoto, S., Zhang, J., Michniewicz, M., Offringa, R., and Friml, J. (2009) PIN auxin efflux carrier polarity is regulated by PINOID kinase-mediated recruitment into GNOM-independent trafficking in Arabidopsis. Plant Cell. 21, 3839-3849.

Kögl, F., and Haagen-Smith, A.J. (1931). Uber die Chemie des Wchsstoffs K. Akad. Wetenschap. Amsterdam. Proc. Sect. Sci. 34, 1411-1416.

Koizumi, K., Sugiyama, M., and Fukuda, H. (2000). A series of novel mutants of *Arabidopsis thaliana* that are defective in the formation of continuous vascular network: calling the auxin signal flow canalization hypothesis into question. Development 127: 3197-3204.

Kudla, J., Batistič, O., and Hashimoto, K. (2010). Calcium signals: the lead currency of plant information processing. Plant Cell 22, 541-563.

Lanteri, M.L., Laxalt, A.M., and Lamattina, L. (2008). Nitric oxide triggers phosphatidic acid accumulation via phospholipase D during auxin-induced adventitious root formation in cucumber. Plant Physiol. 147, 188-198.

Lanteri, M.L., Pagnussat, G.C., and Lamattina, L. (2006). Calcium and calcium-dependent protein kinases are involved in nitric oxide- and auxin-induced adventitious root formation in cucumber. J. Exp. Bot. 57, 1341-1351.

Lee, J.S., and Evans, M.L. (1985). Polar transport of auxin across gravistimulated roots of maize and its enhancement by calcium. Plant Physiol. 77, 824-827.

Lee, S.H., and Cho, H.T. (2006). PINOID positively regulates auxin efflux in Arabidopsis root hair cells and tobacco cells. Plant Cell 18, 1604-1616.

Legue, V., Blancaflor, E., Wymer, C., Perbal, G., Fantin, D., and Gilroy, S. (1997). Cytoplasmic free Ca2t in Arabidopsis roots changes in response to touch but not gravity. Plant Physiol. 114, 789-800.

Leyser, O. (2006). Dynamic integration of auxin transport and signalling. Curr. Biol. 16, R424-R433.

Liang, F., and Sze, H. (1998). A high-affinity Ca2+ pump, ECA1, from the endoplasmic reticulum is inhibited by cyclopiazonic acid but not by thapsigargin. Plant Physiol. 118, 817-825.

Liu, Y., and Zhang, S. (2004) Phosphorylation of 1-aminocyclopropane-1-carboxylic acid synthase by MPK6, a stress-responsive mitogen-activated protein kinase, induces ethylene biosynthesis in Arabidopsis. Plant Cell 16, 3386-3399.

Ljung, K., Bhalerao, R.P., and Sandberg, G. (2001). Sites and homeostatic control of auxin biosynthesis in Arabidopsis during vegetative growth. Plant J. 28, 465-474.

Ljung, K., Hull, A.K., Celenza, J., Yamada, M., Estelle, M., Normanly, J., and Sandberg, G. (2005). Sites and regulation of auxin biosynthesis in Arabidopsis roots. Plant Cell 17, 1090-1104.

Luan, S., Kudla, J., Rodriguez-Concepcion, M., Yalovsky, S., and Gruissem, W. (2002). Calmodulins and calcineurin B-like proteins: calcium sensors for specific signal response coupling in plants. Plant Cell 14, S389-S400.

Luschnig, C., Gaxiola, R.A., Grisafi, P., and Fink, G.R. (1998). EIR1, a root-specific protein involved in auxin transport, is required for gravitropism in Arabidopsis thaliana. Genes Dev. 12, 2175-2187.

Lytton, J., Westlin, M., and Hanley, M.R. (1991). Thapsigargin inhibits the sarcoplasmic or endoplasmic reticulum Ca-ATPase family of calcium pumps. J. Biol. Chem. 266, 17067-17071.

Marchant, A., Bhalerao, R., Casimiro, I., Eklöf, J., Casero, P.J., Bennett, M., and Sandberg, G. (2002).

AUX1 promotes lateral root formation by facilitating indole-3-acetic acid distribution between sink and source tissues in the Arabidopsis seedling. Plant Cell 14, 589-597.

Matsuoka, K., Bassham, D.C., Raikhel, N.V., and Nakamura, K. (1995). Different sensitivity to wortmannin of two vacuolar sorting signals indicates the presence of distinct sorting machineries in tobacco cells. J. Cell Biol. 130, 1307-1318.

Mayer, U., Ruiz, R.A.T., Berleth, T., Misera, S., and Jurgens, G. (1991). Mutations affecting body organization in the Arabidopsis embryo. Nature 353, 402-407.

McElroy, D., Chamberlain, D. A., Moon, E. and Wilson, K. J. (1995). Development of gusA reporter gene constructs for cereal transformation: Availability of plant transformation vectors from the CAMBIA molecular genetic resource service. Mol. Breed. 1, 27-37.

Meskiene, I., Baudouin, E., Schweighofer, A., Liwosz, A., Jonak, C., Rodriguez, P.L., Jelinek, H., and Hirt, H. (2003). The Stress-induced protein phosphatase 2C is a negative regulator of a mitogen-activated protein kinase. J. Biol. Chem. 278, 18945-18952.

Michniewicz, M., Zago, M.K., Abas, L., Weijers, D., Schweighofer, A., Meskiene, I., Heisler, M.G., Ohno, C., Zhang, J., Huang, F., et al. (2007). Antagonistic regulation of PIN phosphorylation by PP2A and PINOID directs auxin flux. Cell 130, 1044-1056.

Mignaco, J.A., Barrabin, H., and Scofano, H.M. (1996). Effects of photo-oxidizing analogs of fluorescein on the sarcoplasmic reticulum Ca2+-ATPase. Functional consequences for substrate hydrolysis and effects on the partial reactions of the hydrolytic cycle. J. Biol. Chem. 271, 18423-18430.

Mockaitis, K., and Estelle, M. (2008). Auxin receptors and plant development: a new signaling paradigm. Annu. Rev. Cell Dev. Biol. 24, 55-80.

Morel, J., Claverol, S., Mongrand, S., Furt, F., Fromentin, J., Bessoule, J.J., Blein, J.P., and Simon-Plas, F. (2006). Proteomics of plant detergent-resistant membranes. Mol Cell Proteomics 5, 1396-1411.

Morris, D.A., Friml. J., and Zažímalová, E. (2004). The transport of auxins. In: plant hormones: Biosynthesis, Signal transduction, Action! Pp, 437-470.

Mostov, K., Su, T., and ter Beest, M. (2003). Polarized epithelial mem- brane traffic: conservation and plasticity. Nat. Cell Biol. 5, 287-293.

Mravec, J., Kubeš, M., Bielach, A., Gaykova, V., Petrášek, J., Skůpa, P., Chand, S., Benková, E., Zažímalová, E., and Friml, J. (2008). Interaction of PIN and PGP transport mechanisms in auxin distribution-dependent development. Development 135, 3345-3354.

Mravec, J., Skůpa, P., Bailly, A., Hoyerová, K., Krecek, P., Bielach, A., Petrásek, J., Zhang, J., Gaykova, V., Stierhof, Y.D., et al. (2009). Subcellular homeostasis of phytohormone auxin is mediated by the ER-localized PIN5 transporter. Nature 459, 1136-1140.

Nagai, T., Ibata, K., Park, E.S., Kubota, M., Mikoshiba, K., Miyawaki, A. (2002). A variant of yellow fluorescent protein with fast and efficient maturation for cell-biological applications. Nat. Biotechnol. 20, 28-9.

Noh, B., Murphy, A.S., and Spalding, E.P. (2001). Multidrug resistance-like genes of Arabidopsis required for auxin transport and auxin-mediated development. Plant Cell 13, 2441-2454.

Normanly, J., Slovin, J.P., and Cohen, J.D. (2004). Auxin biosynthesis and metabolism. In: Plant hormones: biosynthesis, transduction, action! pp. 36-62, Davies P. J. (ed.), Kluwer Academic Publishers Ithaca, NY.

Nühse, T.S., Stensballe, A., Jensen, O.N., and Peck, S.C. (2004). Phosphoproteomics of the Arabidopsis plasma membrane and a new phosphorylation site database. Plant Cell 16, 2394-2405.

Müller, A., Guan, C., Gälweiler, L., Tänzler, P., Huijser, P., Marchant, A., Parry, G., Bennett, M., Wisman, E., and Palme, K. (1998). AtPIN2 defines a locus of Arabidopsis for root gravitropism control. EMBO J. 17, 6903-6911.

Okada, K., Ueda, J., Komaki, M.K., Bell, C.J., and Shimura, Y. (1991). Requirement of the Auxin Polar Transport System in Early Stages of Arabidopsis Floral Bud Formation. Plant Cell 3, 677-684.

Ottenschläger, I., Wolff, P., Wolverton, C., Bhalerao, R. P., Sandberg, G., Ishikawa, H., Evans, M. and Palme, K. (2003). Gravity-regulated differential auxin transport from columella to lateral root cap cells. Proc. Natl. Acad. Sci. USA 100, 2987-2991.

Oliviusson, P., Heinzerling, O., Hillmer, S., Hinz, G., Tse, Y.C., Jiang, L., and Robinson, D.G. (2006). Plant retromer, localized to the prevacuolar compartment and microvesicles in Arabidopsis, may interact with vacuolar sorting receptors. Plant Cell 18, 1239-1252.

Paciorek, T., Zazimalova, E., Ruthardt, N., Petrášek, J., Stierhof, Y.D., Kleine-Vehn, J., Morris, D.A., Emans, N., Jurgens, G., Geldner, N., and Friml, J. (2005). Auxin inhibits endocytosis and promotes its own efflux from cells. Nature 435, 1251-1256.

Pearson, G., Robinson, F., Beers Gibson, T., Xu, B.E., Karandikar, M., Berman, K., and Cobb, M.H. (2001). Mitogen-activated protein (MAP) kinase pathways: regulation and physiological functions. Endocr. Rev. 22, 153-183.

Pencík, A., Rolcík, J., Novák, O., Magnus, V., Barták, P., Buchtík, R., Salopek-Sondi, B., and Strnad, M. (2009). Isolation of novel indole-3-acetic acid conjugates by immunoaffinity extraction. Talanta 80, 651-655.

Peng, J., Elias, J.E., Thoreen, C.C., Licklider, L.J. and Gygi, S.P. (2003). Evaluation of multidimensional chromatography coupled with tandem mass spectrometry (LC/LC-MS/MS) for large-scale protein analysis: the yeast proteome. J. Proteome Res. 2, 43-50.

Perera, I.Y., Hung, C.-Y., Brady, S., Muday, G.K., and Boss, W.F. (2006). A universal role for inositol 1,4,5-trisphosphate-mediated signaling in plant gravitropism. Plant Physiol. 140, 746-760.

Petrášek, J., Mravec, J., Bouchard, R., Blakeslee, J.J., Abas, M., Seifertova, D., Wiśniewska, J., Tadele, Z., Kubes, M., Covanova, M., et al. (2006). PIN proteins perform a rate-limiting function in cellular auxin efflux. Science 312, 914-918.

Petrásek, J., and Friml, J. (2009) Auxin transport routes in plant development. Development 136, 2675-2688.

Pimpl, P., Movafeghi, A., Coughlan, S., Denecke, J., Hillmer, S., and Robinson, D.G. (2000). In situ localization and in vitro induction of plant COPI-coated vesicles. Plant Cell 12, 2219-2235.

Plieth, C., and Trewavas, A.J. (2002). Reorientation of seedlings in the earth's gravitational field induces cytosolic calcium transients. Plant Physiol. 129, 786-796.

Poovaiah, B.W., Yang, T., and van Loon, J.J. (2002). Calcium/calmodulin-mediated gravitropic response in plants. J. Gravit. Physiol. 9, P211-P214.

Quan, R., Lin, H., Mendoza, I., Zhang, Y., Cao, W., Yang, Y., Shang, M., Chen, S., Pardo, J.M., and Guo, Y. (2007). SCABP8/CBL10, a putative calcium sensor, interacts with the protein kinase SOS2 to protect Arabidopsis shoots from salt stress. Plant Cell 19, 1415-1431.

Quintero, F.J., Garciadeblás, B., and Rodríguez-Navarro, A. (1996). The SAL1 gene of Arabidopsis, encoding an enzyme with 3'(2'),5'-bisphosphate nucleotidase and inositol polyphosphate 1-phosphatase activities, increases salt tolerance in yeast. Plant Cell 8, 529-537.

Rashotte, AM., Brady, S.R., Reed, R.C., Ante, S.J., Muday, G.K. (2000). Basipetal auxin transport is required for gravitropism in roots of Arabidopsis. Plant Physiol. 122, 481-490.

Rashotte, A.M., DeLong, A., and Muday, G.K. (2001). Genetic and chemical reductions in protein phosphatase activity alter auxin transport, gravity response, and lateral root growth. Plant Cell 13, 1683-1697.

Raven, J.A. (1975). Transport of indoleacetic acid in plant cells in relation to pH and electrical potential gradients and its significance for polar IAA transport. New Phytol. 74, 163-172.

Reinhardt, D., Pesce, E.R., Stieger, P., Mandel, T., Baltensperger, K., Bennett, M., Traas, J., Friml, J., and Kuhlemeier, C. (2003). Regulation of phyllotaxis by polar auxin transport. Nature 426, 255-260.

Robert, H.S., and Offringa, R. (2008) Regulation of auxin transport polarity by AGC kinases. Curr. Opin. Plant Biol. 11, 495-502.

Robles, P., Fleury, D., Candela, H., Cnops, G., Alonso-Peral, M.M., Anami, S., Falcone, A., Caldana, C., Willmitzer, L., Ponce, M.R., et al. (2010). The RON1/FRY1/SAL1 gene is required for leaf morphogenesis and venation patterning in Arabidopsis. Plant Physiol. 152, 1357-1372.

Rubery, P.H., and Sheldrake, A.R. (1974). Carrier-mediated auxin transport. Planta 188, 101-121.

Sabatini, S., Beis, D., Wolkenfelt, H., Murfett, J., Guilfoyle, T., Malamy, J., Benfey, P., Leyser, O., Bechtold, N., Weisbeek, P., et al. (1999). An auxin-dependent distal organizer of pattern and polarity in the Arabidopsis root. Cell 99, 463-472.

Sachs T (1981). The control of the patterned differentiation of vascular tissues. Adv Bot Res 9, 151-162.

Salisbury, F.B., and Ross, C.W. (1992). Plant Physiology. Belmont, CA: Wadsworth. pp.357-407, 531-548.

Sanchez, J.-P., and Chua, N.-H. (2001). Arabidopsis PLC1 is required for secondary responses to abscisic acid signals. Plant Cell 13, 1143-1154.

Sauer, M., Balla, J., Luschnig, C., Wiśniewska, J., Reinöhl, V., Friml, J., and Benková, E. (2006a). Canalization of auxin flow by Aux/IAA-ARF-dependent feed-back regulation of PIN polarity.

Genes Dev. 20, 2902-2911.
Sauer, M., Paciorek, T., Benková, E., and Friml, J. (2006b). Immunocytochemical techniques for whole-mount in situ protein localization in plants. Nat. Protoc. 1, 98-103.
Scarpella, E., Marcos, D., Friml, J., and Berleth, T. (2006). Control of leaf vascular patterning by polar auxin transport. Genes Dev. 20, 1015-1027.
Schwab, R., Ossowski, S., Riester, M., Warthmann, N., and Weigel, D. (2006). Highly specific gene silencing by artificial microRNAs in Arabidopsis. Plant Cell 18, 1121-1133.
Seaman, M.N. (2005). Recycle your receptors with retromer. Trends Cell Biol. 15, 68-75.
Shevell, D.E., Leu, W.-M., Gillmor, C.S., Xia, G., Feldmann, K.A., and Chua, N.-H. (1994). *EMB30* is essential for normal cell division, cell expansion, and cell adhesion in Arabidopsis and encodes a protein that has similarity to Sec7. Cell 77, 1051-1062.
Shin, H., Shin, H.S., Guo, Z., Blancaflor, E.B., Masson, P.H., and Chen, R. (2005). Complex regulation of Arabidopsis AGR1/PIN2-mediated root gravitropic response and basipetal auxin transport by cantharidin-sensitive protein phosphatases. Plant J. 42, 188-200.
Shishova, M., and Lindberg, S. (2010). A new perspective on auxin perception. J. Plant Physiol. 167, 417-422.
Steinmann, T., Geldner, N., Grebe, M., Mangold, S., Jackson, C.L., Paris, S., Gälweiler, L., Palme, K., and Jürgens, G. (1999). Coordinated polar localization of auxin efflux carrier PIN1 by GNOM ARF GEF. Science 286, 316-318.
Stepanova, A.N., Robertson-Hoyt, J., Yun, J., Benavente, L.M., Xie, D.Y., Dolezal, K., Schlereth, A., Jürgens, G., and Alonso, J.M. (2008) TAA1-mediated auxin biosynthesis is essential for hormone crosstalk and plant development. Cell 133, 177-191.
Stoddart, J.L. (1983). In: The biochemistry and physiology of gibberellins, Vol.2, pp.1-55, Crozier, A. ed. Praeger, New York.
Sondhi, D., Xu, W., Songyang, Z., Eck, M.J., and Cole, P.A. (1998) Peptide and protein phosphorylation by protein tyrosine kinase Csk: insights into specificity and mechanism. Biochemistry 37, 165-172.
Sorefan, K., Girin, T., Liljegren, S.J., Ljung, K., Robles, P., Galván-Ampudia, C.S., Offringa, R., Friml, J., Yanofsky, M.F., and Østergaard, L. (2009) A regulated auxin minimum is required for seed dispersal in Arabidopsis. Nature 459, 583-586.
Sukumar, P., Edwards, K.S., Rahman, A., DeLong, A., and Muday, G.K. (2009) PINOID kinase regulates root gravitropism through modulation of PIN2-dependent basipetal auxin transport in Arabidopsis. Plant Physiol. 150, 722-735.
Swarup, K., Benková, E., Swarup, R., Casimiro, I., Péret, B., Yang, Y., Parry, G., Nielsen, E., De Smet, I., Vanneste, S., et al. (2008). The auxin influx carrier LAX3 promotes lateral root emergence. Nat. Cell Biol. 10, 946-954.
Swarup, R., Friml, J., Marchant, A., Ljung, K., Sandberg, G., Palme, K,, and Bennett, M. (2001). Localization of the auxin permease AUX1 suggests two functionally distinct hormone transport pathways operate in the Arabidopsis root apex. Genes Dev 15: 2648-2653
Swarup, R., Kramer, E.M., Perry, P., Knox, K., Leyser, H.M., Haseloff, J., Beemster, G.T., Bhalerao, R., and Bennett, M.J. (2005). Root gravitropism requires lateral root cap and epidermal cells for transport and responset to a mobile auxin signal. Nat. Cell Biol. 7, 1057-1065.
Sze, H., Liang, F., Hwang, I., Curran, A.C., and Harper, J.F. (2000). Diversity and regulation of plant Ca2+ pumps: insights from expression in yeast. Annu. Rev. Plant Physiol. Plant Mol. Biol. 51, 433-462.
Tang, R.-H., Han, S., Zheng, H., Cook, C.W., Choi, C.S., Woerner, T.E., Jackson, R.B., and Pei, Z.-M. (2007). Coupling diurnal cytosolic Ca2+ oscillations to the CAS-IP3 pathway in Arabidopsis. Science 315, 1423-1426.
Tao, Y., Ferrer, J.L., Ljung, K., Pojer, F., Hong, F., Long, J.A., Li, L., Moreno, J.E., Bowman, M.E., Ivans, L.J., et al. (2008) Rapid synthesis of auxin via a new tryptophan-dependent pathway is required for shade avoidance in plants. Cell 133, 164-176.
Tanaka, H., Dhonukshe, P., Brewer, P.B., and Friml, J. (2006) Spatiotemporal asymmetric auxin distribution: a means to coordinate plant development. Cell Mol. Life Sci. 63, 2738-2754.
Thimann, K.V. (1977). Hormone action in the whole life of plants. Amherst: The University of Massachusetts.
Tiruppathi, C., Song, W., Bergenfeld, M., Sass, P., and Malik, A.B. (1997). Gp60 activation mediates albumin transcytosis in endothelial cells by tyrosine kinase-dependent pathway. J. Biol. Chem. 272, 25968-25975.

Toyota, M., Furuichi, T., Tatsumi, H., and Sokabe, M. (2008). Critical consideration on the relationship between auxin transport and calcium transients in gravity perception of Arabidopsis seedlings. Plant Signal Behav. 3, 521-524.

Tsiantis, M., and Hay, A. (2003). Comparative plant development: the time of the leaf? Nat. Rev. Genet. 4, 169-180.

Vieten, A., Sauer, M., Brewer. P.B., and Friml, J. (2007). Molecular and cellular aspects of auxin-transport-mediated development. Trends Plant Sci. 12, 160-168.

Ulmasov, T., Murfett, J., Hagen, G., and Guilfoyle, T.J. (1997). Aux/IAA proteins repress expression of reporter genes containing natural and highly active synthetic auxin response elements. Plant Cell 9, 1963-1971.

Utsuno, K., Shikanai, T., Yamada, Y., and Hashimoto, T. (1998). Agr, an Agravitropic locus of Arabidopsis thaliana encodes a novel membrane-protein family member. Plant Cell Physiol. 39, 1111-1118.

Vanneste, S., and Friml, J. (2009). Auxin: a trigger for change in plant development. Cell 136, 1005-1016.

Vieten, A., Sauer, M., Brewer, P.B., and Friml, J. (2007). Molecular and cellular aspects of auxin-transport-mediated development. Trends Plant Sci. 12, 160-168.

Weijers, D., Van Hamburg, J.P., Van Rijn, E., Hooykaas, P.J. and Offringa, R. (2003). Diphtheria toxin- mediated cell ablation reveals interregional communication during Arabidopsis seed development. Plant Physiol. 133, 1882-1892.

Weijers, D., Sauer, M., Meurette, O., Friml, J., Ljung, K., Sandberg, G., Hooykaas, P., and Offringa, R. (2005). Maintenance of embryonic auxin distribution for apical-basal patterning by PIN-FORMED-dependent auxin transport in Arabidopsis. Plant Cell 17, 2517-2526.

White, P.J., and Broadley, M.R. (2003). Calcium in plants. Ann. Bot. 92, 487-511.

Willemsen, V., Friml, J., Grebe, M., van den Toorn, A., Palme, K., and Scheres, B. (2003). Cell polarity and PIN protein positioning in Arabidopsis require STEROL METHYLTRANSFERASE1 function. Plant Cell 15, 612-625.

Wilson, P.B., Estavillo, G.M., Field, K.J., Pornsiriwong, W., Carroll, A.J., Howell, K.A., Woo, N.S., Lake, J.A., Smith, S.M., Millar, A.H., et al. (2009). The nucleotidase/phosphatase SAL1 is a negative regulator of drought tolerance in Arabidopsis. Plant J. 58, 299-317.

Wiśniewska, J., Xu, J., Seifertova, D., Brewer, P.B., Ruzicka, K., Blilou, I., Rouquie, D., Benková, E., Scheres, B., and Friml, J. (2006). Polar PIN localization directs auxin flow in plants. Science 312, 883.

Woodward, A.W., and Bartel, B. (2005). Auxin: regulation, action, and interaction. Ann. Bot. 95, 707-735.

Wymer, C.L., Bibikova, T.N., and Gilroy, S. (1997). Cytoplasmic free calcium distributions during the development of root hairs of Arabidopsis thaliana. Plant J. 12, 427-439.

Xiong, L., Lee, B.-h., Ishitani, M., Lee, H., Zhang, C., and Zhu, J.-K. (2001). FIERY1 encoding an inositol polyphosphate 1-phosphatase is a negative regulator of abscisic acid and stress signaling in Arabidopsis. Genes Dev. 15, 1971-1984.

Xiong, L., Lee, H., Huang, R., and Zhu, J.-K. (2004). A single amino acid substitution in the Arabidopsis FIERY1/HOS2 protein confers cold signaling specificity and lithium tolerance. Plant J. 40, 536-545.

Xu, J., and Scheres, B. (2005). Dissection of Arabidopsis ADP-RIBOSYLATION FACTOR 1 function in epidermal cell polarity. Plant Cell 17, 525-536.

Xu, J., Hofhuis, H., Heidstra, R., Sauer, M., Friml, J., and Scheres, B. (2006). A molecular framework for plant regeneration. Science 311, 385-388.

Xu, X., Hotta, C.T., Dodd, A.N., Love, J., Sharrock, R., Lee, Y.W., Xie, Q., Johnson, C.H., and Webb, A.A.R. (2007). Distinct light and clock modulation of cytosolic free Ca2+ oscillations and rhythmic CHLOROPHYLL A/B BINDING PROTEIN2 promoter activity in Arabidopsis. Plant Cell 19, 3474-3490.

Yang, T., and Poovaiah, B.W. (2003). Calcium/calmodulin-mediated signal network in plants. Trends Plant Sci. 8, 505-512.

Yang, Y., Hammes, U.Z., Taylor, C.G., Schachtman, D.P., and Nielsen, E. (2006). High-affinity auxin transport by the AUX1 influx carrier protein. Curr. Biol. 16, 1123-1127.

Zádníková, P., Petrásek, J., Marhavy, P., Raz, V., Vandenbussche, F., Ding, Z., Schwarzerová, K., Morita, M.T., Tasaka, M., Hejátko, J., et al. (2010). Role of PIN-mediated auxin efflux in apical hook development of Arabidopsis thaliana. Development 137, 607-617.

Zegzouti, H., Anthony, R.G., Jahchan, N., Bogre, L., and Christensen, S.K. (2006). Phosphorylation and activation of PINOID by the phospholipid signaling kinase 3-phosphoinositide-dependent protein kinase 1 (PDK1) in Arabidopsis. Proc. Natl. Acad. Sci. USA 103, 6404-6409.

Zhang, J., Nodzyński, T., Pěnčík, A., Rolčík, J., and Friml, J. (2010). PIN phosphorylation is sufficient to mediate PIN polarity and direct auxin transport. Proc. Natl. Acad. Sci. USA 107, 918-922.

Zhao, Y. (2008) The role of local biosynthesis of auxin and cytokinin in plant development. Curr. Opin. Plant Biol. 11, 16-22.

Zhong, R., Burk, D.H., Morrison, W.H. III, and Ye, Z.-H. (2004). FRAGILE FIBER3, an Arabidopsis gene encoding a type II inositol polyphosphate 5-phosphatase, is required for secondary wall synthesis and actin organization in fiber cells. Plant Cell 16, 3242-3259.

Zhou, H., Iwasaki, H., Nakamura, T., Nakamura, K., Maruyama, T., Hamano, S.-i., Ozaki, S., Mizutani, A., and Mikoshiba, K. (2007). 2-Aminoethyl diphenylborinate analogues: selective inhibition for store-operated Ca2+ entry. Biochem. Biophys. Res. Commun. 352, 277-282.

Zhou, H.W., Nussbaumer, C., Chao, Y., and DeLong, A. (2004). Disparate roles for the regulatory A subunit isoforms in Arabidopsis protein phosphatase 2A. Plant Cell 16, 709-772.

Zourelidou, M., Müller, I., Willige, B.C., Nill, C., Jikumaru, Y., Li, H., and Schwechheimer, C. (2009). The polarly localized D6 PROTEIN KINASE is required for efficient auxin transport in Arabidopsis thaliana. Development 136, 627-636.